

IMPACT STUDY:PHOTOVOLTAIC DISTRIBUTED GENERATION ON POWER SYSTEM

SMRUTIREKHA SAHOO

The School of Business, Society and Engineering

Course: Degree Project

Course Code: ERA401

Subject: Energy Technology

Credits: 30.0 hp

Program: [Master Programme in Sustainable
Energy System]

Supervisor: [Maher Azaza, EST, MDH]

Examiner: [Fredrik Wallin, EST, MDH]

Company Supervisor: [Johanna Rosenlind,
Mälarenergi Elnät AB]

Datum: [2016-06-15]

E-post:

[sso14001@student.mdh.se]

ABSTRACT

The grid-connected photo-voltaic (PV) system is one of the most promising renewable energy solutions which offers many benefits to both the end user and the utility network and thus it has gained the popularity over the last few decades. However, due to the very nature of its invariability and weather dependencies, the large scale integration of this type of distributed generation has created challenges for the network operator while maintaining the quality of the power supply and also for reliable and safe operations of the grids. In this study, the behavioral impact of large scale PV system integration which are both steady and dynamic in nature was studied. An aggregate PV model suited to study the impacts was built using MATLAB/Simulink. The integration impacts of PV power to existing grids were studied with focus on the low voltage residential distribution grids of Mälarenergi Elnät AB (10/0.4 kV). The steady state impacts were related to voltage profile, network loss. It was found that the PV generation at the load end undisputedly improves the voltage profile of the grid especially for the load buses which are situated at farther end of the grid. Further, with regard to the overvoltage issue, which is generally a concern during the low load demand period it was concluded that, at a 50% PV penetration level, the voltage level for the load buses is within the limit of 103% as prescribed by the regulator excepting for few load buses. The voltage level for load buses which deviate from the regulatory requirement are located at distance of 1200 meter or further away from the substation. The dynamic impact studied were for voltage unbalancing in the grid, which was found to have greater impact at the load buses which is located farther compared to a bus located nearer to the substation. With respect to impact study related to introduction of harmonics to the grid due to PV system integration, it was found that amount of harmonic content which was measured as total harmonic distortion (THD) multiplies with integration of more number of PV system. For a 50 % penetration level of PV, the introduced harmonics into the representative network is very minimal. Also, it was observed from the simulation study that THD content are be less when the grid operates at low load condition with high solar irradiance compared to lower irradiance and high load condition.

Keywords:

DC-AC inverter, DC-DC boost converter, Dynamic PV model, Grid-connected PV system, Harmonic distortion, LV grid-modelling, Overvoltage, THD, Voltage unbalancing, VSI

PREFACE

This thesis is the final part of the Master's in Sustainable Energy System Programme. The work is carried out in association with Mälarenergi Elnät AB and Future Energy Centre at Mälardalen University in Västerås. This study would not have been completed without the aid of guidance, facility, encouragement from different persons and organizations. This brings me opportunity to thank everyone who were involved in supporting me with this work with their insightful thoughts and ideas.

Foremost, I would like to express my special appreciation to my supervisor Dr. Maher Azaza, researcher at the Department of EST, Mälardalen Högskola (MDH). I would like to thank him for encouraging with my research work and for his valuable comments.

My sincere gratitude for my examiner Dr. Fredrik Wallin at MDH for his insightful comments which enabled me assessing my work and make necessary correction in the report.

I would also like to thank my supervisor at Mälarenergi Elnät AB, Dr. Johanna Rosenlind for giving me this opportunity to work with her and get ideas of the research from various meetings, also from a pool of researchers and for her supervision during the work.

I would also like to show my special gratitude for Mr. Anders Malmquist for letting me understand the Mälarenergi Elnät and for all round support during my work at Mälarenergi Elnät AB.

My fellow colleagues at Mälarenergi, Mr. Patrik Zетроström and Mr. Svante Monie deserve special appreciation for behaving as literal encyclopedia for me during the thesis work. I literally banked on them for understanding the Swedish grid and end consumers.

A special thanks to Dr. Subrat Kumar Sahoo, my husband and best friend for his continuous support and for the help in understanding all nitty-gritty involved in Simulink.

SUMMARY

Grid connected photo-voltaic (PV) generation has emerged as the main stream of renewable energy source during the past years. However, these kind of generation are un-dispatchable due to the natural variability. The PV system are connected to the grid with many intermediate level of conversion and those are basically electronic components with non-linear characteristics. Furthermore, most of the new PV generation has been installed in the distribution grid as distributed generation, connected at the load end of the network and have customer oriented characteristics. These kind of grid connected PV system installation has given rise to problems concerning the power quality issues of the grid. Network operators are preparing themselves for upgrading and strengthening the grid to be able to integrate and manage more of this renewable electricity source in their systems. In the above backdrop, this thesis work is an attempt to investigate the impacts of the PV integration on the low voltage side network of the grid.

The impacts of PV system are both of steady and dynamic in nature. Hence, different modelling techniques are required to study the different kinds of impact. An aggregate model of grid-connected PV system was built for this purpose and was used for simulating the integration of PV generation on a large-scale to the modelled LV grid to study the steady state and dynamic impacts. A representative low voltage residential distribution system feeder of Mälarenergi Elnät was selected to study the steady state impacts related to overvoltage, voltage improvement and loss reductions. The representative grid network model was built using components/library from Simscape Power System tool of MATLAB/Simulink. The grid operates at nominal three phase line to line voltage of 400 V, supplied from 500 kVA 11/0.4 kV distribution transformer. The network comprises 16 number of distribution feeder nodes as load buses and the load for those distribution feeders were modelled as lump load. The integration of PV generator is done at each such feeder nodes.

The study approached the integration impacts by comparison method of the distribution grids without PV generation integrated and with PV generation integrated for peak (maximum) load and low (minimum) load conditions and with different level of solar irradiance. The PV generator functions at unitary power factor, hence produces only active power. The overvoltage issues were checked for minimum load condition with high irradiance and the voltage improvement was checked for maximum load condition with a lower level of irradiance. The impacts study revealed that integration of solar PV generation for the distribution grids in general caused an increase in voltage profile, decrease in voltage drop and losses. Further, it was learnt that the overvoltage which occurred during the low load condition is within the limit allowed by regulator (except for few nodes at far end), whereas, the same PV system generation from a low level of irradiance helped in improving voltage at the time of peak load condition.

Further, a dynamic model of PV system suitable for studying its interactions with the grid system was developed using the MATLAB/Simulink tool. The modelling involved a detailed model of PV systems with inverter interface and with the control blocks. The model was simulated for getting electrical characteristic of photo-voltaic generation with the dynamic response of the system to rapid changes in irradiance and temperature. The harmonic impacts were studied for maximum load and minimum load condition. The harmonic content was

found less for the minimum load condition. The voltage unbalancing which is a phenomenon due to uneven distribution of load and solar installation among the three phases of network supply system was found to be prominent to the far end load buses compared to the load buses near to substation.

1	INTRODUCTION	1
1.1	Background	2
1.2	Research Question.....	2
1.3	Purpose.....	3
1.4	Delimitation.....	3
1.5	Method	4
1.6	Report outline	5
2	GRID CONNECTED PV SYSTEM CHARACTERSTICS, CHALLENGES AND TREND .	6
2.1	Global solar irradiation in Sweden.....	6
2.2	Solar policy framework in Sweden.....	6
2.3	PV installation trend in Sweden	7
2.4	Power Quality Regulation Standard	8
2.5	Challenges of grid-connected PV system.....	9
2.5.1	<i>Interference with Voltage regulation</i>	<i>10</i>
2.5.2	<i>Overvoltage and Losses</i>	<i>10</i>
2.5.3	<i>Voltage unbalancing</i>	<i>11</i>
2.5.4	<i>Harmonic Distortion</i>	<i>11</i>
2.5.5	<i>Voltage stability.....</i>	<i>12</i>
2.6	Inverters' Reactive Power Support.....	13
3	COMPONENTS OF GRID CONNECTED PV SYSTEM	16
3.1	Photovoltaic cell electrical characteristics.....	17
3.2	DC-DC converter and maximum power point tracking (MPPT) controller.....	19
3.3	DC-AC inverter.....	21
3.4	Filter circuit.....	23
3.5	Instantaneous p-q theory, Clarke and Park transformation	23
3.5.1	<i>Stationary reference frame (Clarke transform)</i>	<i>24</i>
3.5.2	<i>Synchronous/Rotating reference frame (Park transform)</i>	<i>26</i>
3.6	Grid synchronisation.....	28
3.7	Control strategies of the inverter power stage.....	30

3.8	Voltage regulation, Load flow	30
4	MODELLING OF GRID-CONNECTED PV SYSTEM AND THE DISTRIBUTION NETWORK.....	32
4.1	PV array modeling	33
4.2	DC-DC converter and MPPT control algorithm.....	39
4.3	DC-AC inverter and control system	43
4.4	Distribution network modelling	50
4.4.1	<i>Grid source</i>	51
4.4.2	<i>Low voltage distribution network</i>	51
4.4.3	<i>Load profile</i>	52
5	RESULT	57
5.1	Overvoltage impact	57
5.2	Voltage unbalancing impact	60
5.3	Harmonic distortion impact	62
6	DISCUSSION.....	66
7	CONCLUSION.....	67
8	FUTURE WORK.....	68
	REFERENCES.....	70
	APPENDIX A: MATLAB SCRIPT FOR PV MODULE MODELLING.....	1
	APPENDIX B: MATLAB SCRIPT FOR P&O ALGORITHM.....	2

LIST OF FIGURES

Figure 1: PV Installation Trend during past 12 years (Lindahl, 2014)..... 8

Figure 2: P-Q capability of 10 kVA Inverter (Ravi Bhatt, August 2011)15

Figure 3: Effect of Inverter size on the reactive power capability.....16

Figure 4: Grid-connected PV system blocks17

Figure 5: I-V characteristic for PV Module (Marcelo Gradella Villalva, MAY 2009) 18

Figure 6: Temperature Dependence of Open Circuit Voltage (Marcelo Gradella Villalva, MAY 2009)..... 18

Figure 7: Flow Chart of P&O Algorithm.....20

Figure 8: Transformation from abc to $\alpha\beta 0$ (Clarke Transformation) (Evju, June 2007) 25

Figure 9: $\alpha\beta$ to dq transformation using Park transformation (Evju, June 2007)..... 27

Figure 10: A basic circuit of PLL 29

Figure 11: Schematic block diagram of PLL (Evju, June 2007) 29

Figure 12: Representative Two Node Grid.....31

Figure 13: Voltage Profile along the feeder from sending end node to receiving end node (Mulenga, 2015) 32

Figure 14: Five Parameter Single Diode Model 34

Figure 15: Block Diagram of the PV Model in Simulink 36

Figure 16: PV Model in Subsystem..... 36

Figure 17: Characteristic I-V Curve under different Temperature 37

Figure 18: Characteristic I-V Curve under different Irradiation 38

Figure 19: Characteristic P-V Curve under different Temperature 38

Figure 20: Characteristic P-V Curve under different Irradiation 39

Figure 21: Schematic Diagram of Boost Converter40

Figure 22: Simulation schematic of boost topology.....41

Figure 23: Simulation Results of the boost converter with control algorithm 42

Figure 24: Schematic block Diagram of Voltage Controller 44

Figure 25: Photovoltaic Output characteristics 46

Figure 26: DC Link Voltage vrs. Modulation Index..... 47

Figure 27: Voltage Source Inverter and Grid reference Output..... 48

Figure 28: THD at 0.5 second time of operation 49

Figure 29: THD after 2 second of operation 50

Figure 30: Schematic Diagram of the representative Mälarenergi Elnät LV grid..... 52

Figure 31: Voltage profile for load buses for peak load condition 56

Figure 32: Voltage profile for the load buses for low load condition..... 57

Figure 33: Voltage Profile at distribution feeder for Case I..... 59

Figure 34: Voltage profile at distribution feeder for case-II..... 59

Figure 35: Overvoltage at minimum load condition with PV Integration..... 60

Figure 36: Voltage sequence at node 5196 before PV integration61

Figure 37: Voltage sequence at node 5196 after PV Integration.....61

Figure 38: Voltage sequence at node 5200 before PV Integration..... 62

Figure 39: Voltage sequence at node 5200 after PV Integration..... 62

Figure 40: THD at maximum load condition at 400 V side 63

Figure 41: THD at maximum load condition at 11kV side 64

Figure 42: THD for minimum load condition at 400V..... 65
 Figure 43: THD at minimum load condition at 11 kV..... 66

LIST OF TABLES

Table 1: Manufacturing Datasheet of PV Model 37
 Table 2: Design Parameter for Boost Converter 42
 Table 3: Design Parameter for 15 kW aggregate model 45
 Table 4: Typical Consumption data for Residential Houses in Scandinavian countries..... 53
 Table 5: Load data for distribution feeders..... 55

NOMENCLATURE

Description	Unit	Indication
Current	Ampere	I
Voltage	Volt	V
Active Power	Watt	P
Reactive Power	Volt Ampere Reactive	Q
Apparent Power	Volt Ampere	S
Short Circuit Current	Ampere	I_{sc}
Open Circuit Voltage	Volt	V_{oc}
Rated Capacity	Watt Peak	W_p
Current at Maximum Power Point	Ampere	I_{MP}
Voltage at Maximum Power Point	Volt	V_{MP}
PV Current Output	Ampere	I_{PV}
PV Voltage Output	Volt	V_{PV}
Resistance	Ohm	R
Inductance	Henry	H
Capacitance	Farad	F
DC-link Voltage	Volt	V_{DC}
Irradiance	Watt/m ²	W/m ²
Energy	Watt-hour	Whr
Frequency	Hertz	Hz

ACRONYMS

AC	Alternate Current
AM	Air Mass
ANN	Artificial Neural Network
CC	Current Control
CSI	Current Source Inverter
DC	Direct Current
DG	Distributed Generation
DSO	Distribution System Operator
DSTATCOM	Distribution Static Compensator
DVR	Dynamic Voltage Restorer
EN	European Network
EU	European Union
FFT	Fast Fourier Transform
GHI	Global Horizontal Irradiance
GTI	Global Tilted Irradiance
IC	Incremental Conductance
IGBT	Insulated Gate Bipolar Thyristor
LTC	Load Tap Changer
LV	Low Voltage
LVRT	Low Voltage Ride Through
MOSFET	Metal Oxide Semiconductor Field Effect Transistor
MPPT	Maximum Power Point Tracking
MV	Medium Voltage
PCC	Point of Common Coupling
PCS	Power Conditioning System
PF	Power Flow
PI	Proportional Integral
P&O	Perturb and Observe
PV	Photo-voltaic
PVDG	Photo-voltaic Distributed Generation
PQ	Power Quality
PWM	Pulse Width Modulation
RES	Renewable Energy Source
STC	Standard Test Condition
THD	Total Harmonic Distortion
VC	Voltage Control
VU	Voltage Unbalancing
VSI	Voltage Source Inverter

1 INTRODUCTION

Environmental consciousness lead to adoption to a sustainable way of producing energy. This is a probable way towards combating the global climate issues. In the era of sustainable energy for all, renewables have entered the mainstream. Among various renewable energy sources (RES), the photo-voltaic (PV) market across the globe has seen steady growth during the past 15 years and is also expected to grow in the future years (REN21, 2015). With an installed capacity of 36.2 Mega Watt peak (MWp) during 2014, PV installation rate in Sweden showed 100% increase over the installation rate during the year 2013. In Sweden, the PV integration is enjoying strong growth rate in recent years because of a growing interest in technology, falling system prices and the direct capital subsidy grant which is effective from the year 2006 (Lindahl, 2014). Such installations help in reducing the losses and improving the voltage profile of the network by supplying the load at the consumer point (Sam KoohiKamali, 2010). Despite its promising success, PV penetration presents potential challenges when connected to the distribution network. The most important characteristic of these PVs is that their output power being fed to the grid is not controlled and is dependent on the instantaneous power from the Sun. Also PV system when integrated to the grid, introduces various interfacing devices with non-linear characteristics.

In conventional power system configuration, generations are located centrally with a corollary that the flow of power is from generation through transmission and distribution network to the end user. The normal direction of power flow is radial/un-directional i.e. from the source (substation) towards the load (customers) in any part of the grid. The power flow causes the voltages to drop through the network from the supply end to the receiving end. On the contrary, the PV installation, referred to as distributed generation (DG), are geographically distributed, of smaller capacity, connected to medium voltage (MV)/low voltage (LV) distribution grid and are usually located closer to the load. The random distributed integration of PV at the distribution side of the power system, creates meshed flow of power in the network.

The potential problem and challenges associated with PV integration can be power quality (PQ) issues such as voltage rise, voltage fluctuation and flickering, voltage unbalancing, voltage instability, current harmonics, voltage harmonics, etc. or the issues affecting the normal operation of power system like load/frequency control, load following, de-sensitization or malfunctioning of protection equipment, overloading of cable and transformers, increase of losses of power lines, interaction with load tap changer (LTC), line voltage regulators or capacitor banks, etc. (M. Karimi, 2016). These issues are barriers that limit the penetration of PV distributed generations (PVDGs) into the power system. The issues very much vary depending on the level of penetration, voltage level at the connection point, grid parameters (capacity and topology), the characteristics of load etc. (Nadeeshani Jayasekara, 2010), (Aldo Canova, 2009), (Minas Patsalides, 2016), (M. Chidi, July 2012),(Jaan Niitsoo, 2015). As the use of solar photo-voltaic continues to expand, concern about its potential impact on the operation of the

electricity grid grow as well. For seamless integration of PV penetration in the power system, its impact on the distribution system has to be addressed in a right manner. Distribution system operators (DSOs) should be prepared to integrate and manage more of this kind of DG into the system.

1.1 Background

In Sweden, the power sector was deregulated in 1996. The objective of deregulation was to make the power sector market more competitive and to give the boost to sustainable source of generation and exposition of the existing network. Under deregulated framework, the DSOs are responsible for planning and operation of their network while fulfilling certain PQ regulation (Huang Yalin, June 2013) . Deregulation of the power market has caused the increased share of renewable energy sources in the generation mix. This had become the prime driver for the transition in the way distribution networks are planned, managed and operated from the past. Small scale renewable distributed generation units are making a way towards the power system network and replacing the large conventional production units. More distributed generation introduced in the distribution network means more dynamic power flows in to the distribution system. In the above backdrop, power systems of the future will most likely be more complex than they have been in the past (Vattenfall, 2007). The DSOs need safe and reliable operation guideline to get through such installations. In the current scenario in Sweden, the residential PV installations do not need to meet any technical standards for the grid integration. However, the DSO must adhere to certain standard as per the prevalent regulation when supplying electric power to the customers. The deployment of PV technology in local distribution grids is usually done in an unplanned way without performing the required studies and this may induce PQ issues. Significant increase in installation of grid-connected PV system which has called for better understanding of those systems. In order to better understand the interaction mechanism between PV integration, and power system and solve these problems modelling of PVDG system and simulation study integrating those models to the existing operational grid is a need. Building accurate models of PV system make possible the evaluation of their behavior in the context of the full network and also lead to the development of appropriate solutions.

1.2 Research Question

Onset of steady growth in penetration rate of PVDG system over the years and the impact associated with it on the power system network, is reason for concern among researchers around the world. Various studies have been conducted to quantify the impacts. These are pertaining to PQ issues and other operational aspects.

This work would include primary research of:

1. What are the typical impacts of large scale PV integration on the network, and the associated challenges faced by DSO while maintaining the quality of the power supply?

2. What are the modelling requirements for analysing the impact of the PV system in to the grid?

To answer the above questions, the present study will assess the impact of PV penetration on one of the representative network the LV distribution system of Mälarenergi Elnät. The impacts can be both of steady state and dynamic in nature. Suitable models for the grid-connected PV system needs to be built in order to reflect the PV power output for Swedish weather condition and for the dynamics introduced in the network due to the introduction of power electronics.

Appropriate analysis tools are required to check distribution networks operating conditions in the evolving scenario. For example, power flow (PF) calculations are typically needed to assess the allowed PVDG penetration level for a given network in order to ensure that voltage and current limits are not exceeded. The power quality issues that would be subject of interest for this study is pertaining to voltage rise, voltage unbalancing, harmonics in the systems in particular.

1.3 Purpose

The work aims to be done in association with Mälarenergi Elnät AB and Mälardalen Högskola as thesis work for Master's Programme in Sustainable Energy System. The focus of the project is to understand the behavioral impact of large scale PV integration for different operating condition of distribution grid. The work would include:

- A literature review in combination with simulations in order to answer the research questions.
- A standardized model of grid connected PV module capable to capture the actual functional characteristics of a PV system
- Understanding the problems related to power quality especially overvoltage and harmonics, voltage unbalancing for different scenarios by way of building suitable model for PV system and distribution grid.

1.4 Delimitation

The following limitations are involved for this thesis work:

- The component parameter selection involved in the modelling of the PV system is purely for simulation study. Hence, the selection is not optimized for cost, efficiency and sizing.
- The grid network modelling only considers bulk load modelling and bulk solar generation in the LV distribution networks at point of common coupling. It doesn't include the house level feeder modelling.
- For studying the unbalancing impact, only few of the distribution feeder node has been simulated, one near to the substation and another farther to substation to see the difference in impact.

- The loads used for simulation are constant active and reactive power (PQ) load without any non-linear characteristics, hence do not represent the dynamics of loads as per real scenario. Further, due to limited time available for thesis, some assumption were made regarding the maximum load and minimum load demand of the network, which can be avoided with good resource of database.
- The loads considered assumed to be equally distributed among the three phases, which could not be the case for real scenario.
- The impact study was only limited to PV penetration level of 50%.

1.5 Method

The proposed work scope under the thesis will contribute in two parts.

The first part of the work would deal with the grid-connected PV system modelling. A literature study pertaining to commonly accepted impacts on the network related to distributed PV integration and the study of the relevant power system standards under European Union (EU) or Swedish regulatory framework pertaining to solar integration would be carried to understand the modelling requirement. The modelling work would be for introducing the main components for PV system and the required controller schemes. The PV modelling part in general focus on the two main conversion parts of a PV generation. The direct current (DC) side consists of PV modules to derive the DC current out of the sun irradiation. The PV system then interfaces the alternate current (AC) network via an inverter. The DC side of the system is equipped with the controllers such as maximum power point tracking (MPPT) or active power control. The control facilities, implemented on the DC side, are mainly focuses on regulation of the output DC voltage of the generator depending on the requirements of the system. The impact of the PV system on the grid operation are provided by extra controllers installed on the AC side. The AC side controllers would be designed considering the PV system dynamic contribution on the grid. The modelling would be performed in Simulink/Simscape Power System tool of MATLAB.

The second part of the work would deal with the analysis impact of PV on power system. The representative grid from Mälarenergi Elnät would be used for study. In order to design a model of a grid, and to carry power flow calculations, power system simulations based tool of MATLAB will be used. Concerning the network, a single line will be simulated in order to evaluate the impacts.

The PV system would be modelled as a constant power generator working with unity power factor (regulated with zero reactive) and would be simulated with a representative distribution feeder model without various typical voltage support equipment. Some power flow simulation will be performed in order to evaluate the influence of connecting multiple of PV systems in a limited residential area. The measuring parameters are feeder voltage profile, the active and reactive power flows, phase voltages and phase angle. Also, the study would include the integration of dynamic PV model, which would show the impacts pertaining to voltage unbalancing and total harmonic distortion.

1.6 Report outline

The report is organized as follows.

In chapter 2, the solar installation trend in Sweden, pertaining regulatory framework and support measures with respect to solar installation has been detailed. A detailed literature study with respect to various impacts and challenges involved with grid-connected PV integration was carried in order to understand the challenges, technical requirements and demands from the power system operator associated with the integration of PV generation. The technical capabilities of inverters relevant to feeder voltage control are also presented.

Chapter 3 introduces analysis approach, discusses modelling requirements, and the concepts of literature that is in line to the subject of integrating PV system to an existing grid. It defines the functionality of individual components and its associated control blocks and the basic concept for designing and selection of the components of grid connected PV system. It also discusses some basic operation of the low voltage distribution network system.

Chapter 4 is dedicated to explain the modelling details of the grid connected PV system. The modelling methodology of the system is divided into five subsystems, for PV module, DC-DC boost converter, DC-AC inverter, the control system blocks and the low voltage grid modelling. The criteria for selection of the relevant subsystem, both internal and external controllers explained based on illustrating parameter definition methods. Finally, the PV system performance based on the external grid operation is presented.

Chapter 5 analyzes the steady state and dynamic impact of the PV integration under different scenarios (maximum load condition and minimum load condition) for different irradiance level.

Chapter 6&7 contents comparison of simulation results from the study with reference to the literature study and summary of the conclusion of this thesis work ending the report.

Chapter 8 contents some thought on the possible future work leading to more development regarding this work.

2 GRID CONNECTED PV SYSTEM CHARACTERISTICS, CHALLENGES AND TREND

This chapter presents a background of the solar irradiance data followed by a short description of the current installation trend of grid-connected PV systems in Sweden over the past years. It includes a study of Swedish regulatory framework and pertaining support measures in facilitation of PV integration in Sweden. The chapter also includes briefing of the challenges associated with grid-connected PV system based on studies that have been attempted in various parts of the world. Also, the literature study includes a brief overview of possible mitigation strategies for different such kind of issues.

2.1 Global solar irradiation in Sweden

Global irradiance or more specifically global horizontal irradiance (GHI) or global tilted irradiance (GTI) is the measured incident radiation power per unit area, and reported in units of Watt/square meter (W/m^2). By integrating over time it is the total radiation energy per unit area for a specified period, such as hours, days, months or years. This quantity is designated global irradiation and the monthly and annual values indicated are given in kWh/m^2 or Mega Joule (MJ/m^2) ($1 kWh/m^2 = 3.6 MJ/m^2$). Often, however, the term global radiation as a general expression is used for both global irradiance (GHI and GTI) and global irradiation. However, in this case it should be clearly indicated whether it is instantaneous or average values of GHI or if it is accumulated values (Skalík, et al., February 2016).

The total amount of solar radiation received by a horizontal (ground) surface is called the global diffused radiation from the rest of the sky and the ground i.e. scattered by atmospheric molecules and particles or reflected by clouds. The solar radiation therefore depends on the weather, on the position on the globe and the season of the year. Sweden has a lower solar radiation than in many countries farther to the south, since the maximum insolation angle is only 58 degrees in the far south. Average global solar radiation in Sweden was about but still received $980 kWh/m^2$ in 2014, which was a little bit less sunny year in Sweden compared with the record year of 2013 of $1000 kWh/m^2$ (IEA-PVPS, 2014).

2.2 Solar policy framework in Sweden

In Sweden, the integration of PV system comes ambit certain regulations. As per Electricity Act, renewable energy is not given priority dispatch. Every kind of electricity has guaranteed access to the electricity grid, and all electricity fed into the grid must be transmitted and distributed. Besides, there is no obligation to purchase electricity generated from renewable energy sources (RES). The main support scheme for RES-E is a quota system. A direct capital subsidy for installation of grid connected PV systems that have been active in Sweden since 2009. Self-consumption through net-metering is offered by some local utilities since 2014.

Additionally, a tradable green certificates scheme exists since 2003, but only around 12% of PV installations are using it so far, because of the insufficient level of support for PV installations. Another example is green certificates, which was introduced in Sweden in 2003. Production resources being classified as renewable then also produce a financial instrument, a green certificate, for each Mega Watthour (MWh) of production. The consumers are mandated to buy green certificates representing a specified share of their electricity consumption. The green certificates are traded on a market and the owners of renewable power plants get revenues also for the green certificates. Thereby they get an increased economic incentive to invest in renewable energy production

2.3 PV installation trend in Sweden

Historically, the Swedish PV market was majorly consisted of a small but stable off-grid market. This domestic off-grid market is still stable and is growing slightly. However, in the last seven years, more grid-connected capacity than off-grid capacity has been installed and as a result grid-connected PV largely outscores off-grid systems across the Europe. The grid-connected market is almost exclusively made up of roof mounted systems installed by private persons or companies. Now talking about in Sweden context, in 2012, and in the same way as in many European countries, the large increase of installed systems occurred within the segment of grid-connected systems. Around 18 Megawatt (MW) were installed in 2013. PV installation rate in Sweden during 2014 showed 100% increase over the installation rate during year 2013 (refer Figure 1) (Lindahl, 2014). A total of 36.2 Megawatt peak (MWp) were installed under 2014, which is almost twice as much as the 19.1 MWp installed under 2013. Historically, Sweden has a stable off-grid PV market, however in recent years, the market for grid-connected PV systems has grown rapidly with an installation of 35.1 MWp in total of 36.2 MW during the year 2014. Private persons and companies contributed to doubling the overall grid connected PV capacity in Sweden. The strong growth in recent years is attributed to falling system prices and a growing interest in PV in Sweden. The report (Lindahl, 2014) states that typical prices for a turnkey residential system has declined from an average of approximately 17 SEK/Wp (excluding VAT) in late 2013, to just over SEK 15/Wp by the end of 2014. For large commercial systems over 20 kWp the average price was about 13 SEK/Wp at the end of 2014. The explanatory reason for the system prices in Sweden have gone down is that the prices for modules and balance of system (BoS) equipment has dropped in the international market. Another reason is that the Swedish market is growing, providing the installation firms a steadier flow of orders and an opportunity to streamline the installation process, thus reduce both labor and the cost margins, and competitive market for business of PV system installation (ibid.).

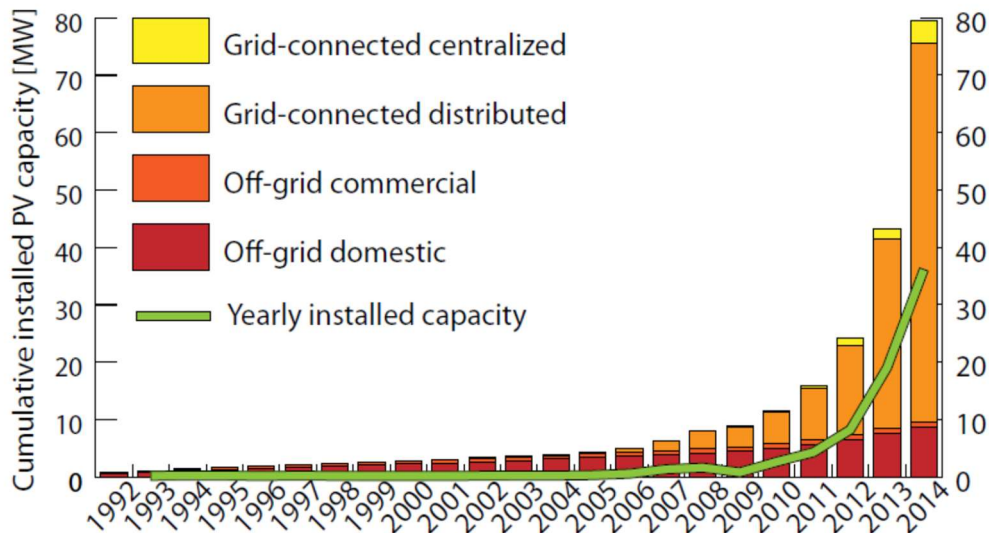


Figure 1: PV Installation Trend during past 12 years (Lindahl, 2014)

2.4 Power Quality Regulation Standard

As explained in the above sections, amongst many sources of RES, the PVDG installation are seeing an upward surge in recent years, with DSOs foreseeing this as a way to expand further, in future. The reason being the ever declining economy of PV system, improvement in PV technology and electronics over the years and support from various incentive schemes. Consequently, DSOs are facing with the challenges of maintaining the allowable levels as per regulatory standards. Some of these standards are the requirements to PQ at the delivery point, e.g. voltage limits: maintenance of the voltage at the point of delivery to each customer within an acceptable range, voltage fluctuations, interruptions and harmonics etc. (EN50160, 2004).

The highest penetration of PV system including production, installation and integration, has been established in Germany, Spain and Italy (Lindahl, 2014). Each of those countries has been following their own national grid codes. However, all European countries are recommended to satisfy the EU standards, EN 50160: Voltage characteristics of electricity supplied by public distribution systems.

As per Grid Code EN 50610 framework, attributes which define power quality include:

- Voltage regulation refers to the maintenance of the voltage at the point of delivery to each customer within an acceptable range.
- Flicker defines the repetitive and rapid changes of voltage, which has the effect of causing unacceptable variations in light output and other effects on power consumers and their equipment.
- Voltage imbalance referring to the grid voltage does not having identical voltage magnitude on each phase, and a 120 ° phase separation between each pair of phases.
- Harmonic distortion means the injection of currents having frequency components which are multiples of the fundamental frequency.

- Direct current injection— A situation which can cause saturation and heating of transformers and motors, and can also cause these passive devices to produce unacceptable harmonic currents.

As per Grid Code EN 50610, the following requirements are general:

- Voltage unbalance for three-phase inverters: max. 3%
- Voltage amplitude variations: max. $\pm 10\%$
- Frequency variations: max. $\pm 1\%$
- Voltage dips: duration $< 1s$, deep $< 60\%$

German grid code is found to be the most updated one. Hence it has been used as the reference code to satisfy the grid requirement in various studies. Previous to 2009, as per German grid code, PV generators were not being allowed to stay connected to the system during grid disturbances. They could not therefore participate in the system improvement during a fault condition. Today, due to the increasing penetration of PV systems, they have to meet required technical specifications such as Low Voltage Ride Through (LVRT) in order to ensure the stability of the system. By LVRT capability, one means that an electric system would remain connected to the grid in case of any temporary voltage drops or load changes. They should not only be able to stay connected to the grid during a disturbance, but also support the grid through reactive power injection during steady state condition contributing to voltage control and injection of short circuit current during a fault condition (VDE, 2011).

Also, it states that admissible voltage changes during normal operation, the magnitude of the voltage change caused by the generating plants must not exceed, in any point of common coupling, a value of 3% compared with the voltage when the generating plants were not connected. The preferred method to calculate the voltage changes is using complex load-flow calculations (ibid.).

2.5 Challenges of grid-connected PV system

The potential problem and challenges associated with PV integration can be broadly grouped into two categories: PQ issues such as: voltage rise, voltage fluctuation and flickering, voltage unbalancing, voltage instability, current harmonics, voltage harmonics, etc. or the issues affecting the normal operation of power system like load/frequency control, load following, desensitization or mal-functioning of protection equipment, overloading of cable and transformers, increase of losses of power lines, interaction with LTC, line voltage regulators or capacitor banks, etc. Various studies have been conducted to quantify the impacts of high PV deployment pertaining to above mentioned PQ issues. The impacts were segregated as per following categories.

2.5.1 Interference with Voltage regulation

A primary objective of distribution system design is to supply customers at a voltage which is within a prescribed range. Distribution system voltage regulation design is based on relatively predictable daily and seasonal changes in loading. In general, loading on the various sections of a feeder follow relatively similar patterns. Without PVDG, power flow is always unidirectional, and monotonically decreasing in real power (kW) magnitude with increasing distance from the substation. The distribution system feeder voltage profile is designed for decreasing over the network length. In the Swedish standard, the allowable voltage drop limit between two buses is 5%, if one of the bus is a household node, while for point of common coupling (PCC) node, it is 3% (Huang Yalin, June 2013). The addition of PVDG to a system, however, can radically shift power flow patterns and make them unpredictable. Depending on the spatial relationship of loads and PVDG, power flow can increase or decrease along a feeder. Net power flow can potentially reverse over a portion of the feeder, or even over the entire feeder if PVDG production exceeds the load present at that time. These load flow variations can make it difficult to maintain adequate voltage regulation. Also, the unconventional load flow patterns can cause distribution system voltage regulation devices, such as step voltage regulators, load tap-changers, and switched capacitor banks to respond inappropriately.

PV integration changes normal voltage profile due to export of excess PV power generated to the grid during the lower load demand and eventually causes the reverse power flow and overvoltage in the network (E. Liu, February 2008). Voltage regulation practice is based on radial power flows but reverse or bi-directional power flow interfere with the effectiveness of standard voltage regulation practice (NREL, August 2003), (Nadeeshani Jayasekara, 2010).

2.5.2 Overvoltage and Losses

The penetration level which is defined as the ratio of nameplate PV power rating (W_p) to the maximum load seen on the distribution feeder (Watt) is the widely used terminology defining scale of integration. The impacts on voltage rise is modest, when maximum PV penetration will be equal or less compared to the minimum load which was considered to be 25% of the maximum load on that specific feeder (Povslen, February 2002) . From the system point of view, there is more margin of feeding of PV power in to network, if the PV power penetrates from only a single LV line than from multiple LV lines connected to the same MV/LV transformer or even multiple MV/LV transformers. The most severe limit occurs in minimum load situations for any case, especially if the power system beforehand is operated to its design limits (Povslen, February 2002). PV with storage system fares better for maintaining voltage profile and in reducing voltage fluctuation (Mohammad T. Arif, October 2014). The impact and consequently threshold of penetration level depends on how sparsely PVDG and load are distributed on the feeder. For a feeder with uniformly distributed load and without fixed reactive compensation, if the DGs are lumped at the remote end of the feeder, the allowable level is about 15%. This issue of overvoltage is more significant when the DG is lumped at the end of the line, than when the DG is lumped at the beginning of the feeder. With DG distributed uniformly along the feeder, the line-rise overvoltage begins to be a significant issue when penetration exceeds 50% (NREL, August 2003). The level of losses in the system also is closely linked to the power flows and thus PVDG integration also impacts energy losses of the system.

The loss in the system shows an ‘U’ trajectory depending on the penetration level. Until certain penetration level losses in the system is reduced beyond which it increases (V́ctor H., May 2006).

The voltage rise problem between two buses are limited by the Swedish standards, which says that the maximum voltage variation at PCC after the connection of a distributed generator is maximum 3%. Therefore, the PV capacity is limited by: $V_{cp} \leq 1.03\% V$, where Where V is the voltage at the PCC before the connection of the PV system (Yalin Huang E. H., 2013).

2.5.3 Voltage unbalancing

Grid-connected PV systems can be attached to one or all three phases. For small-scale production, it is common with single-phase connected systems due to the price of the inverter. Feeding in current into only one phase can cause asymmetry in the grid if the attached amount of power is not equal for each phase. Voltage unbalance (VU) in the power system occurs when the magnitude of voltage among the three phases differs in amplitude or the phases deviate from each other from the normal 120-degree difference or both (P. Trichakis, 2006). As a general practice, the residential loads are equally distributed among the three phases of distribution feeders (Short, 2004). Uneven load distribution to different phases or uneven generation from single phase DGs can cause voltage unbalanced condition in the network (Mohammad T. Arif, October 2014). The rooftop PV installation by residential customers are mostly unplanned, random and not equally distributed among the phases. Combined together it creates the VU in the network. The probability of VU is more at the end of the feeder than to the beginning of nodes. Besides, the sensitivity of VU is also dependent on the characteristics of load of the phase in which the PV is installed, on the location and rating of the PVs. (Farhad Shahnian R. M., 2010). The devices such as distribution static compensator (DSTATCOM) and dynamic voltage restorer (DVR) as mitigation measure when connected to the feeder reduces VU and overvoltage issues to certain extent (Farhad Shahnian A. G., 2011).

As per EN 50160 standard, the following requirements pertaining to VU must be met by the DSOs:

- Voltage unbalance for three-phase inverters: max. 3%
- Voltage amplitude variations: max. $\pm 10\%$

2.5.4 Harmonic Distortion

Harmonic distortion is another major impact that has to be considered during the integration of PVDG systems (Rangy Sunny, December, 2013), (Mohammad T. Arif, October 2014). Harmonics are sinusoidal components of voltage or current signals with the frequency equal to an integer multiple of the fundamental frequency. The main source of harmonics currents in distribution system are non-linear loads. Harmonic currents translate into harmonic voltages through the grid impedance. The other potential cause of harmonics may be due to saturation of transformers caused by higher voltage during light load demand conditions or amplified by resonance in the utility network (Man, 2011). The harmonic voltage levels in LV

networks must be kept within the prescribed levels to ensure reliable operation of all the equipment connected in the network. The European network operators are abided as per the harmonic voltage limits specified in EN 50160. Distorted voltage and current in the distribution system can cause in undue effects in the network such as over-loading, over-voltages, mechanical stress in the network, unreliable operation of protection devices, and lowering the efficiency of appliances. The distortion affects also the end users fed through the PCC (Jaan Niitsoo, 2015). The major source of harmonics are the inverters with solid semiconductor switches used for conversion of DC to DC or DC to AC, injecting voltage harmonics and current harmonics to the system and thus result in power harmonics. The harmonic generation of a PV system is primarily dependent on the inverter technology, solar irradiance level, ambient temperature, load characteristics, and the supply system characteristics (Florentin Batrinu, May 2006).

As far as voltage distortion is concerned, the effect of the PV plant operation is insignificant compared to the harmonic distortion of the currents generated by the PV system (Florentin Batrinu, May 2006). The study (S.V. Swarna Kumary, 2014) showed that, both for at maximum PV generation as well as at minimum PV generation, the level of harmonics of voltage and current are high at far end feeder bus node as compared to bus node, near the distribution transformer. It can be described either as intrinsic or extrinsic effects. Intrinsic harmonic distortions are related to inverter technologies, e.g. component selection (switches) and control loop non-linearity, and limited pulse-width modulation (PWM) resolution. Connection to a weak and unbalanced electrical grid can be considered as an extrinsic effect on the output power of a PV system (Pedro A. B. Block, March 2014). While operating at low solar irradiance levels e.g. at the time of sunrise and sunset, during cloudy days, current total harmonic distortion (THD) values can increase significantly, as the THD factor is inversely proportional to the output active power of the PV system. However, THD significantly reduces with the increase in the active power output from the PV system and is least when the PV power output reaches its nominal value (Jaan Niitsoo, 2015). The THD is also less, when the PV is operates at a lower or minimum loading condition (Jaan Niitsoo, 2015). The different voltage control techniques produce different order of harmonics on the output voltage (Patil, November 2013). The standard EN50160 stipulates maximum THD level of 8% in the supply voltage. The higher the percentage, the more distortion in the voltage/current signal it creates (EN50160, 2004).

2.5.5 Voltage stability

Voltage stability is defined as the state of operation where in the all bus voltages in the grid are maintained at a steady acceptable level under normal operating conditions or under disturbances within the prescribed norm (EN50160, 2004). Voltage stability is achieved when the demand of reactive power in the network is met from the generations. The inverters without any voltage control regulation are responsible for keeping the power factor of the PV system at unity, which means that there will be no exchange of reactive power between the inverter and the grid. But in real scenario, most of the PV system consume or inject reactive power into the grid depending on the network and transformer losses, on the output active power from the PV and also the conversion technology. Withdrawal of reactive power by large scale PV system connected to a weak grid creates static voltage instability problem (Xu

Xiaoyan, April 2009). Furthermore, the uncertainty associated with PVDG, predominantly due to fast changing climatic conditions such as cloud covers or due to connection and disconnection of PV system causes fluctuation in the power output. This sudden change in the power output cause output voltage fluctuations and flicker at the end consumer point. This kind of phenomenon is referred to as voltage instability. As reported in (SANDIA Report, February 2008), voltage fluctuation caused by cloud transients was regarded to be smooth and slow and hence do not create serious voltage stability problems, with a note of caution that fluctuation might be a problem when PV penetration exceeds 20%.

2.6 Inverters' Reactive Power Support

The existing power network or grid is an integration of multiple stages of power transmission i.e. from generation to transmission, transmission to distribution and finally to the consumer. The grid had been designed to transmit electricity generated from large centralized power plant. The direction of current flow is from high voltage level to low voltage level due to resistance and inductance of the cable. The PVDG is mostly installed near to the load point and hence connected to the distribution network of the utility grid. When such distributed generation integration increases into the distribution side of the network, power flow direction gets altered. The most likely issues associated with high penetration of PV is the voltage regulation, because it is directly correlated to the amount of reverse power flow (NREL, February 2008).

The service entrance voltage at the consumer point is most important from the DSO perspective. Most utilities use LTC transformer to regulate the substation bus voltage. Distribution transformers are available with and without no-load taps (meaning the taps are to be changed without load) with standard taps of ± 2.5 and ± 5 . Utilities can use this feature to provide a fixed boost for customers on a circuit with low primary voltage (SANDIA Report, February 2008). Voltage control can also be achieved with devices such as voltage regulators and capacitor banks which have localized controls. These schemes work well for today's radial circuits but they do not handle circuit reconfigurations and voltage impacts of distributed generation well, resulting in limits on the ways in which circuits can be configured and imposing important limits on the penetration of PVDG.

Many inverters have the capability of providing reactive power to the grid in addition to the active power generated by their PV cells. The PV generators that are not equipped with a voltage controller, the connected bus voltage fluctuates during periods of large change in irradiance. These fluctuations become more significant with higher penetrations of PV generation. Voltage control using the PV inverter can help reduce the voltage fluctuations caused by the changes in irradiance and tends to make system more stable following a fault (Yun Tiam Tan, June 2007). Besides, if reactive compensation of PV inverters is allowed when grid voltage at the PCC becomes too low or too high, the voltage problem can effectively be solved.

The reactive characteristic of PV station can also be changed by control the power factor at the AC side of the inverter. However, it is at the cost of reducing the output power of the inverter.

Constant power factor control of the inverter may not resolve the voltage problem practically. The detailed control information of the power factor should be calculated by practical case. . Also, reactive power compensation can be done by changing the power factor at the AC side of inverter. But this method will cause over-voltage at some level of output. How to define the power factor of the inverter should be analyzed by practical projects. The ideal way is to control the power factor dynamically and to install flexible compensation device. If the PV station integrated to grid is controlled as a voltage source, i.e., the control aim is to maintain constant voltage output at AC side of the inverter, the inverter should generate certain reactive power to adjust its output voltage. Under voltage-mode control, the inverter could generate reactive power to keep the AC voltage of the inverter constant.

When the PV station is controlled as a current source, i.e., $\cos\phi = 1.0$, the absorbed reactive power is always kept as zero regardless of the output. However, in practical application, PV station would absorb some reactive power because of line and transformer loss. The detailed absorbed reactive power is related to the output of the PV station. For large output power, the PV station needs a lot of reactive power and voltage instability problem may occur. When the PV station is controlled as a current source, dynamic compensation at the lower side of the transformer could improve the voltage stability. When the PV station is controlled as a voltage source, the reactive power generated or absorbed by the inverter can be adjusted to maintain the voltage at the parallel point constant. But the regulation capability is related to the capacity of the inverter and its power factor range (Xu Xiaoyan, April 2009).

Currently most inverters used for PV generators are designed to operate at unity power factor. Reactive power is neither absorbed nor produced. If PV generation is implemented on a large-scale, there is a need to make better use of the PV plant to help with voltage control. However, inverters are capable of providing reactive power along with the active power. The apparent power rating (S) of the inverter can be resolved into components of P and Q given by equation (1):

$$S = \sqrt{P^2 + Q^2} \quad (1)$$

Depending on the inverter rating and the amount of DC power available at the input, the P-Q capability of the inverter can be determined as shown in Figure 2.

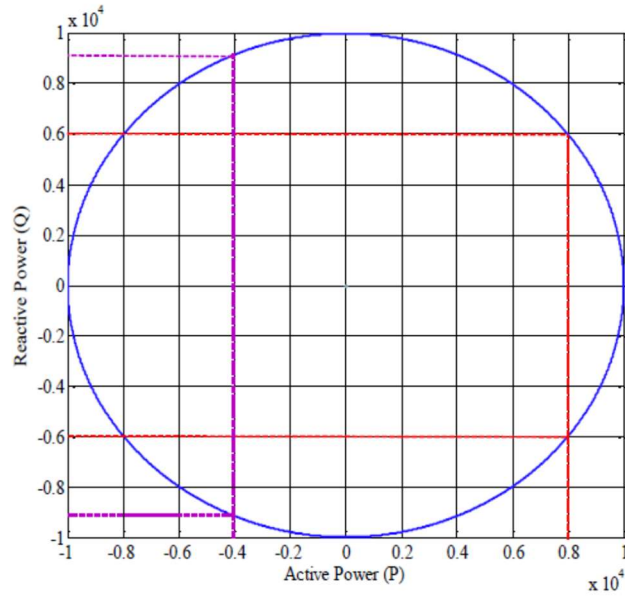


Figure 2: P-Q capability of 10 kVA Inverter (Ravi Bhatt, August 2011)

The P-Q capability is the ability of the PV system to provide active and reactive power instantaneously. An intelligent controller implemented here is responsible for generating/absorbing the maximum active power (P) and generating/absorbing the maximum reactive power (Q) that the system can handle. By means of proper switching, the inverter can be operated in a four-quadrant mode. One can refer Figure 2, that if, 8 kW is the amount of DC power available at the input (P_{in}), then by introducing the proper phase to the output current, the inverter can deliver 6 kVAR of leading or lagging reactive power. Similarly, for power output (P_{in}) of 4 kW i.e. when bridge is operating as active rectifier, it can deliver/absorb 9.16 kVAR. If the power at the dc bus (P_{in}) is equal to S, then the inverter loses its reactive power capability; on the other hand, if P_{in} is zero, then the inverter capacity can be dedicated to provide reactive power only. However, there are some losses associated with the inverter, and so, P_{in} cannot be zero. The proper inverter size can be selected in order to provide a specific amount of voltage regulation. The normal practice is to select an inverter with $S = P_{inmax}$ where P_{inmax} is the maximum active power that the inverter injects into the grid. Over-sizing the inverter just by 5% provide 32% additional capacity of reactive power as shown in the power triangle of Figure 3 (Ravi Bhatt, August 2011).

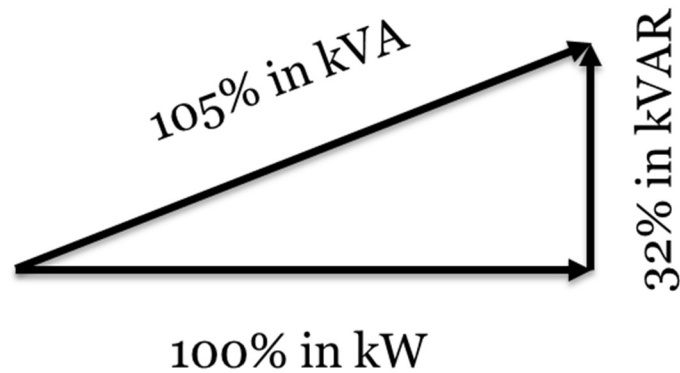


Figure 3: Effect of Inverter size on the reactive power capability

3 COMPONENTS OF GRID CONNECTED PV SYSTEM

This chapter includes literature study briefly defining various components involved in a grid-connected PV system. It includes description of the electrical characteristics PV module, presents a description of the components in a three-phase dual-stage PV system, and further discusses different algorithm and control system involved on the DC and AC side of the System. Understanding the dynamics of grid-connected PV system helps in understanding the impact on the grid system.

The output from PV module is DC and the utility grid operates in AC characterized by certain level of voltage and frequency. Often the output voltage from the PV Module is not sufficient to integrate it into the grid. Hence, connection of the PV Array to the utility grid is generally done through several intermediate levels. The conversion from DC to AC can be achieved either in single stage or dual stage (June Seok Lee, January 2013). PV system circuit topology with DC-DC converter is termed as dual stage. The building blocks of a typical PV system is shown in Figure 4. In the system, the DC output from PV system is passed through a DC-DC converter to boost up PV voltage to a level suitable to integrate to an inverter. The boosted DC voltage will interface the utility grid by means of DC-AC inverter, which is used for enforcing sinusoidal voltage waveform with matching phase frequency and voltage with that of grid. The system also contains controller which focus mainly on the DC and AC side operation of the PV system. A control mechanism is required in order to supply the desired amount of power to the grid from the PV system and to facilitate the operation of PV system at maximum efficiency.

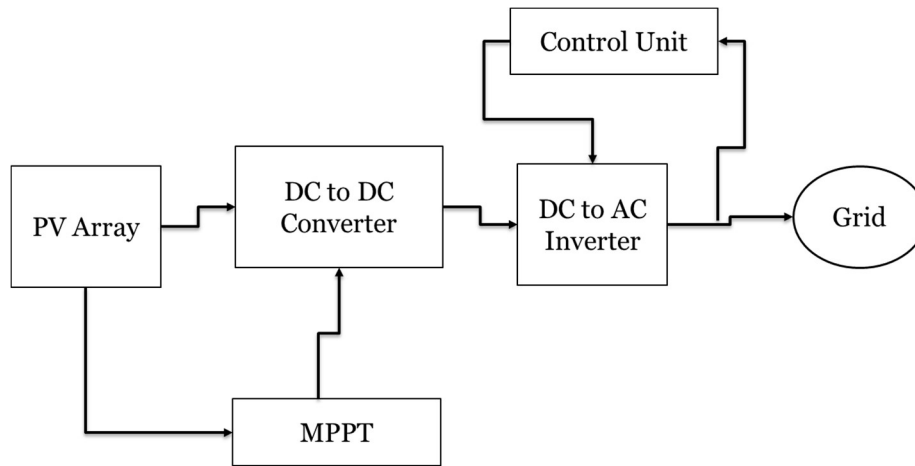


Figure 4: Grid-connected PV system blocks

3.1 Photovoltaic cell electrical characteristics

The basic unit of a photo-voltaic (PV) system is the PV cell, which are arranged in series to form the cell series string and putting together one or more of such strings forms the PV module. A PV cell is an electrical device that converts the electrical energy of light directly into electricity. When sunlight strikes the surface of a PV cell, the PV cell generates photo current, resulting in a flow of current when the PV cell is connected to an electrical load. The PV module if many put in series is called modules string, multi-folding the voltage times the number of modules in series. Such PV module string also referred as PV array, when connected in parallel, makes the current multifold (Tao Ma, 2014).

The performance of a PV module is mostly affected by PV cell configuration, irradiance, and module temperature. In order to predict the output power of the PV module it is important to understand the relationship between these effects and the power output. Short circuit current (I_{sc}), represents the maximum current flowing while the output terminals of the PV cells are short circuited. Higher levels of irradiance will cause more electrons to flow off the PV cells to the load attached hence, the short circuit current I_{sc} is directly proportional to the solar insolation (irradiation). However, the amount of voltage produced by the PV module is affected by the irradiance value, but the effect is very small. A typical PV module I-V curve representing the basic points such as short circuit current I_{sc} open circuit voltage V_{oc} , and the maximum power point (MPP) is presented in

Figure 5.

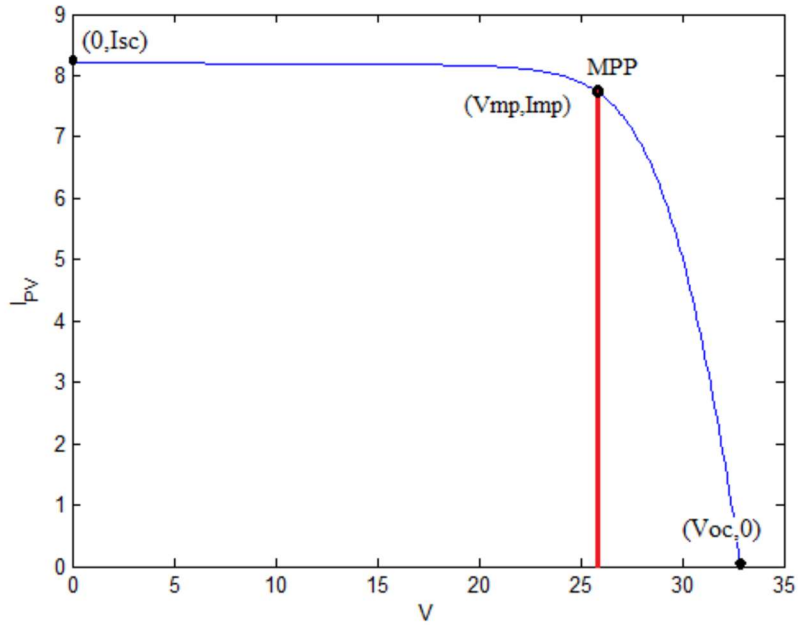


Figure 5: I-V characteristic for PV Module (Marcelo Gradella Villalva, May 2009)

Open circuit voltage V_{oc} , is the maximum voltage which provides the PV cell while its terminals are open circuited. The open circuit voltage is affected from the temperature variation which is inversely proportion to the temperature as shown in Figure 6. The voltage reduces with increase of the temperature, on the other hand the current increase with temperature, but only slightly, so the net result is a decrease in power and efficiency. (Marcelo Gradella Villalva, May 2009).

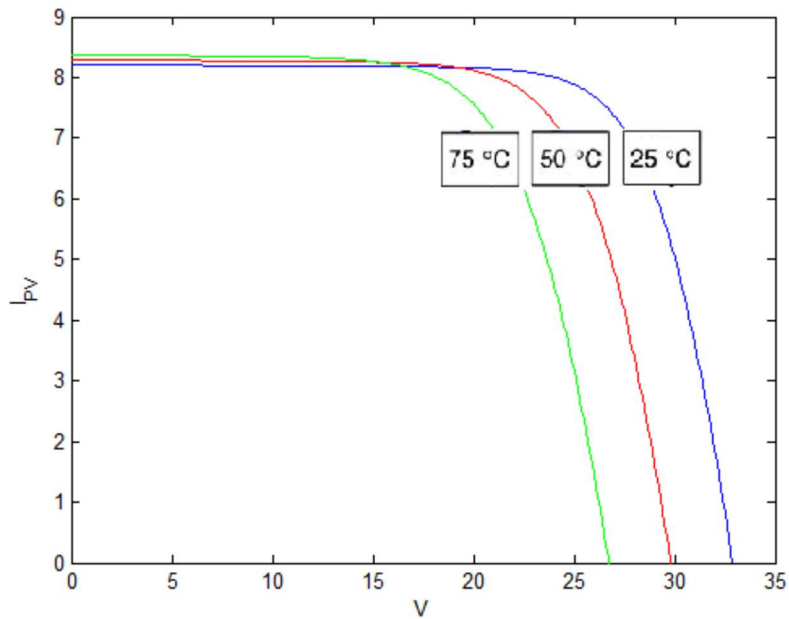


Figure 6: Temperature Dependence of Open Circuit Voltage (Marcelo Gradella Villalva, May 2009)

Maximum power point (MPP), is the point shown in the I-V curve where the PV cell is provided with the maximum possible electric power. The voltage of this point is called the maximum power voltage (V_{mp}) and the related current is the maximum power current (I_{mp}). The amount of maximum power is highly influenced by the level of irradiation as well as the ambient temperature of the PV. Maximum power point is one of the objective be achieved during the PV system operation.

Rated power output, is output of a PV under standard condition. Considering standard test condition (STC) categories of PV modules, standard condition is described for the following situation: $G= 1000 \text{ W/m}^2$, $T= (25\pm 2 \text{ }^\circ\text{C}$, $AM= 1.5 \text{ AM}$, where G is the vertical irradiance, T is the ambient temperature and AM indicates the air mass.

3.2 DC-DC converter and maximum power point tracking (MPPT) controller

The relation between V_{PV} , I_{PV} produced from PV module is highly non-linear and influenced by incident solar irradiation on the module and temperature of the cell. Hence, the combination of the current and voltage that maximizes the output power changes with the atmospheric parameters. Utilization of maximum power from PV Array needs some conversion device with functionality of tracking the maximum power point (MPP) for various operating conditions. The controller is either implemented in the DC-DC converter for a PV system with dual stage conversion or in the DC-AC inverter for a single stage conversion. A DC-DC converter is a static device which converts or transfers the DC power from one circuit to another from fixed voltage to variable and vice versa. DC-DC converter also helps in regulating the PV output voltage to the required level (Evju, June 2007).

There are a number of MPPT techniques. All of these methods require an algorithm to specify the location of the operating point with respect to the maximum power point (Tan, February 2004) (Yun Tiam Tan, June 2007). MPPT will ensure that, PV modules operate in such way maximum voltage, V_{mp} and maximum current, I_{mp} of the modules will be attained and produce maximum power P_{mp} . There are several techniques in the literature used in order to illustrate the function of MPPT. The artificial neural network (ANN), the fuzzy-logic, perturb and observe (P&O) and incremental conductance(IC) method are examples of different applied MPPT techniques. Among all proposed strategies, the P&O method is a widely used approach in MPPT because it is simple, it requires only measurements of V_{PV} and I_{PV} , and it can track the maximum power point quite accurately through variations in irradiance and temperature. As its name indicates, the P&O method works by perturbing V_{PV} and observing the impact of this change on the output power of the PV array.

Figure 7 **Error! Reference source not found.** is a flow chart of the P&O algorithm. At each cycle, V_{PV} and I_{PV} are measured to calculate $P_{PV}(k)$. The value of $P_{PV}(k)$ is compared to the value $P_{PV}(k - 1)$ calculated at the previous cycle. If the output power has increased, V_{PV} is adjusted further in the same direction as in the previous cycle. If the output power has decreased, V_{PV} is perturbed in the opposite direction as in the previous cycle. V_{PV} is thus

perturbed at every MPPT cycle. When the maximum power point is reached, V_{pv} oscillates around the optimal value $V_{pv,MPPT}$. This causes a power loss that increases with the step size of the perturbation. If this step width is large, the MPPT algorithm responds quickly to sudden changes in operating condition. On the other hand, if the step size is small the losses under stable or slowly changing conditions will be lower but the system will not be able to respond quickly to rapid changes in temperature or irradiance (Tan, February 2004).

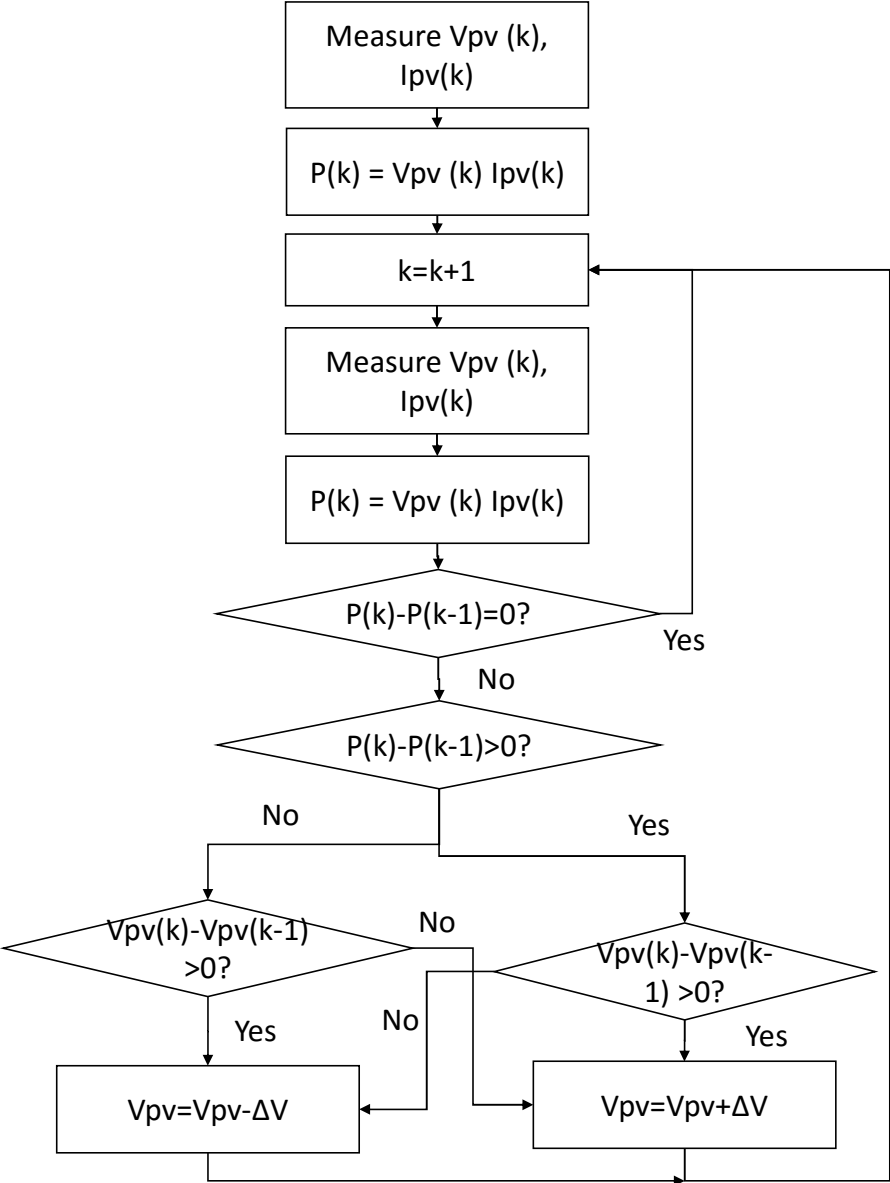


Figure 7: Flow Chart of P&O Algorithm

In dual stage inverters, the output from the DC-DC converter is a low ripple DC voltage, as the DC-DC converter handles MPPT, boosts the voltage level (if required) and output current regulation while the DC-AC inverter switches at the grid frequency to unfold the rectified sine wave (Evju, June 2007).

3.3 DC-AC inverter

The DC-AC inverter connects the PV array to the utility grid. Inverter acts as bridge to transfer the DC power that produces from PV system to the grid network which operates in AC. The technical requirement from inverters are to produce good-quality sine-wave output, and to follow the frequency and voltage of the grid. The topology of the inverter varies and it depends upon the output voltage level and power level of PV array and utility grid interconnection voltage (Massawe, June 2013). The primary topology consideration is whether or not to use a single stage or dual stage conversion.

Inverter technology is the key technology to have reliable and safety grid interconnection operation of PV system. To meet with these requirements, up to date technologies of power electronics are applied for PV inverters. Two main classes of DC-AC inverters are:

- Line commutated
- Self-commutated

Self-commutated inverters are of interest for this study. By means of high frequency switching of semiconductor devices with PWM technologies, high efficiency conversion with high power factor and low harmonic distortion power can be generated (Mohamed A. Eltawil, 2010). Most common of switchable power electronic components are design using insulated gate bipolar transistor (IGBT) or the metal oxide semiconductor field effect transistor (MOSFET). The choice of switch to be used is one of the challenges. The switching power devices possibly used in the inverter topology can be either IGBTs or MOSFETs. For high power applications and output voltage rating higher than 150V, the IGBT can be used as power device. In spite of its lower on-state voltage drop, higher power density and lower cost respect to the MOSFET, the IGBT has higher switching losses and limited switching frequency (Evju, June 2007).

Further, the grid-connected inverters for PV Array application are divided into the following categories:

- Current Source Inverter (CSI), or
- Voltage Source Inverter (VSI).

The VSI is fed from a DC-link capacitor which is connected in parallel with PV panels, whereas CSI, the inverter is fed from a large DC-link inductor. In VSI, the DC side is connected to the DC side of the PV module. In today's scenario, a voltage-source PWM converter is generally preferred over a current-source PWM converter. The main reason being the use of semiconductor switch IGBT, which is integrated with a free-wheeling diode, is more cost-effective in constructing the voltage source PWM converter than the current-source PWM converter. Another reason is that the DC capacitor which is indispensable for the voltage-source PWM inverter is more compact and less heavy than the DC inductor for the current-source PWM inverter (Hirofumi Akagi, 2007). Besides, VSI is the type of inverter where the independently controlled AC output is a voltage waveform. The output voltage waveform is unaffected by the load condition of the integrated network. For a dual stage PV inverter system, when voltage amplification from the PV arrays at the input capacitor is essential, then DC-AC

VSI handles both the output current regulation and DC bus voltage regulation (Massawe, June 2013). In these inverters the magnitude of the input DC voltage is essentially constant in magnitude and it is possible to control both the output voltage and frequency of the inverters (Yun Tiam Tan, June 2007).

A VSI is also capable of operating in all four quadrants. Theoretically, the voltage at PCC of a grid-connected VSI can be dynamically regulated by controlling the reactive power injected/absorbed by the VSI to/from the power grid. Therefore, the capability of a PV system that is integrated to the grid via a VSI to regulate the network voltage would enable the PV system to be utilized as a dynamic voltage regulator in the network at all times.

The controller strategies of DC-AC Inverter can be of two types voltage controlled type (VC) or current controlled type (CC). The VC is not appropriate for a grid connected inverter since the voltage on the PV output is generally dictated by the grid power condition. In this condition, the current controlled type are more suitable for DG application. CC inverter is used to inject a predetermined amount of current. Hence, with the effective value of the grid voltage being approximately constant, the PV system transfers a predetermined level of power to the grid (Evju, June 2007). MPPT can be implemented with CC PV inverters by monitoring both the PV output voltage and current, and maximizing the power by varying the amount of exported power (Amakye Dickson, May 2014.). A current controller has the advantage of being less susceptible to voltage phase shifts and to distortion in the grid voltage, thus it reduces the harmonic currents to a minimum, whereas, VC can result in overloading of the inverter due to small phase errors, and large harmonic currents may occur if the grid voltage is distorted (Evju, June 2007).

A significant factor while choosing for inverter components is the conversion efficiency. The key components involved for efficiency optimization are transistor devices, magnetic, and parasitic loads. The selection of switching frequency is another key factor and always a trade-off between switching losses, magnetic component costs, power quality, cooling system requirements, audible noise, and equipment size and weight. Another key design aspect for the inverters would be the performance of grid connected PV systems which is the power injected into the grid must meet utility power quality requirements. The primary trade-offs that drive power quality, are the transistor switching frequency used and the sizing of output filter components. Considering a fixed size of filter, higher switching frequencies result in better power quality as measured by THD, total demand distortion and the levels of individual harmonics. This is at the expense of higher switching losses. The size of filter components is designed as per the magnitude of the ripple current at the switching frequency. This ripple current decreases as the switching frequency increases (Evju, June 2007).

Another topology selection for the DC-AC inverter are as single-phase or three-phase. A single-phase inverter is mostly used in small residential grid-connected PV system with capacity up to approximately 5-6 kW, however, the use of a three-phase inverter has some advantages over single-phase inverter. In case of three-phase inverter, the power is distributed equally in all three phases unlike in single-phase inverters, hence, the three-phase inverter under balanced load conditions will have a constant instantaneous load power. This advantage remove the

need for capacitive storage elements under the balanced load conditions to meet the grid code requirement (Evju, June 2007).

3.4 Filter circuit

The power from the PV system to the grid is typically done through a DC-AC inverter which PWM modulated. Hence, the output from inverter is not purely sinewave, hence content harmonics. The said harmonics in the output voltage of the inverter is usually attenuated by connecting a filter between the inverter and the grid in order to cope with the power quality requirements of the utility. The filters can be of various designs as per the required degree of attenuation of the harmonic content.

A first order filter which consists of one inductor (L) in series with the mains is the most commonly used filter. This kind of filter is easy to make, and it has no resonance problems as higher order filters may have. The major drawback of first order filter is the huge size of the inductor needed to achieve a reasonable attenuation of the current harmonics. However, this kind of filter is found to be an efficient option when used with high frequency PWM converters.

Higher order filters with combinations of inductors and capacitors (LC/LLC/LCL), can solve the purpose of giving a better attenuation of the harmonics with a smaller size of the components, but it also makes the design complex. The most common higher order filters are the second order LC filter and the third order LCL filter. Among higher order filters, the LC filter is seldom used in grid connected systems, since the resonance frequency of the filter will vary with the inductance value of the grid. A correctly designed LCL filter give a better attenuation than a LC filter for the same size, better stability and cost performance and with lower grid harmonic stability (Erhan Demirok, 2009), (Evju, June 2007).

3.5 Instantaneous p-q theory, Clarke and Park transformation

The PV systems required to be interfacing to the utility grid through Power Condition System (PCS) with some controller scheme. Control of the PCS can be divided into two parts: controlling the DC-DC converter to extract maximum power from the array while boosting the terminal voltage, and controlling the DC-AC VSI to inject three-phase sinusoidal currents into the grid. The first stage of the PCS is a DC-DC boost converter responsible for extracting maximum power from the PV array and increasing its output voltage. The second stage of the PCS is a current controlled VSI that converts the DC power of the array into AC power and injected it into the grid.

The control technique relies on transforming the three-phase currents and voltages into a rotating or stationary reference frame and then regulates the resulting reference frame current components (Ahmed S. Khalifa, Sept. 2010). Hence, the control schemes for the built model will involve the use of transformations between the three-phase system and different two-phase systems. In order to avoid controlling three current/voltages separately,

transformations from a three-phase system to different two-phase systems has to be made. These are based on the fact that in a balanced three-phase system there are only two independent current/ voltages, thus the third current/voltage can be expressed by the other two. These systems are often referred to as reference frames, where the frame is the axis system of the transformed system.

3.5.1 Stationary reference frame (Clarke transform)

The p-q theory is based on set of instantaneous powers defined in the dime domain. The p-q theory first transforms voltages and currents from the abc to $\alpha\beta 0$ coordinates and then define the instantaneous power on these coordinates. The p-q theory uses the $\alpha\beta 0$ transformation, also known as the Clarke transformation. The Clarke transformations consists of a real matrix that transform the three phase voltages and currents into a two-phase system, or a transform into the 'stationary reference frame'. Both the three-phase and the two-phase system is said to be stationary, because the axes are locked in one position.

The transformation is made by applying the Clarke transformation in equation (2) where the three-phase quantities must be phase values. By inverting the coefficient matrix, the three-phase quantities can be found as a function of the two-phase quantities.

$$\begin{bmatrix} X_\alpha \\ X_\beta \\ X_0 \end{bmatrix} = \frac{2}{3} \begin{bmatrix} 1 & -\frac{1}{2} & -\frac{1}{2} \\ 0 & \frac{\sqrt{3}}{2} & -\frac{\sqrt{3}}{2} \\ \frac{1}{2} & \frac{1}{2} & \frac{1}{2} \end{bmatrix} \cdot \begin{bmatrix} X_a \\ X_b \\ X_c \end{bmatrix} \quad (2)$$

The transformation can also be defined as a change of coordinate system, from a three axis (phase) system to a two axis (phase) system as shown in Figure 8. It can be seen from the abc system that only two phases is needed to express the vector X_{abc} and thus it can be expressed in the $\alpha\beta$ system as the vector X_{ab} without any loss of information. In the figure, Figure 8, ω is the angular speed of the vector, and θ is the instantaneous angle of the vector. If X is the grid voltage, then ω represents the grid frequency, and θ represents the instantaneous phase angle.

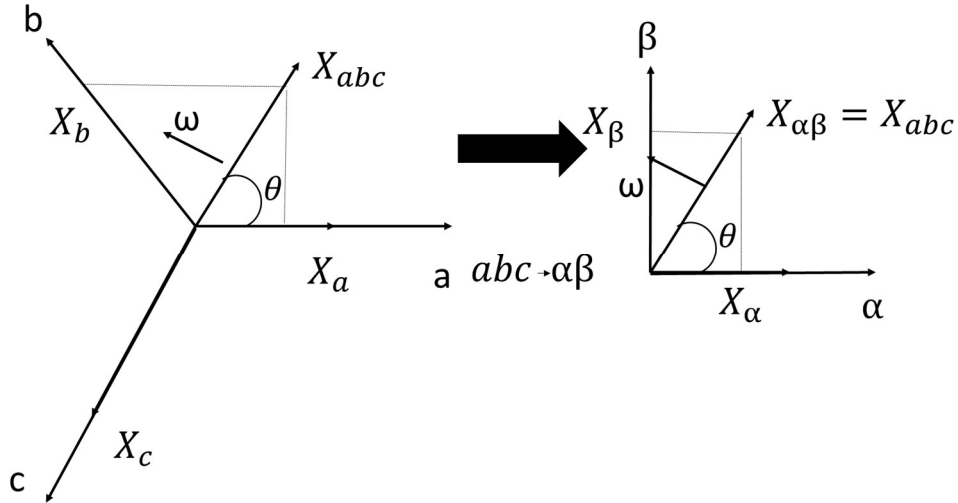


Figure 8: Transformation from abc to $\alpha\beta$ (Clarke Transformation) (Evju, June 2007)

Usually the three-phase quantities are assumed symmetrical, and thus the zero-sequence component can be ignored. With use of instantaneous power theory in the control scheme of inverter, makes it possible to control of real and reactive power (G. C. Pyo, 2008).

Voltage and current are given by equation (3):

$$v_a(t) = \sqrt{2}V \sin\omega t, i_a(t) = \sqrt{2}I \sin(\omega t - \phi) \quad (3 \text{Error! No sequence specified.})$$

From equation (2), the instantaneous power can be computed as by (4)

$$\begin{aligned} p_a(t) &= v_a * i_a = VI \cos\phi [1 - \cos 2\omega t] - VI \sin\phi \sin 2\omega t \\ &= P(1 - \cos 2\omega t) - Q \sin 2\omega t \end{aligned} \quad (4)$$

Then the current can be written as :

$$i_a(t) = \sqrt{2}I (\cos\phi \sin \omega t - \sin\phi \cos\omega t) \quad (5 \text{Error! No sequence specified.})$$

Then the current can be divided into two components as (6). One i_α is the component which is in-phase with the voltage $v_a(t)$, and the other i_β is the component which is perpendicular to $v_a(t)$. So

$$I = i_\alpha + i_\beta, i_\alpha = (\sqrt{2} \cos\phi) \sin \omega t, i_\beta = (\sqrt{2}I \sin\phi) \cos\omega t \quad (6 \text{Error! No sequence specified.})$$

Finally, instantaneous power is calculated and separated into two terms $p(t)$ and $q(t)$ as equation (7).

$$P_a(t) = v_a(i_\alpha + i_\beta) = v_a * i_\alpha + v_a * i_\beta = p(t) + q(t),$$

where $p(t) = v_a i_\alpha = VI \cos\phi (1 - \cos 2\omega t)$, $q(t) = v_a i_\beta = VI \sin\phi \sin 2\omega t$

**(7Error!
No
sequence
specified.)**

The first term $p(t)$ contributes to the power transfer, but the second term $q(t)$ reciprocates between the circuits, not transfers energy. $p(t)$ is called as the instantaneous real power and $q(t)$ is referred as the instantaneous imaginary power. The three-phase instantaneous power can be obtained as equation (8) where p the instantaneous real power is and p_0 is the instantaneous zero-sequence power.

$$P_{3\phi}(t) = v_a i_a + v_b i_b + v_c i_c = v_\alpha i_\alpha + v_\beta i_\beta + v_0 i_0$$

$$= p_\alpha + p_\beta + p_0 = p + p_0$$

**(8Error!
No
sequence
specified.)**

Stationary reference frame transformation conserves three-phase instantaneous power, right side and left side of equation (8) is equal. When there is no zero-sequence component the instantaneous active and reactive power is given by equation (9) and (10). The factor $3/2$ is introduced in order to have the power from all three phases.

$$P_{\alpha\beta} = \frac{3}{2}(V_\alpha I_\alpha + V_\beta I_\beta) \tag{9}$$

$$Q_{\alpha\beta} = \frac{3}{2}(V_\beta I_\alpha - V_\alpha I_\beta)$$

**(10Error!
No
sequence
specified.)**

3.5.2 Synchronous/Rotating reference frame (Park transform)

In this system the axis system is no longer locked, and rotates following an arbitrary vector, hence referred as “synchronous/rotating reference frame”. In grid connected inverters, it is most common to lock the axis system to a voltage or current (usually the grid voltage). In Figure 9, the d-axis is locked to the vector X_{ab} , and therefore $X_{ab} = X_d$ and $X_q = 0$. The axis system will then rotate with an angular speed of ω , and have an instantaneous angle of θ (referred to the stationary system).

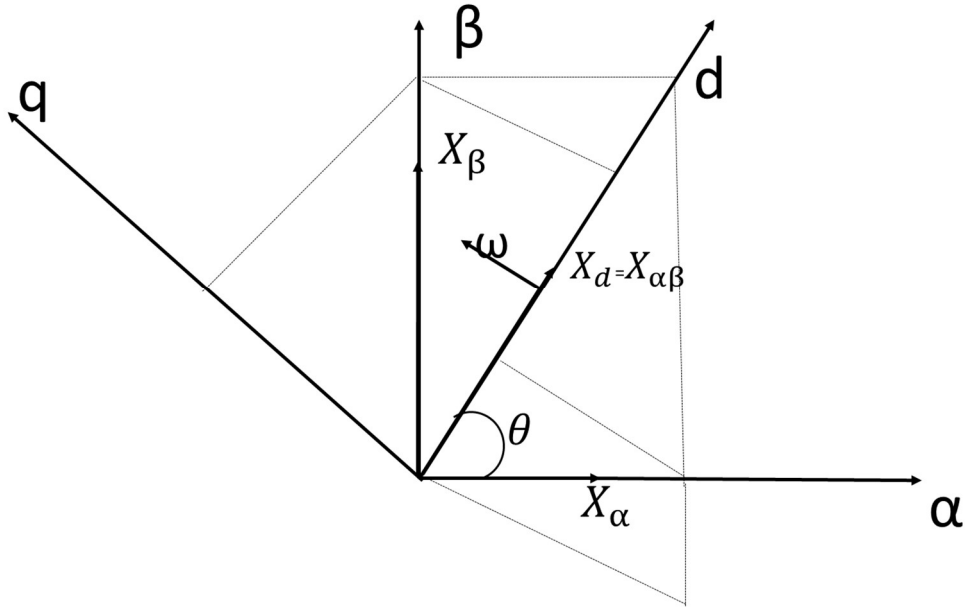


Figure 9: $\alpha\beta$ to dq transformation using Park transformation (Evju, June 2007)

Assuming the system is balanced; the dq transformation can be used to convert the three-phase currents injected by the inverter, into three constant DC components defined as the direct, quadrature and zero components: I_d , I_q and I_o respectively. The relation between the natural (abc) and the rotating frames ($dq0$) is given in equation (11) (Ahmed S. Khalifa, Sept. 2010).

$$\begin{bmatrix} I_d \\ I_q \\ I_o \end{bmatrix} = \sqrt{\frac{2}{3}} x T x \begin{bmatrix} I_a \\ I_b \\ I_c \end{bmatrix} \quad \text{(21Error! No sequence specified.)}$$

$$T = \begin{bmatrix} \cos(\omega t) & \cos(\omega t - 2\pi/3) & \cos(\omega t + 2\pi/3) \\ -\sin(\omega t) & \sin(\omega t - 2\pi/3) & \sin(\omega t + 2\pi/3) \\ \frac{1}{\sqrt{2}} & \frac{1}{\sqrt{2}} & \frac{1}{\sqrt{2}} \end{bmatrix}$$

Where T is the transformation matrix and ω is the frequency of rotation of the reference frame in rad/sec. Real and reactive powers injected by the inverter can be calculated in dq frame by using equation (12) and (13):

$$P = V_d I_d + V_q I_q \quad \text{(12Error! No sequence specified.)}$$

$$Q = V_q I_d + V_d I_q \quad \text{(13Error! No sequence specified.)}$$

Where, V_d , V_q are the dq voltages at the point of common coupling, I_d and I_q are the dq components of the injected current. A phase locked loop was used to lock on the grid frequency in such a way that V_q was set to zero. In that case, calculations of real and reactive powers were decoupled and simplified to equation (14):

$$P = V_d I_d, Q = V_d I_q \quad (14 \text{Error! No sequence specified.})$$

Which means that if the grid voltage is relatively constant, I_d and I_q can control real and reactive power injections from the PV array. In order to inject real power from the inverter, I_d was controlled to follow a specified reference signal I_{d_ref} (reference current extracted from the dynamics of the DC link capacitor). Reactive power injection is set to zero if the PV generator operates ta unity power factor and thus, $I_{q_ref} = 0$. A constant DC voltage across the capacitor meant that the power that went into it from the PV array matched the power going out to the inverter. The relationship is depicted as in equation (15):

$$\frac{d}{dt} V_{DC}^2 = \frac{2}{C} (P_{in} - P_{out}) \quad (15 \text{Error! No sequence specified.})$$

Where in V_{DC} is the DC link capacitor voltage. The input power P_{in} to the capacitor was controlled to be the maximum PV array output power by the DC-DC converter. It was the task of the inverter, however, to control the output power P_{out} from the capacitor to keep its voltage constant. A proportional integral (PI) controller is used to extract the reference current I_{d_ref} from the error mismatch between P_{in} and P_{out} . Having this information, the command voltages V_{d_com} and V_{q_com} for the inverter gates PWM can be obtained. The command voltages are transformed back to the natural abc frame where they will be used as the PWM modulating signals for the inverter. These signals are normalized with respect to the DC link voltage to have maximum amplitude of 1 V for comparison with a high frequency carrier signal (Ahmed S. Khalifa, Sept. 2010).

3.6 Grid synchronisation

The current delivered through the inverter to the grid has to be synchronized with the grid voltage and phase angle because of the following reasons:

- In order to deliver power at a power factor within the limits in the standards, or within limits given by the utility if there is need for reactive power compensation.
- Reduce the harmonic current content, by applying a “clean” reference current.
- Minimize the grid connection transients.

There are several methods for grid synchronization. Phase locked loop (PLL) synchronization method is one of them. A PLL is an electronic circuit with a voltage or current driven oscillator that is constantly adjusted to match in phase with the (and thus lock on) the frequency of an input signal. A PLL produces an output signal which synchronizes in phase and frequency with the input signal, using a negative feedback loop. The PLL controls the internal signal such that, the error in phase between input and output is kept to a minimum, and the frequency is equal

at input and output. A basic PLL circuit often consists of three components, a phase detector, a loop filter and a voltage controlled oscillator. The basic circuit is shown in Figure 10.

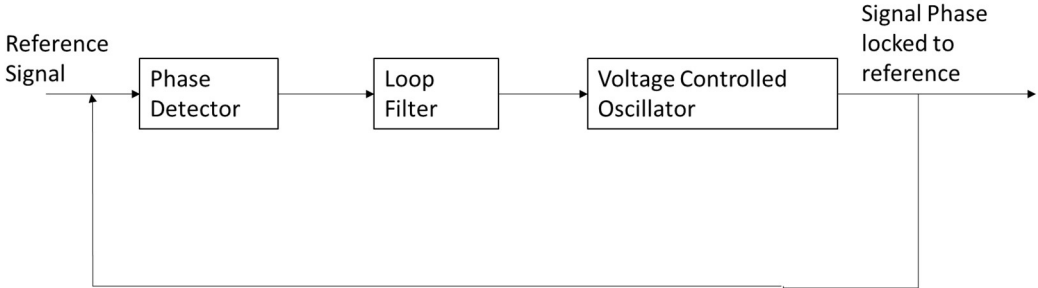


Figure 10: A basic circuit of PLL

The phase detector is implemented by transforming the voltages into the dq system. In this, the phase angle is detected by synchronizing the PLL rotating reference frame and the utility voltage vector. By using the phase locked angle in the dq transformation, the phase difference between the reference signal and the phase locked signal can be extracted by applying the arctangent function. This gives the exact phase difference. Also the phase difference can be indirectly found setting the direct axis reference voltage to zero results in the lock in off the PLL output on the phase angle of the utility voltage vector. The loop filter can be some sort of regulator, which brings the phase error to zero. This is usually a PI regulator, but also higher order regulators can be used. A higher order system increases the dynamics of the system and enhances the filtering capabilities, but it also increases the complexity. After the loop filter, which output is the frequency, a voltage controlled oscillator is applied. This is usually a simple integrator, which gives the phase locked angle as output. With the PLL no delays are introduced, so the phase locked angle will be in phase with the grid angle. A schematic model based on one presented in Figure 11, and shows the basic principle of a phase lock loop with its transformations of the three-phase voltages. In this loop the arctan2 function is applied as the phase detector, giving the exact phase difference. In addition, the instantaneous frequency and amplitude of the voltage vector are also determined. When the difference between grid phase angle and the inverter phase angle is reduced to zero ($\Delta\theta = 0$), the PLL became active (Stefania Conti, 2005), (Evju, June 2007).

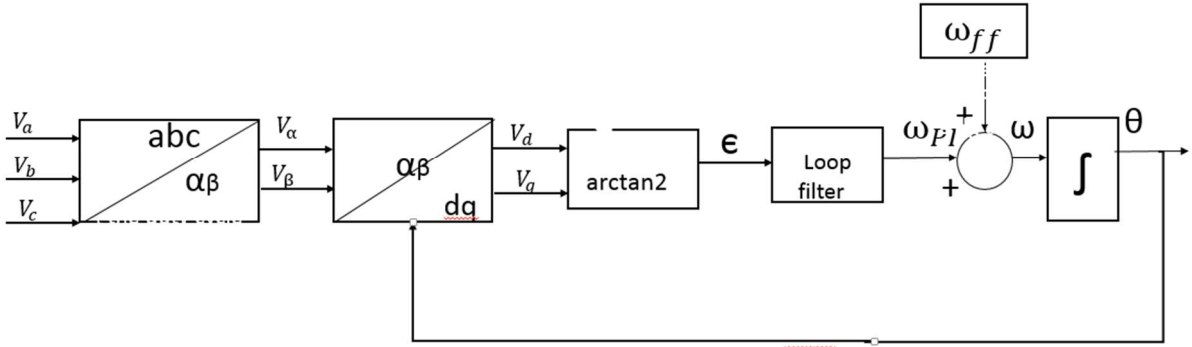


Figure 11: Schematic block diagram of PLL (Evju, June 2007)

3.7 Control strategies of the inverter power stage

The inverters convert the DC input to an AC output with the use of PWM switching techniques. There are several ways of implementing PWM in order to shape the output waveform of AC power output (voltage, current). Carrier-based PWM (CB-PWM) is the most common way to modulate the switching signal. In sinusoidal PWM, which is also a CB-PWM technique, three reference sinusoidal signals are compared to a triangular wave generating logical signals controlling the switches. In this modulation technique, there are multiple numbers of output pulses with different widths (regulated as per the duty cycle) per each half cycle. The width of each pulse varies in proportion to the amplitude of the sine wave evaluated at the center of each pulse. The gating signals are generated by comparing a sinusoidal reference signal with a high frequency triangular signal. The reference signal frequency is responsible in determining the frequency of the inverter output voltage (Evju, June 2007).

Modulation Index (M) is defined as ratio of amplitude of modulating waveform to amplitude of carrier waveform. The modulation index controls the amplitude of the output voltage. For $M < 1$, signifies that, PWM inverter is operating at under modulation condition and for $M > 1$, signifies that PWM inverter is operating at over modulation condition. Over modulation can lead to large AC magnitude voltage even with a poor spectral content in the voltage. Besides, over modulation condition also cause more harmonic contents in the output voltage. Hence, PWM inverter are designed to operate at under modulation condition. If it is operated at over modulation condition, then the relation between modulating wave and output voltage becomes non-linear (Evju, June 2007).

3.8 Voltage regulation, Load flow

Voltage profile is defined as the mathematical representation of the voltage level at a point, node or bus of an electric network. Voltage regulation is the act of maintaining the voltage profile at the customer's premises (also known as service voltage), or the load side of the point of common coupling (PCC) within the acceptable range. The service voltage is directly dependent on feeder voltage (when considered on the same voltage base) and is equal to the feeder voltage minus the voltage drop across the transformer and the feeder conductor. Loads require active and reactive power, and the related current that supplies the active and reactive power causes the voltage drop on feeder conductors (NREL, February 2008). Hence, voltage drop on the feeder is a consequence of current flow and the impedance (resistance and reactance) of the feeder conductor, transformer, and load. Voltage drop along the distribution feeder is inevitable and it is, in fact, required in order to move power from the substation to the customers. The voltage regulation practice applied to distribution systems is based on the radial power flow from the substation to the load.

As the operating condition of the network changes i.e. under low load, high load condition etc., it is important that the service voltage to be remained within a specified limit. Typically, two (boundary) operating conditions of the feeder are to be considered: feeder voltage should not drop below the minimum during peak load condition, and it should not exceed the maximum during light load condition. It is the responsibility of the transmission and distribution grid

operators to maintain the service voltage profile of the grid within acceptable limits. Even in times of system upgrades such as integration of new power generating units and operations, grid parameters must be maintained within stable operating conditions.

The concept of voltage profile and voltage drop of an electric grid can be derived and explained by considering a system shown in Figure 12, that has a short transmission line represented with impedance ($Z = R + jX$), sending end voltage (V_1), receiving end voltage (V_2), and connection of a load (P, Q) at the receiving end.

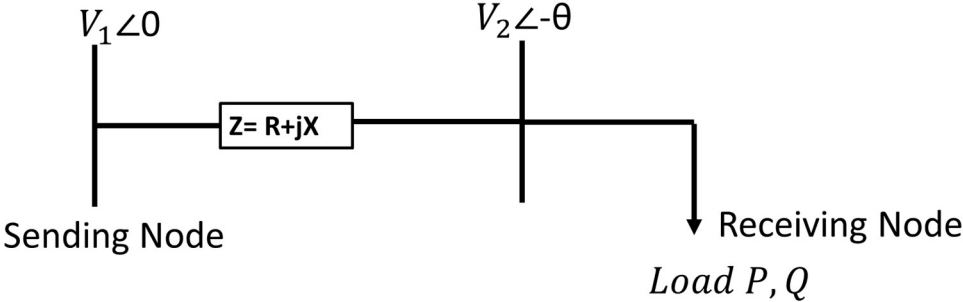


Figure 12: Representative Two Node Grid

The voltage relationship between point 1 and point 2 is described as in equation (16) :

$$\bar{V}_1 = \bar{V}_2 + IZ \tag{36}$$

Error! No sequence specified.

Where in, I is current flow from the sending end node to receiving end node of the network. Further, the voltage at receiving end node can be expressed as equation (17):

$$|V_2| = |V_1| - \left(\frac{RP + XQ}{|V_1|} \right) \tag{17}$$

The voltage drop ΔU is, which is a product of the line parameters (R and X), the load active and reactive power consumption at the receiving node. It is expressed as:

$$\Delta U = \frac{RP + XQ}{|V_1|} \tag{48}$$

Error! No sequence specified.

For a given grid with feeders at points A, B, C and D, and with feeder distances of a, b, c and d kilometers (kms) from the sending end node, the voltage profile is shown in Figure 13. The distances are in increasing order with feeder 'A' closer to the sending node with the distance 'a' and the feeder 'D' at farthest point a distance of 'd' kms from the sending end node. The figure shows feeder voltage profile at distances from the sending end voltage which is the desired voltage level of 1 p.u..

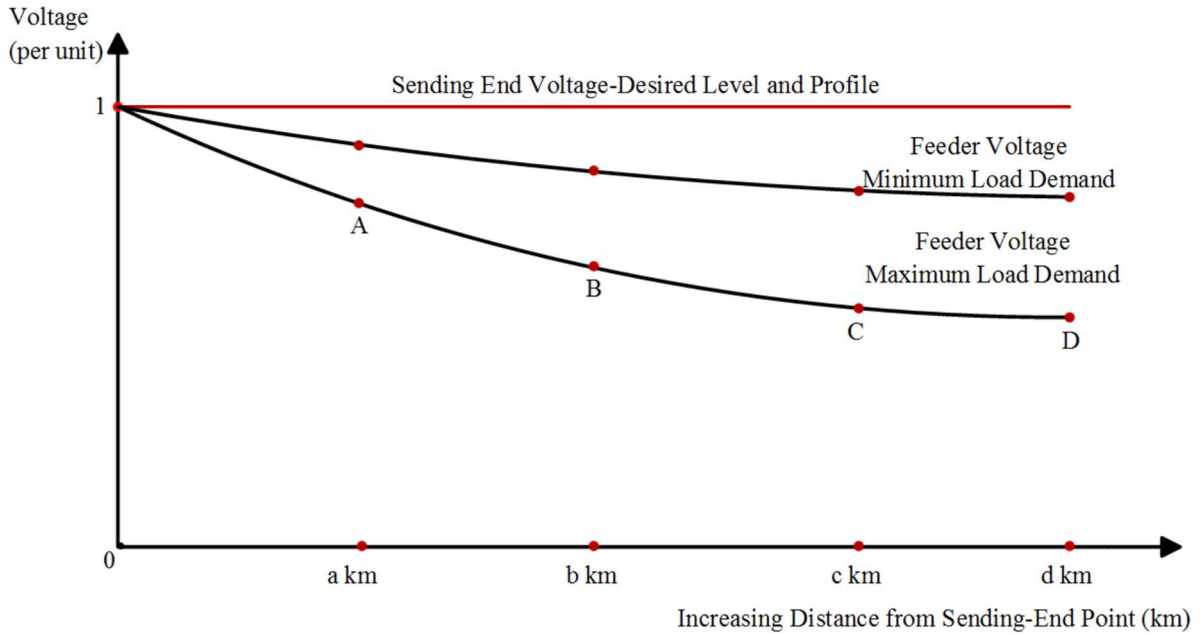


Figure 13: Voltage Profile along the feeder from sending end node to receiving end node (Mulenga, 2015)

The voltage level reduces with increase in the distance from the sending end voltage as shown in (Mulenga, 2015). This is due to an increase in line parameters (R and X) shown by equation (17) and (18) that causes the voltage level and profile to reduce. The active and reactive losses of the line can be expressed by equations (19) and (20).

$$P_{Loss} = |I|^2 R = \frac{P^2 + Q^2}{|V_2|^2} R \quad (59 \text{Error! No sequence specified.})$$

$$Q_{Loss} = |I|^2 X = \frac{P^2 + Q^2}{|V_2|^2} X \quad (20 \text{Error! No sequence specified.})$$

Here, from the two node system, it could be seen that power to enter at node 1 and leave node 2. With the help of a power flow study is power system electrical quantities is determined with some quantities known while others unknown. These quantities are voltage magnitude ($|V|$), voltage or load angle (δ), active power (P), reactive power (Q) and apparent power (S). During the process of power flow, line loadings, voltage drops and losses are also determined (Mulenga, 2015).

4 MODELLING OF GRID-CONNECTED PV SYSTEM AND THE DISTRIBUTION NETWORK

This chapter introduces modelling work for grid-connected PV system and the representative grid network. Grid connected PV system modelling is the foundation of studying operating

characteristics of PV system when connected to utility grid. The kind of PV system model used for the study is based on dual stage conversion topology. In the system, the PV generation have been modelled for an output I-V and P-V characteristics with varying temperature and solar irradiance. A DC-DC boost converter have been used to boost the DC output voltage from PV Array to a suitable voltage level to integrate it to a DC-AC inverter. Also, the DC-DC converter have been designed to track the maximum power point of PV module. The boosted DC voltage is modelled to interface the utility grid by means of a PWM based VSI. The output voltage wave shape of PWM inverter is square PWM wave. Therefore, a filter circuit have been used for coupling the inverter to the grid. The filter circuit does the functionality of converting PWM square wave to pure sine wave. The model also contains controller which focus mainly on the DC and AC side operation of the PV system. The outputs from the grid connected PV model both DC and AC under varying condition of temperature for irradiance are presented. From the grid side, the data pertaining to the steady state grid voltage level both for the high and load condition are presented from the simulation of load flow study. Models of both PV system and grids were built in Simulink/ Simscape Power Systems platform. Simscape Power Systems software allows the user to build powers system model by using the Simulink environment.

4.1 PV array modeling

The most important factor affecting the accuracy of PV system simulation is the modelling of the PV cell. A PV cell can be represented with an equivalent circuit comprising either one or two anti-parallel diodes (D) with an internal resistance (R_s) and shunt /parallel resistance (R_p). Such kind of representation of a PV system is called five-parameter (5-p) model. If the circuit have one diode is called one-diode model and if it has two parallel diodes named as two-diode model. Researches based on two-diode model found to be more accurate in predicting the behavior I-V curve of the real time, particularly at the time low irradiation and partial shading conditions hence a preferable choice in terms of accuracy, however, its computational requirement is much more demanding in comparison to one-diode five-parameter model (Kashif Ishaque Z. S., September 2011) .The one-diode five-parameter model is a well balanced between computational complexity and accuracy (Tao Ma, 2014). Based on the above theory, the one-diode model with five parameters is chosen for this study and the equivalent PV cell electrical circuits is presented in Figure 14.

The report (Kun Ding, December 2012) have been referred to, in order to extract parameters for getting the I-V, P-V curve for the PV module. The model used for the study is suitable to determining the electrical characteristics of PV- module from the given datasheet from the manufacturer and also suitable for obtaining maximum PV installation output power under condition of non-uniform irradiance. The proposed model is built using MATLAB/Simulink function from the mathematical equations of photo current and photovoltaic voltage as presented in the following equations (21) and (22).

$$I = I_{ph} - I_D - I_p = I_{ph} - I_o \left(e^{\frac{V+IR_s}{V_t}} - 1 \right) - \frac{V + IR_s}{R_p}$$

**(21Error!
No
sequence
specified.)**

Where I_{ph} is photocurrent (A)

I_D is current of parallel diode (A)

I_0 is the reverse saturation current of the diode (A)

V_t is diode thermal voltage (V) $= V_t = \frac{AkT}{q}$,

q is the electron charge (1.602×10^{-19} C),

A is the curve fitting factor, and

k is Boltzmann constant (1.38×10^{-23} J/K)

R_s is the series resistance

R_p is the parallel resistance

The series resistance (R_s) and parallel resistance (R_p) has the effect on the I-V characteristics of the PV system. The parallel resistance affects the output current and the series resistance affect the output voltage from the system (Tao Ma, 2014).

If the PV array are composed of several modules N_s connected in series and several strings N_p in parallel, the output current I_A and the output voltage V_A above can be modified as per equation (22):

$$I_A = N_p I_{ph} - N_p I_0 \left(e^{\frac{1}{V_t} \left(\frac{V_A + I_A R_s}{N_s} \right)} - 1 \right) - \frac{N_p}{R_p} \left(\frac{V_A + I_A R_s}{N_s} \right) \quad (22 \text{Error! No sequence specified.})$$

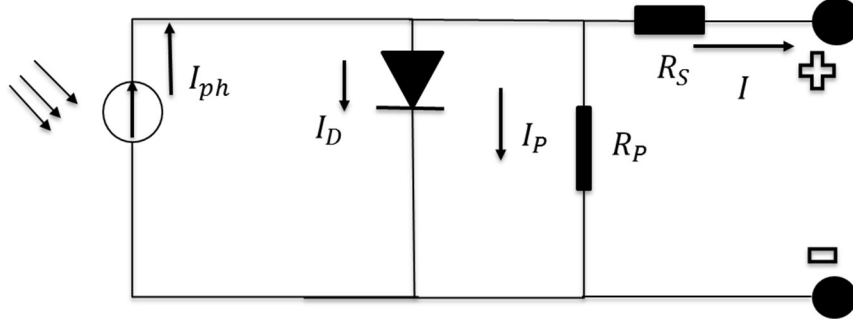


Figure 14: Five Parameter Single Diode Model

The simplification of the equation (22) under ideal operating condition gives equation (23) and equation (24) as presented:

$$I_{ref} = I_{SC,ref} \left(1 - k_{ref} \frac{V_{ref} + R_s I_{ref}}{V_{oc,ref}} - 1 \right) \quad (23)$$

$$k_{ref} = \frac{\left(\frac{V_{MPP,ref} + R_s I_{MPP,ref}}{V_{oc,ref}} - 1 \right)}{\sqrt{1 - \frac{I_{MPP,ref}}{I_{SC,ref}}}} \quad (24)$$

I_{ref} is the output current at STC.

$I_{SC,ref}$ is the short-circuit current at STC , given by the manufacturer.

V_{ref} is the output voltage under STC.

$V_{oc,ref}$ is the open-circuit voltage under STC, given by the manufacturer.

k_{ref} is the coefficient of I_{SC} and I_o under reference condition.

$V_{MPP,ref}$ is the output voltage at MPP under STC given by the manufacturer.

$I_{MPP,ref}$ is the output current at MPP under STC given by the manufacturer.

The PV module are rated for STC but does not operate under STC during normal conditions. Consequently, the performance of the PV module varies as per the actual operating conditions. The output voltage of the PV module V_{OC} decreases with the temperature. Therefore, the open-circuit voltage of the PV module has a negative temperature coefficient. Also, higher temperature results in larger photocurrent. Consequently, the output current of the PV module has a characteristic of positive temperature coefficient. The effect of changes of temperature and irradiance should be considered in the PV module model. To achieve I-V, P-V characteristics of a PV module in varying temperature and irradiance, the following mathematical expressions for correction of current and voltage are being used (Kun Ding, December 2012):

$$I_{SC} = I_{SC,ref} \left[1 + \alpha(T - T_{ref}) \right] \frac{S}{S_{ref}} \quad (25)$$

$$V_{OC} = V_{oc,ref} \left[1 + a \ln \frac{S}{S_{ref}} + \beta(T - T_{ref}) \right] \quad (26)$$

T is the temperature of PV module.

T_{ref} is the reference PV module temperature under STC .

α is the temperature coefficient of I_{SC} given by the manufacturer.

β is the temperature coefficient of V_{OC} given by the manufacturer.

S is the in-plane solar irradiance, S_{ref} is the reference irradiance under STC.

a is the irradiance correction factor of V_{OC} .

The translation equation of output current and voltage to the operating condition are (Kun Ding, December 2012):

$$I_{PV} = I_{ref} \frac{I_{sc}}{I_{SC,ref}} \quad (27)$$

$$V_{PV} = V_{ref} + (V_{OC} - V_{OC,ref}) + R_s(I_{ref} - I) \quad (28)$$

Where, I_{PV} is the current output from the PV Module at the operating condition.

V_{PV} is the voltage output from the PV Module at the operating condition.

The block diagram of the MATLAB/Simulink based PV Module model is shown in Figure 15. The

Figure 16 represents a subsystem of the PV Model.

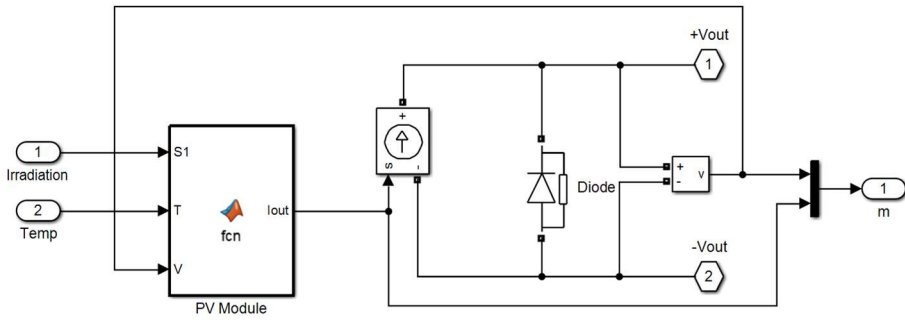


Figure 15: Block Diagram of the PV Model in Simulink

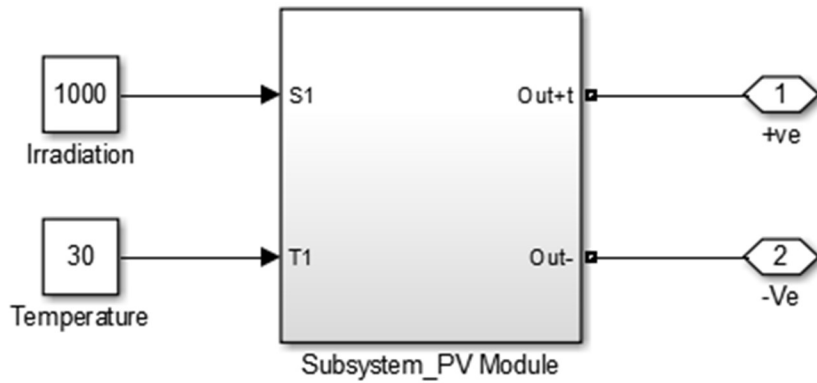


Figure 16: PV Model in Subsystem

The used manufacturer data for building the PV model is given in Table 1. The function script file containing the equation for the PV model is attached as Appendix A.

Table 1: Manufacturing Datasheet of PV Model

Electrical Characteristics of EGING 50 Watt		
Parameters	Variable	Value
Maximum Power	P_{max}	50 Watt
Open Circuit Voltage	V_{oc}	22 Volt
Short Circuit Current	I_{sc}	3 Amp
Voltage at P_{max}	V_{mpp}	17.98 Volt
Current at P_{max}	I_{mpp}	2.77 Amp
Temperature coefficient of I_{sc}	α	0.04%/°C
Temperature coefficient of V_{oc}	β	-0.33%/°C

Figure 17 and Figure 18 represents the simulation results of the characteristic I-V under varying condition of temperature and irradiance respectively. Figure 19 and Figure 20 represents the simulation results of the characteristic P-V under varying condition of temperature and irradiation respectively.

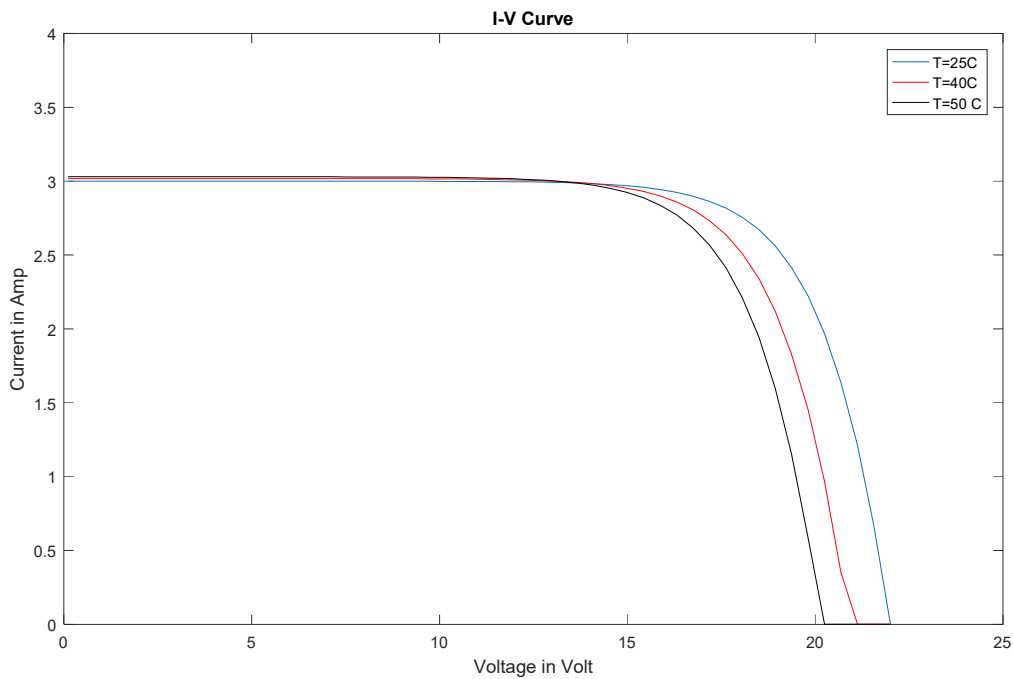


Figure 17: Characteristic I-V Curve under different Temperature

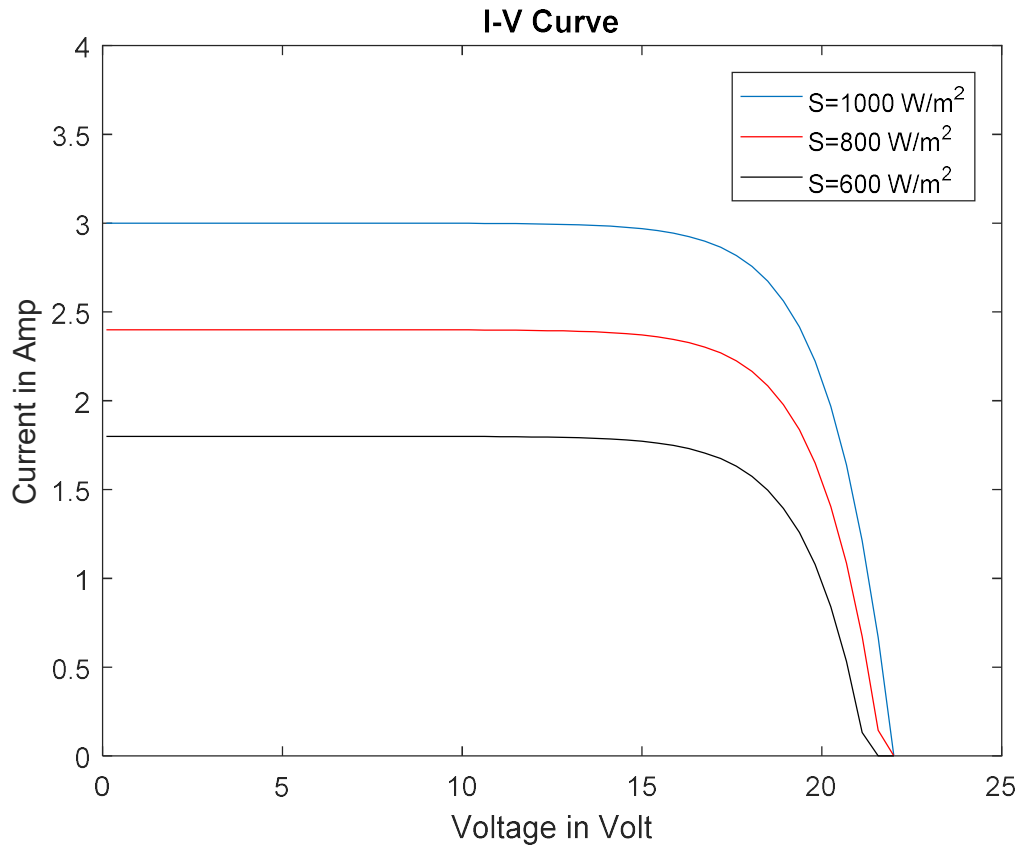


Figure 18: Characteristic I-V Curve under different Irradiation

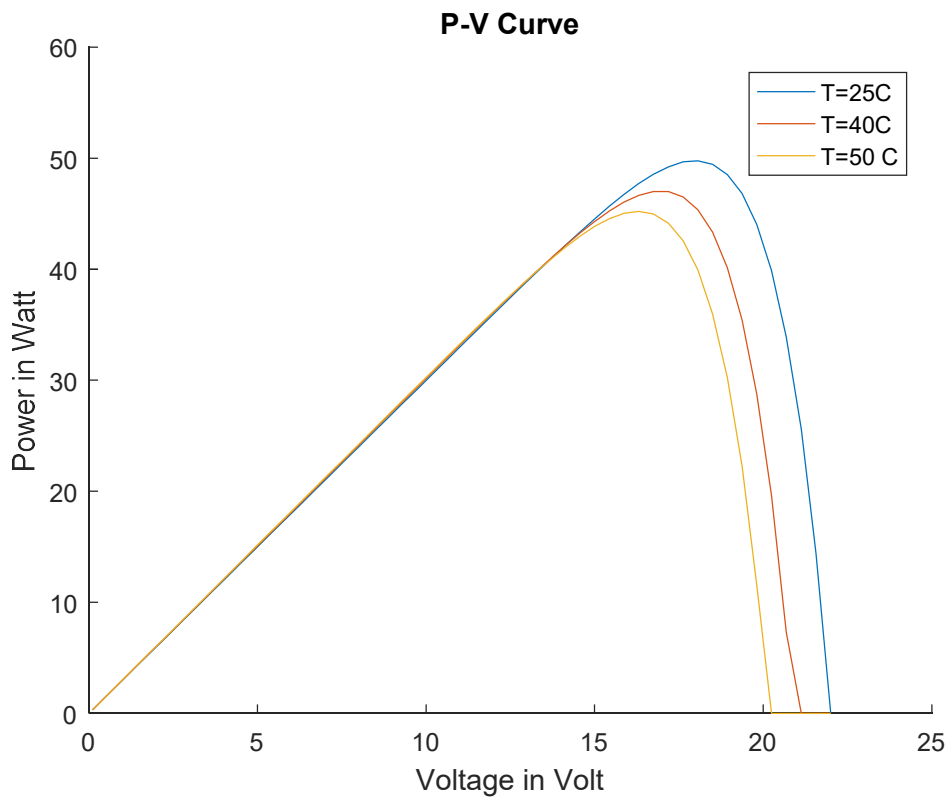


Figure 19: Characteristic P-V Curve under different Temperature

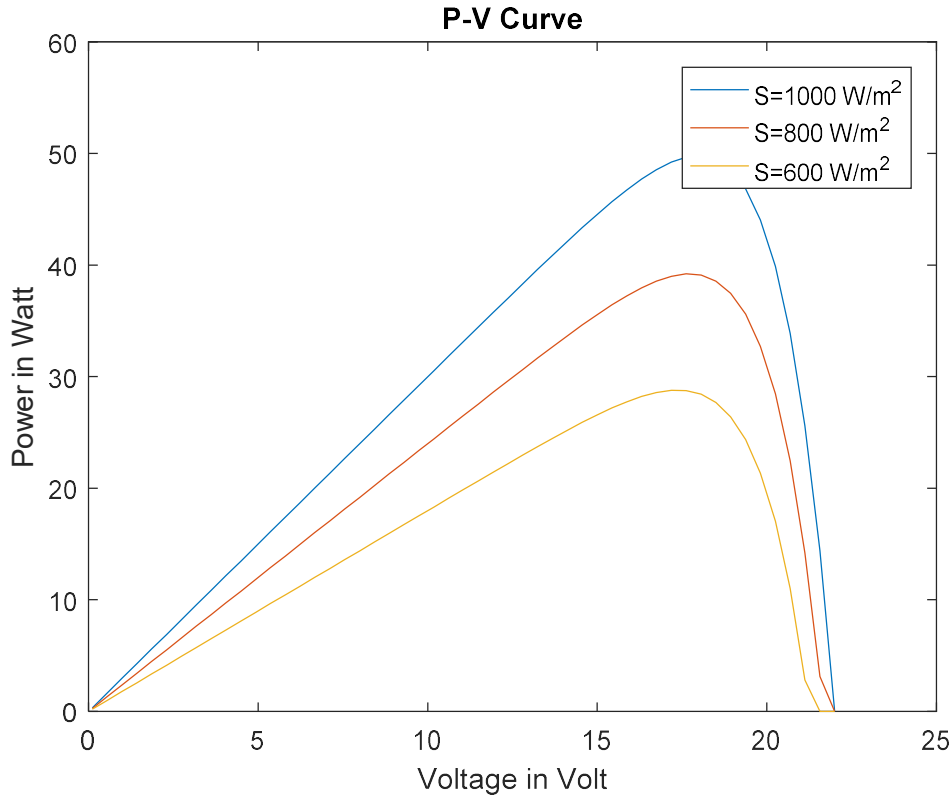


Figure 20: Characteristic P-V Curve under different Irradiation

4.2 DC-DC converter and MPPT control algorithm

The DC-DC boost converter was modeled to extract maximum power output from the PV array with a P & O algorithm. It also has been used to increase the terminal voltage. The gain from boost converter is directly proportional to the duty cycle (D) and relation is presented in equation (29) below:

$$\frac{V_{DC}}{V_{PV}} = \frac{1}{1 - D} \quad (29)$$

Where in V_{DC} is output DC-link voltage.

V_{PV} is the output DC voltage from the PV array.

The input voltage coming from PV panel changes with atmospheric conditions. Therefore, with the variation of duty cycle the maximum power point of PV module can be achieved (S.M.A.Faisal, 2011). The schematic diagram of the boost converter built using Simulink is presented in Figure 21.

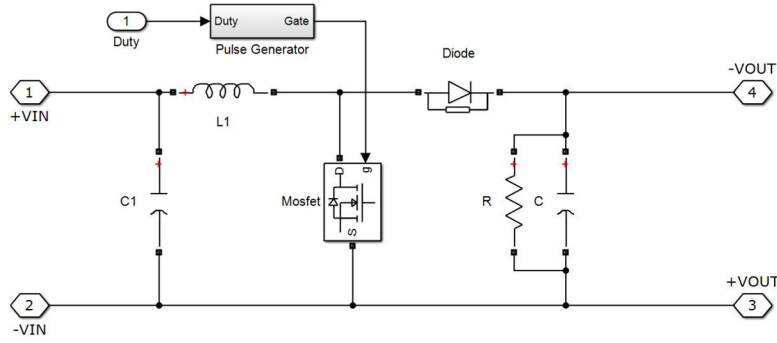


Figure 21: Schematic Diagram of Boost Converter

In the model, MOSFET switch has been used. When the MOSFET switch is ON, the current through the inductor increases and the inductor starts to store energy. When the MOSFET switch is closed, the energy stored in the inductor starts dissipating. The current from the voltage source and the inductor flows through the fly back Diode D to the load. The Voltage across the load is greater than the input voltage and is dependent on the rate of change of the inductor current. Thus the average voltage across the load is greater than the input voltage and is determined with help of the duty cycle of the gate pulse to the MOSFET switch (Williams K. Francis, December 2014). The controller for DC-DC converter, produces duty cycle which is dependent on PV module 's voltage and power. Value of duty cycle is then compared to a high frequency saw tooth wave signal, so that the comparator produces a PWM signal that is fed to MOSFET switch in the DC to DC converter. The duty ratio of the PWM signal depends on the value of duty cycle. Furthermore, the frequency of the PWM signal is the same as the frequency of the saw tooth waveform (Kun Ding, December 2012).

The used relation for choosing the parameters of boost converter components is as per below equations (M.D Singh, 2011):-

$$\text{Inductor, } L_1 \geq \frac{V_{DCM} * D_m * (1 - D_m)}{\Delta i F_{sw}} \quad (30)$$

$$\text{Input Capacitor, } C_1 \geq \frac{I_m * D_m^2}{0.02 * (1 - D_m) * V_{PVM} * F_{sw}} \quad (31)$$

$$\text{Output Capacitor, } C \geq \frac{I_m * D_m}{\Delta v * F_{sw}} \quad (32)$$

F_{sw} = switching frequency,

Δv = ripple voltage for capacitor,

I_m = output current at maximum output power,

D_m = duty cycle at maximum input power,

Δi = ripple current for inductor,

V_{PVM} = input voltage at maximum power point,

V_{DCM} = maximum of output voltage.

Three numbers of modelled PV Module is placed in series, with varying input solar irradiation and temperature. The simulation schematic is presented in Figure 22. MPPT algorithm is inserted into the MTTLAB embedded block to form the MPPT block. The outputs (i.e. the current and voltage terminals) of the PV module are fed into the MATLAB embedded block while the output of the MPPT is routed to the MOSFET of the DC-DC boost converter. The MATLAB m-script file used for P&O algorithm has been attached as in Appendix B.

The design parameters of boost inductor are presented in Table 2. The controller would allow to change the output of PV Array with a smaller step in each control cycle. The controller sense both voltage and current output from the PV array, and compare the output power from the previous cycle. If the output power will be increased, ‘perturbation’ will continue to work in the same direction, else in the changed direction.

The control parameters for MPPT algorithm are as follows:

- the initial duty of pulse width modulation is 0.5 (as per the equation (29))
- ΔD is 0.01 and the duty step in perturb and observe is .02 and the control period is 50 μ s.

The Figure 23 show the results from some of the simulation results studies.

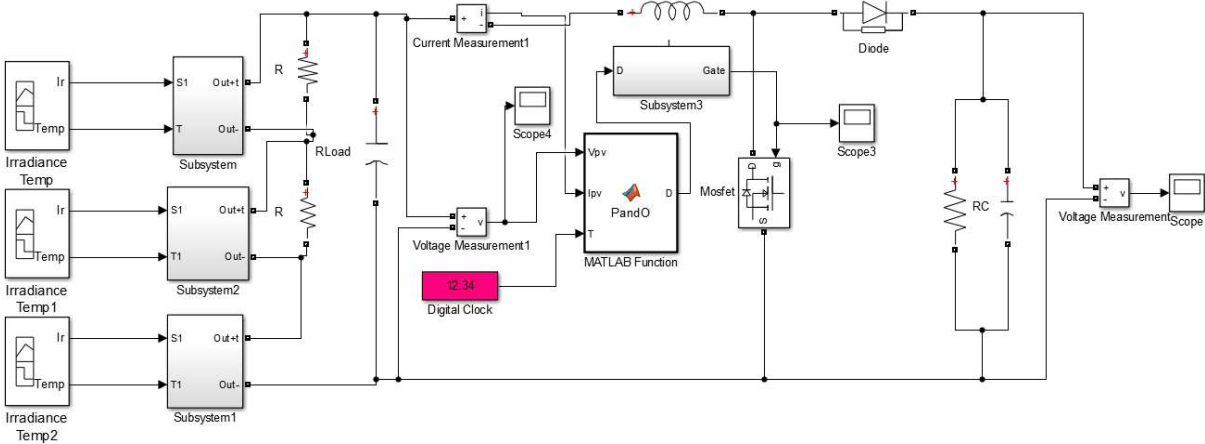


Figure 22: Simulation schematic of boost topology

Table 2: Design parameter for Boost converter

Design parameter for Boost Converter		
	Parameter	Value
Input capacitor	C_1	1.7 mH
Input inductor	L_1	10 μ F
DC-link capacitor	C	470 μ F
Load	R	86 Ω
Switching frequency	f_s	10 kHz
Voltage input	V_{DCM}	54 Volt
Voltage output	V_O	104 Volt

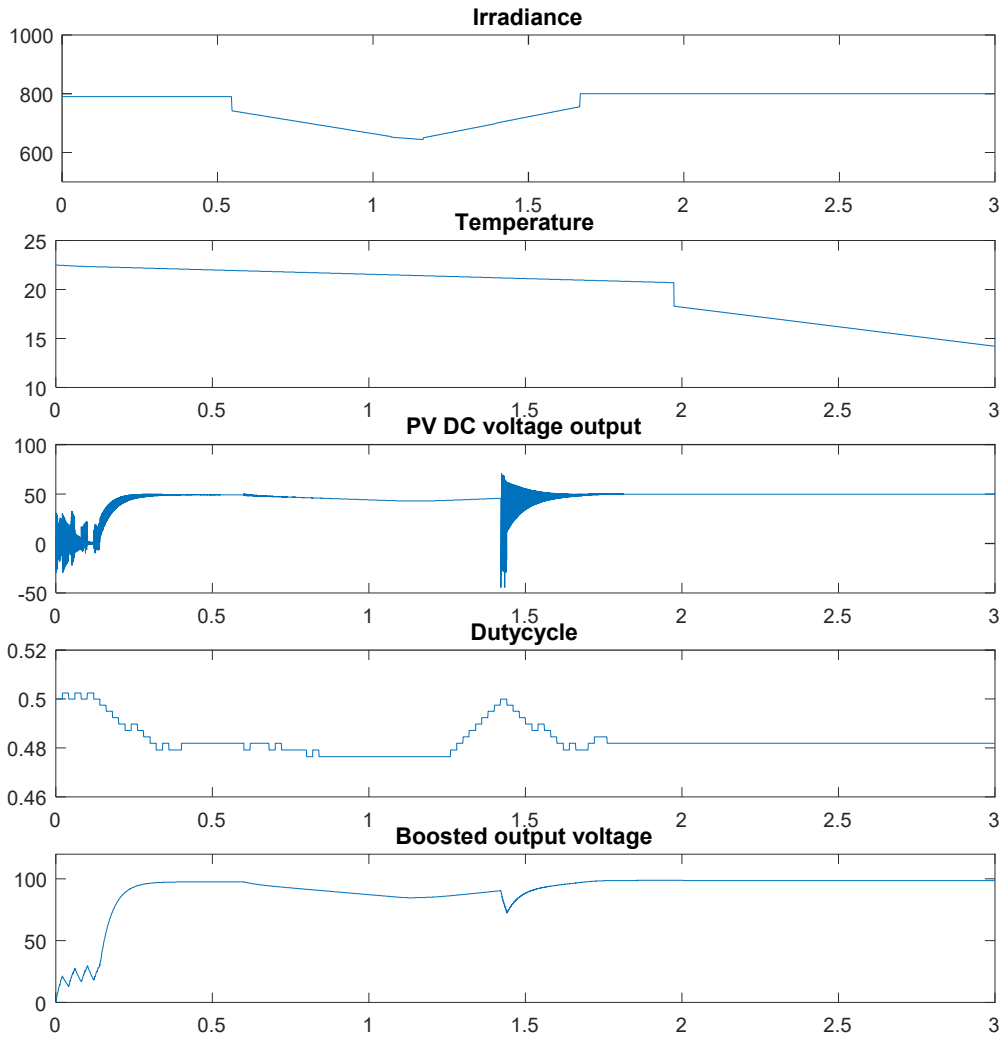


Figure 23: Simulation Results of the boost converter with control algorithm

The change in the duty cycle adjusted with every control period by the MPPT controller to extract the maximum power from the module is shown with time (t) Seconds in Figure 23. It can be observed that, there is a ripple at the PV array output voltage at 1.5s of the simulation,

due to change in irradiance level, which could be smoothened by changing duty cycle of the boost converter operation with functioning of MPPT algorithm. Also, it shows that the voltage at load is boosted from output voltage from PV module.

4.3 DC-AC inverter and control system

For satisfactory operation of the inverter and to obtain an undistorted current waveform, a minimum DC-link voltage is needed to be maintained at. Also, in order to have full control of the inverter operation, it is important that, the six diodes of the inverter switches must be polarized negatively at all value of ac-voltage supply. Hence, to keep the diodes blocked, a higher DC-link voltage than the peak DC voltage generated by the diodes is needed. Theoretically for diode inverter, the maximum DC output voltage is the peak value of line-to-line RMS voltage (Sanjuan, 2010). Hence, the DC-link voltage V_{DCmin} should be greater than the peak line-to-line RMS voltage $\sqrt{2}V_{LL(rms)}$ represented in equation (33).

$$V_{DCmin} > \sqrt{2}V_{LL(rms)} = \sqrt{2}\sqrt{3}V_{LN(rms)} \quad (33)$$

Further, it is a common practice to oversize the DC-link capacitor for about 15-20% to take care of the DC-link capacitor ripple voltage (Sanjuan, 2010). Thus, taking into consideration of above criterion, if the output AC voltage of the inverter is specified for 400 V line to line (r.m.s.), the estimated DC-link voltage would be approximately 680 V.

A Simulink/ Simscape Power Systems library block 'Universal Bridge' is used in the model for representing the three level bridge VSI. The chosen semiconductor switches are IGBT. The inverter takes the V_{DC} as voltage input, while 12 gate pulses are generated (from the controller) to provide three-phase sinusoidal voltage.

The control system of the AC side operation of the inverter measure three-phase sinusoidal voltage and current from the PCC (the point which PV System is integrated to the utility grid). Later this three-phase voltage and current are converted into rotating dq-frame. DC voltage and DC current are taken as input to the MPPT control which gives the d-axis reference current i_{d_ref} . An inner current controller compares the reference grid currents i_{d_ref}, i_{q_ref} with the dq frame component of the actual grid currents i_{d_meas}, i_{q_meas} . These comparisons provide modulating switching signals which are further converted to gate pulse signals to the PV inverter using the PWM generator.

The three phase sinusoidal signals at the AC side of PV inverter are varied with time at the grid frequency ω_o and so as the dq frame variable. The control signals for operation of the inverter need to be time invariant. Therefore, by using a PLL, the angular velocity of dq frame variable is matched with the grid angular frequency. Then, the control variable becomes synchronized with the grid and can be used for control actions (Farhan Mahmood, May , 2014).

DC-link voltage control is realized by simply measuring the DC voltage V_{dc_meas} from the DC-link and compared it with a DC voltage reference V_{dc_ref} . The DC voltage reference is given as a constant value of 680 V. The error is fed to the PI Controller that regulates V_{DC} such that actual DC voltage should follow the reference DC voltage. The yield error is passed through the PI block from the Simulink/ Simscape Power Systems library with the proportional K_{p_VDCreg} and integral gain K_{i_VDCreg} to yield the i_{d_ref} . The i_{q_ref} is set to zero to operate the PV system at unity power factor. The schematic block diagram is shown in Figure 24.

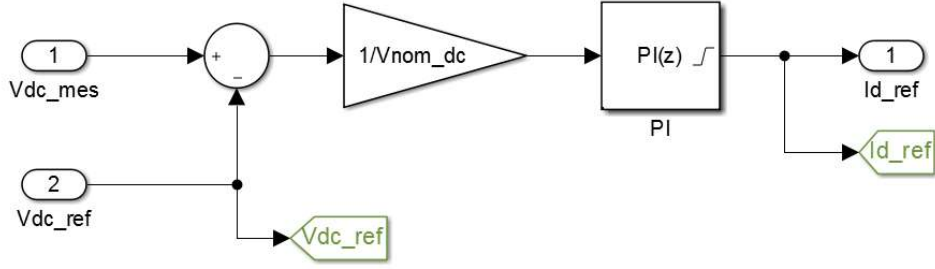


Figure 24: Schematic block Diagram of Voltage Controller

Current control scheme is implemented to ensure that i_{d_meas}, i_{q_meas} follow their references i_{d_ref}, i_{q_ref} . The i_{d_ref} generated by the DC voltage controller, while i_{q_ref} is set at zero. The control inputs $e_d = i_{d_ref} - i_{d_meas}$ and $e_q = i_{q_ref} - i_{q_meas}$ given to the respective compensators controller K_{p_Ireg} and integral gain K_{i_Ireg} with which finally give the modulating signals for feeding to the PWM control.

The terminal voltage of the inverter is controllable through PWM modulation. Hence, by controlling these modulating signals the output voltage can be controlled. Therefore, modulating signals m_d, m_q in the dq reference frame are converted back to the abc reference frame as m_a, m_b and m_c which correspond to the three phase sinusoidal voltage reference signals (V_a, V_b and V_c). Three-phase reference signals (V_{abc}) are compared with a triangular carrier signal using a pulse width modulation scheme to provide the final gate pulse control signals to the inverter.

The simulation step is carried by integrating a 15 kW PV system model into a basic distribution grid. PV array consists of around 50 numbers of PV modules with configuration of 5 PV modules connected in series to form a single string and 10 strings connected in parallel. The maximum voltage (V_{MP}), and maximum current (I_{MP}) each PV module is considered as 54.7V and 5.58 A respectively. The PV array is connected to a low voltage AC bus at 400 V. Then a step up transformer boosts the low voltage of a medium voltage of 11 kV. The transformer is connected an infinite source grid via a feeder with a length of 1 km. The grid is having active load of 400 kW and reactive load of 100 kVAR.

Table 3: Design parameter for 15 kW aggregate model

Design Parameter for detailed 15 kW PV Model		
	Parameter	Value
Input capacitor	L_1	10 mH
Input inductor	C_1	100 μ F
DC-link capacitor	C	2000 μ F
Switching frequency	f_s	1.5 kHz
Voltage output	V_{PV}	274 Volt
DC-link voltage	V_{DC}	680 Volt
Power output	W_P	15 kW
Filter	L	5 mH
Grid AC voltage (line to line)	$V_{LL (r.ms.)}$	400 Volt

The Figure 25 shows the DC output from the 15 kW PV Array under varying condition of the irradiance and temperature. It can be seen that the duty cycle of MPPT controller changes in order to keep the output voltage of the PV array at maximum operating point.

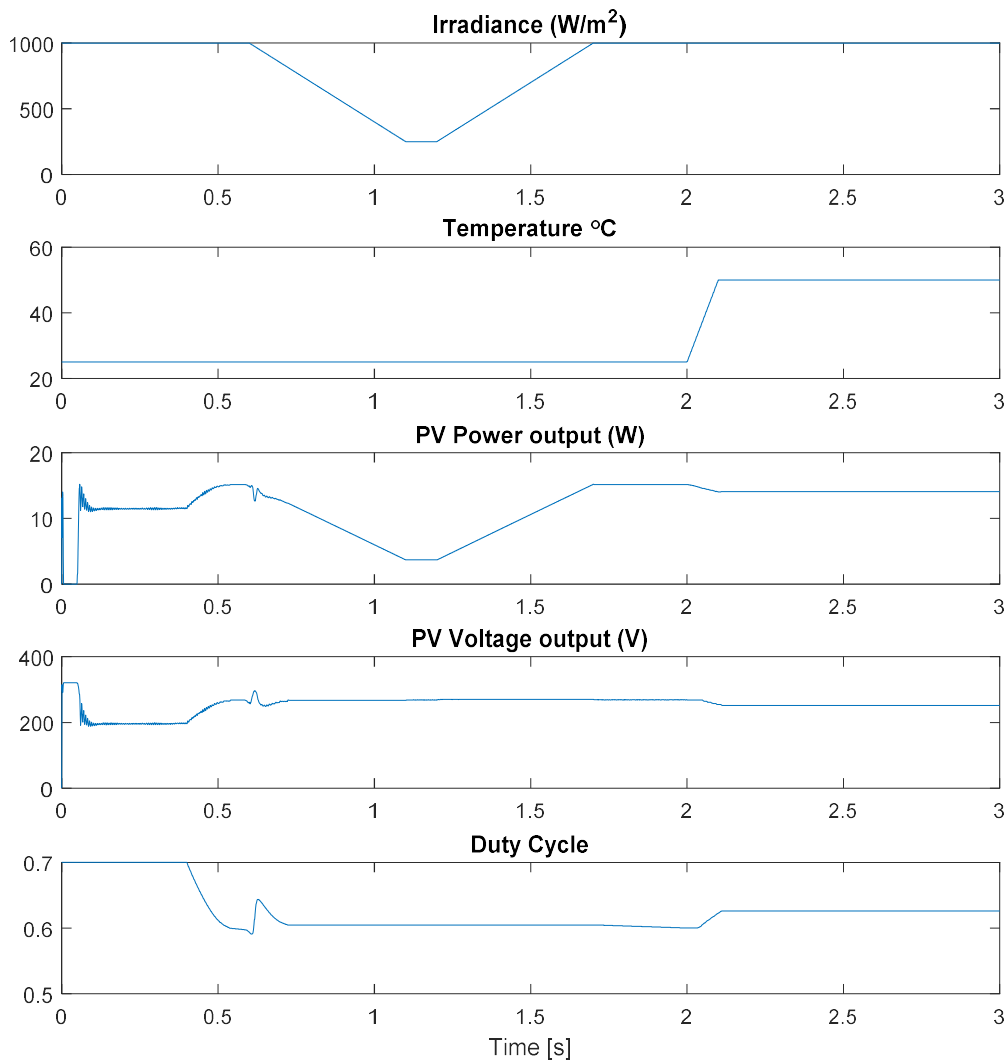


Figure 25: Photovoltaic output characteristics

Figure 26 shows the functioning of DC controller in order to keep the DC-link voltage at constant value of 680 V which is also the set DC reference voltage.

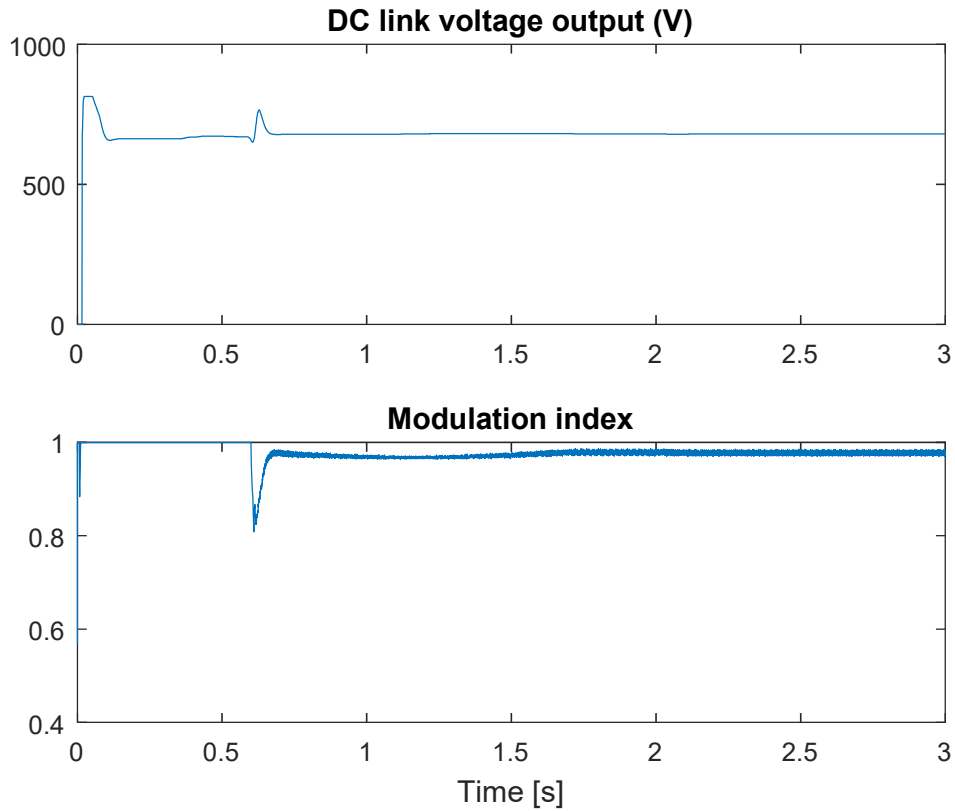


Figure 26: DC-link voltage vrs. Modulation index

Figure 27 shows AC line to line voltage from the DC-AC inverter before and after the filter circuit. This show that the output square wave from the VSI is been translated to pure sinusoidal wave by use of a filter circuit. Also, the grid reference voltage and current which has been taken as the reference for the control system is shown.

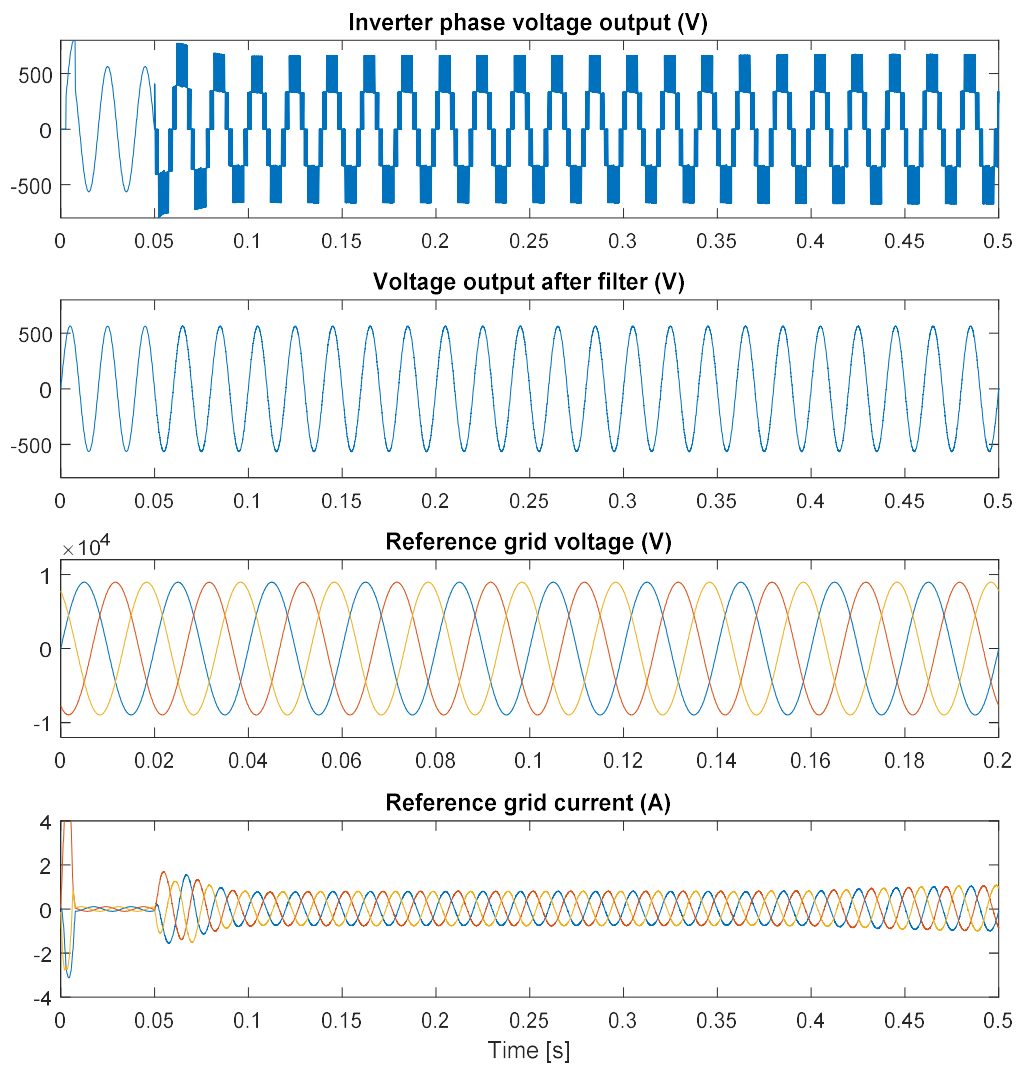


Figure 27: Voltage Source Inverter and Grid Reference Output

The introduction of the PV system introduces the harmonics to the grid. The harmonics injected to the particular grid is measured using Fast Fourier Transform (FFT) tool of Simscape Power System. The harmonic measurement differs at different time of operation as can be shown Figure 28 and Figure 29 at 0.5 second and 2 second of operation.

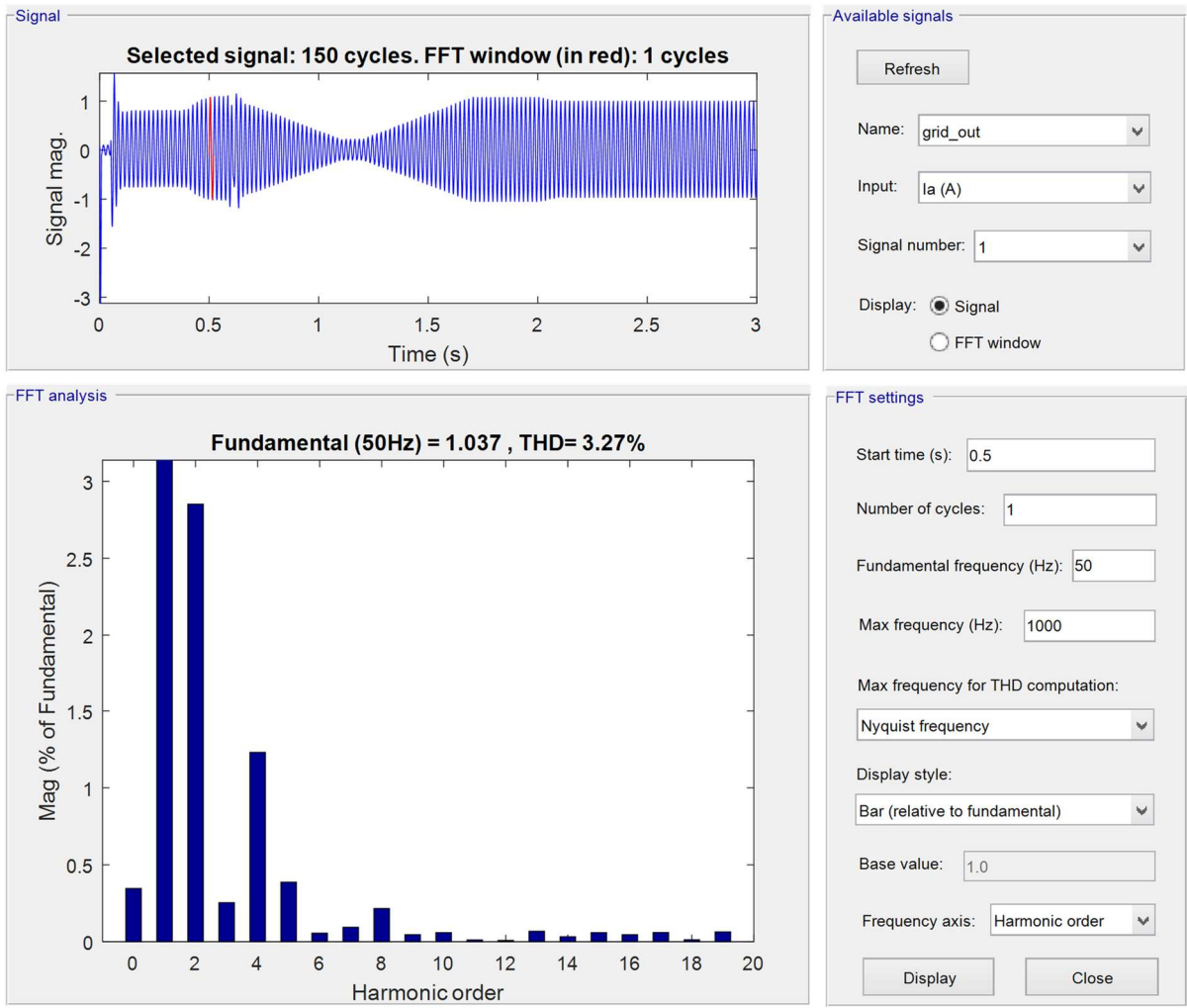


Figure 28: THD at 0.5 second time of operation

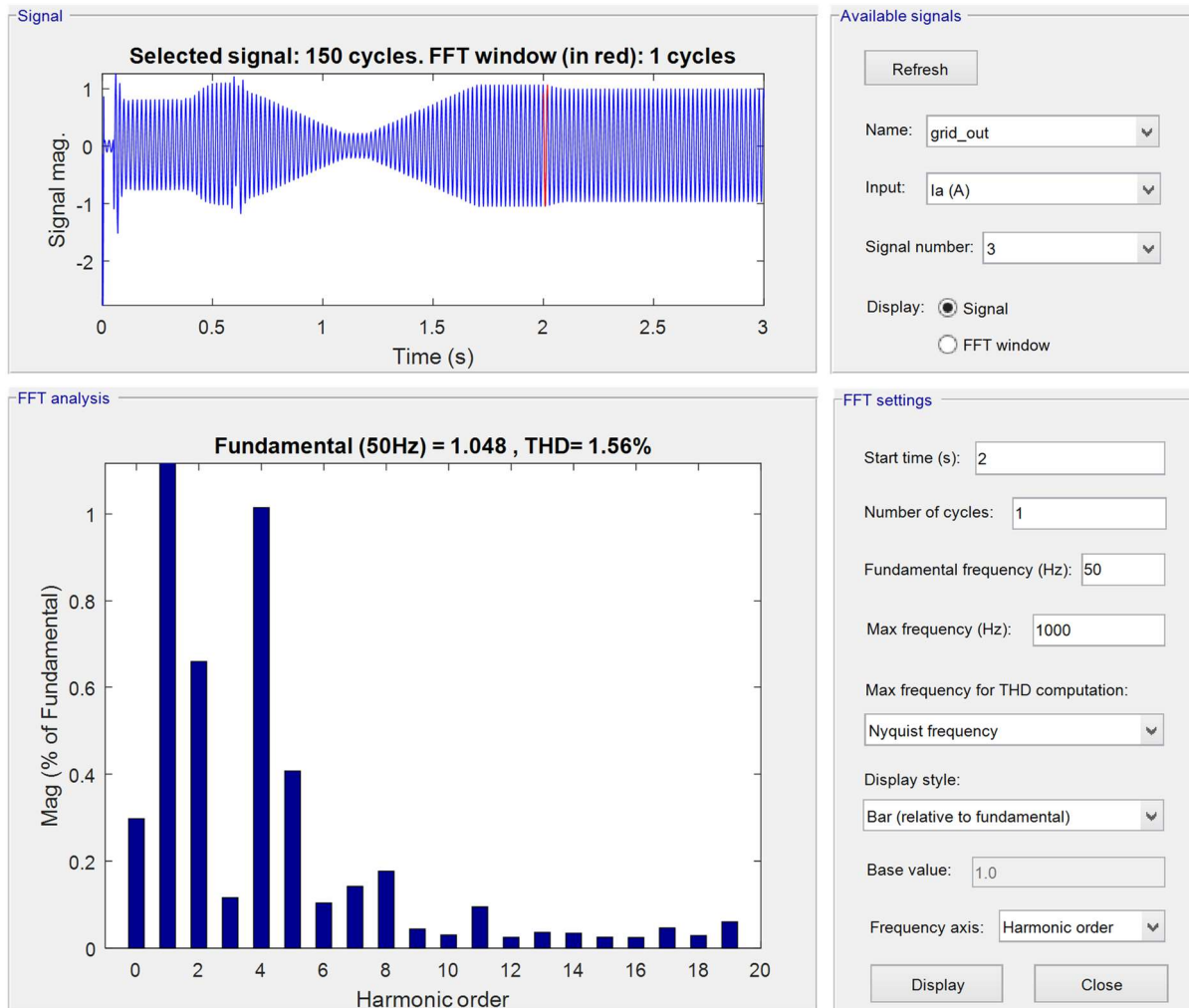


Figure 29: THD after 2 second of operation

4.4 Distribution network modelling

In this section, the actual grid network of Mälarenergi Elnät with real time operation data is built to study the steady state behavior of the grid under peak load and low load condition. The electrical distribution network was built using Simscape Power Systems tool of Simulink. Simulink library has all typical model of power equipment i.e. transformers, lines, machines, and power electronics. The advantages of modelling the distribution network in Simulink platform is simple like click and drag procedures. Simulink uses MATLAB computational engine and users can uses MATLAB toolbox to receive and sending linear or non- linear signals in continuous or as discreet time stamps.

A part of the LV network is modelled for representing LV side of the network, which is connected to the 11 kV side of the Mälarenergi Elnät. The grid model comprised following components/sub-system.

4.4.1 Grid source

The 11 kV grid behaves as the grid source in the network and considered as the slack bus as well. A three-phase source block available in Simscape library is used as a grid source in the network model. The power source block specifications used for the analysis are for the base voltage of 11 kV, three-phase short circuit level 10 MVA. The frequency is 50 Hz as of EU power system. A low voltage distribution transformer (DT) with DYN11 configuration is considered in the network model. The DT specifications with respect to winding voltage ratio, and transformer rated capacity are considered as 11 kV/400 V, and 500 kVA respectively. The phase to phase voltage of primary and the secondary side has been set as per representative electrical network parameters. The transformer resistance and reactance have been chosen by default. Magnetizing inductance and resistance are generally very high and here kept as default value. Five LV distribution lines start from the substations. A 11 KV feeder has been used between the grid source and the high voltage end of the transformer at substation ET 3053. The measured length of the line per phase is 2358 meter. The cable parameter with respect to the positive sequence values of resistance, inductance, and capacitance of the line are considered to be 0.125 Ω /km, 0.3 mH/km and 1.56 μ F respectively. The voltage level at LV grids supplied by MV/LV transformer substation is assumed to be constant and no variation in MV grid is taken into consideration for the study. However, voltage control in manually operated tap-changing transformer may cause change in the voltage profile on the LV sides. However, for the study such variation has not been taken into consideration.

4.4.2 Low voltage distribution network

The representative distribution system chosen for the study is a standard LV grid configuration for residential urban areas. The considered distribution system is radial and supplied by a medium-voltage transformer (11/0.4 kV) equipped with a tap changer. The distribution system includes five main feeders with laterals and distributed loads. The topology of the LV network was built with use of database in Trimble of Målaenergi Elnät AB. The built in network model is for 16 load buses, which are the distribution feeders emerging from the five main feeders with a nominal three-phase voltage level of 400V. Each load bus represents the point of common coupling or the distribution feeder section for the residential buildings. Each load bus serves different number of houses. The single line diagram of the electrical network model of the ET 3053 is presented Figure 30.

The ‘Three-Phase Distributed Parameters Line’ block has been used for modelling all the distributed lines in the network. The Distributed Parameter Line block implements an N-phase distributed parameter line model with lumped losses. The distribution feeder specification parameters are like; resistance 0.125 Ω /km, inductance 0.24 mH/km, and capacitance C=1.56 μ F/km. The actual feeder length data is taken from the database of Målaenergi Elnät AB. All the load buses are modelled as PQ buses.

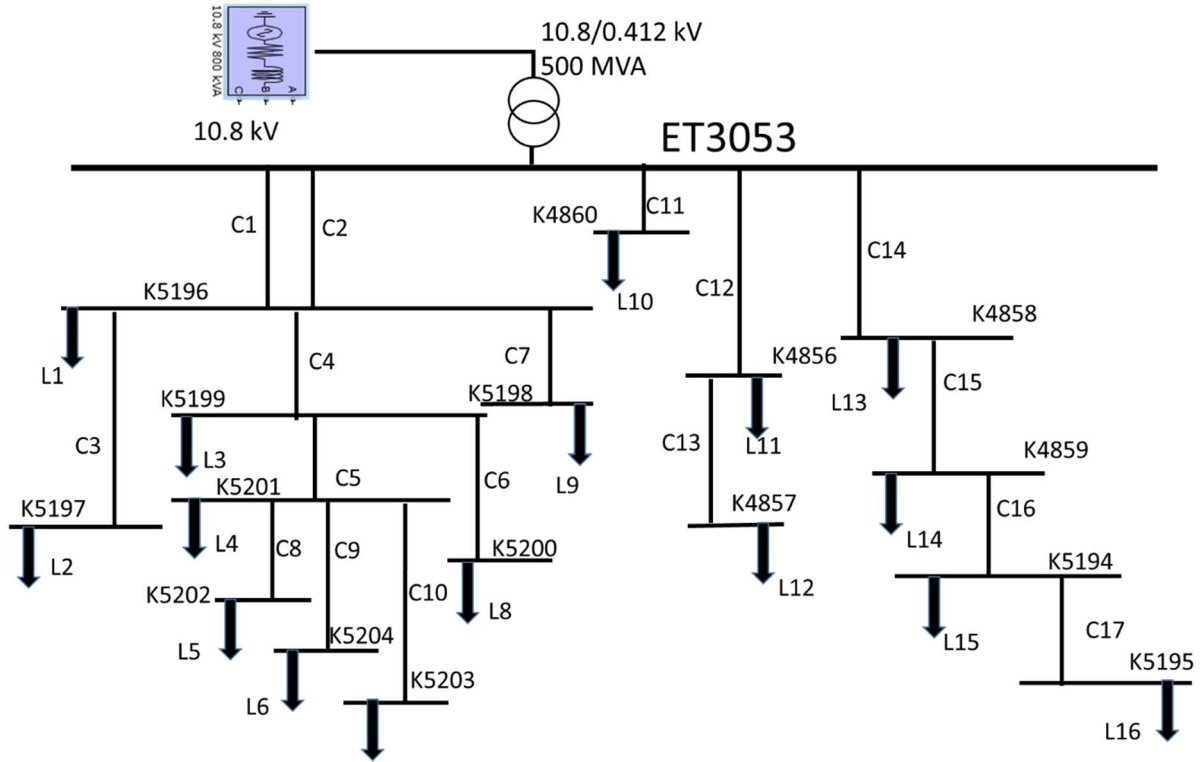


Figure 30: Schematic Diagram of the representative Mälarenergi Elnät LV grid

4.4.3 Load profile

The hourly load profile data is a requirement to study the steady state parameters of the network. Hence, the data pertaining to consumption for the houses supplied from the ET 3053 (11/0.4 kV) substation was collected with help of the database in Trimble of Mälarenergi Elnät AB. The consumption data for the houses were only available on year basis. Also, the annual consumption data was not available for all the houses fed from the particular substation. Hence, in absence of hourly consumption data, Velander's formula has been used in the study for computing the peak demand from the individual house. The formula is very much fitted for the Scandinavia residential house load profiles and widely used for converting the annual consumption data in to peak load power data. The relation between annual consumption and peak load is as per equation (32):

$$P_{max} = k_1 * E + k_2 * \sqrt{E} \quad (32)$$

Where k_1, k_2 are the empirical coefficients, which varies depending on the type of house.

E is the annual consumption for the residential houses.

P_{max} is the peak power from the house.

The typical residential load profile of houses in Sweden is categorized for three groups based on hourly load profiles and those are (Neimane, 2001):

- Domestic house without electrical heating (district heating supply)

- Houses with electrical heating
- Large House with electrical heating

The standard annual consumption data for the above type residential houses is presented in Table 4.

Table 4: Typical Consumption data for Residential Houses in Scandinavian countries

Annual household demand for different houses in the LV grid			
	Annual Consumption [kWh/year]	Mean [kWh]	Peak Power in kW(using Velander's formula)
House with electrical heating	18789	2.14	9.06
Houses with District heating	7624	0.87	6.88
Large House with electrical heating	38402	4.38	15.65

As per above annual load consumption data, the peak load of houses with district heating, houses with electrical heating and large houses with district heating is considered around 6.88 kW, 9.06 kW and 13.65 kW respectively (Neimane, 2001). Also in order to compute the low load from the houses, the typical residential daily load profile of a house with electrical heating, house with district heating and cottage with electrical heating were collected. The minimum load for house with district heating, cottage with electrical heating and large cottage with district heating is considered around 0.87 kW, 2.146 kW and 4.65 kW respectively. It is assumed that the distribution feeder is supplying to mix of end user customers with district heating loads and with direct electrical heating for both small and big houses at ratio of 6:4. After computing the possible maximum load using the Velander's formula, low load for individual type of houses, the weighted average peak load and low load is computed for each load bus/distribution feeder based on the number of houses served from that distribution feeder. Also, a coincident factor of 0.6 is multiplied to arithmetic sum of the all the loads for every houses, in order to compute the incident peak load and low load for the distribution feeders which later used for computation of the load flow,

All the loads represented in the simulation are for house appliances, hence a power factor of 0.9 has been used in the study. The lumped active and reactive load data for the distribution feeders at high load and low load conditions is presented in

Table 5.

Table 5: Load data for distribution feeders

Distribution Network Load Data					
Feeder No.	No. of houses	Peak Load		Low load	
		Resistive load in kW	Inductive load in kVAR	Resistive load in kW	Inductive load in kVAR
4858	15	63.88	30.94	9.0	4.3
4859	7	29.81	14.44	4.2	2.0
5194	4	17.04	8.25	2.4	1.2
5195	6	25.55	12.38	3.6	1.7
4860	12	51.11	24.75	7.2	3.5
4856	9	38.33	18.56	5.4	2.6
4857	7	29.81	14.44	4.2	2.0
5196	8	34.07	16.50	4.8	2.3
5197	4	17.04	8.25	2.4	1.2
5198	4	17.04	8.25	2.4	1.2
5199	5	21.29	10.31	3.0	1.4
5201	4	17.04	8.25	2.4	1.2
5200	6	25.55	12.38	3.6	1.7
5202	6	25.55	12.38	3.6	1.7
5203	7	29.81	14.44	4.2	2.0
5204	5	21.29	10.31	2.991	1.45

For the load model “Three Phase Series RLC Load” block has been used. The nominal voltage level has been set according to the configuration of the representative distribution network which is at 400 V and the frequency was set to 50 Hz. The load is modelled as constant “PQ” load, hence, in the field of active and reactive power, the resistive and inductive load parameters for the respective distribution feeder were given. The VI measurement block is connected near to each load tapping point. This block is used to measure instantaneous three-phase voltage and current measurements in a circuit. This block is connected in between two other Simscape Power Blocks in the network. In addition, a single connector load flow bus is connected at each load tapping point in order to capture the steady state voltage value in p.u. with respect to reference nominal voltage. Since the loads in the system are equally distributed among the three phases, only single connector load flow bus has been used.

The load flow performs a balanced positive sequence load flow. For power system model build in Simulink, Powegui block is necessary for simulation and needs to place in the build model. Powegui block has two parts, first part is the simulation and configuration options and the second part is the analysis tools. From the first part of Powegui block need to select whether the model should run either in continuous, discrete or phasor method. For the application of the model involved in the study, simulation needs to run in discrete with standard sample time of 50 micro seconds. In load flow tab the frequency was set to 50Hz, a base power 10 MVA and PQ tolerance of 0.0001(p.u.). Maximum iteration for load flow analysis was chosen as 50 (by default). Voltage and Power units are in V and kW respectively.

Power/load flow is a load flow study performs the analysis on time based. This analysis is able to determine the bus voltage and power consumption (active and reactive) of a load against a period of time. Power flow studies therefore gives the results of simulation on an instant based scenario. Some simulations have been carried out in different conditions of the systems. The first simulation is aimed to evaluate the steady state parameters along the LV distribution line, with peak load condition. The parameters for the simulation are:

- voltage value supplied from the MV/LV substation of 412V;
- maximum condition of load

The results from the simulation study is presented in Figure 31. As per European standard, the nominal AC voltage of 230V at the point of supply in single phase line to neutral and 400 V in three phase line to line with a tolerance of $\pm 10\%$ has to be maintained at low voltage distribution network side. The voltage profile at the distribution feeder shows a good performance of the network without the PV integration, with all the load bus voltage profile within the required regulatory requirement of $\pm 10\%$.

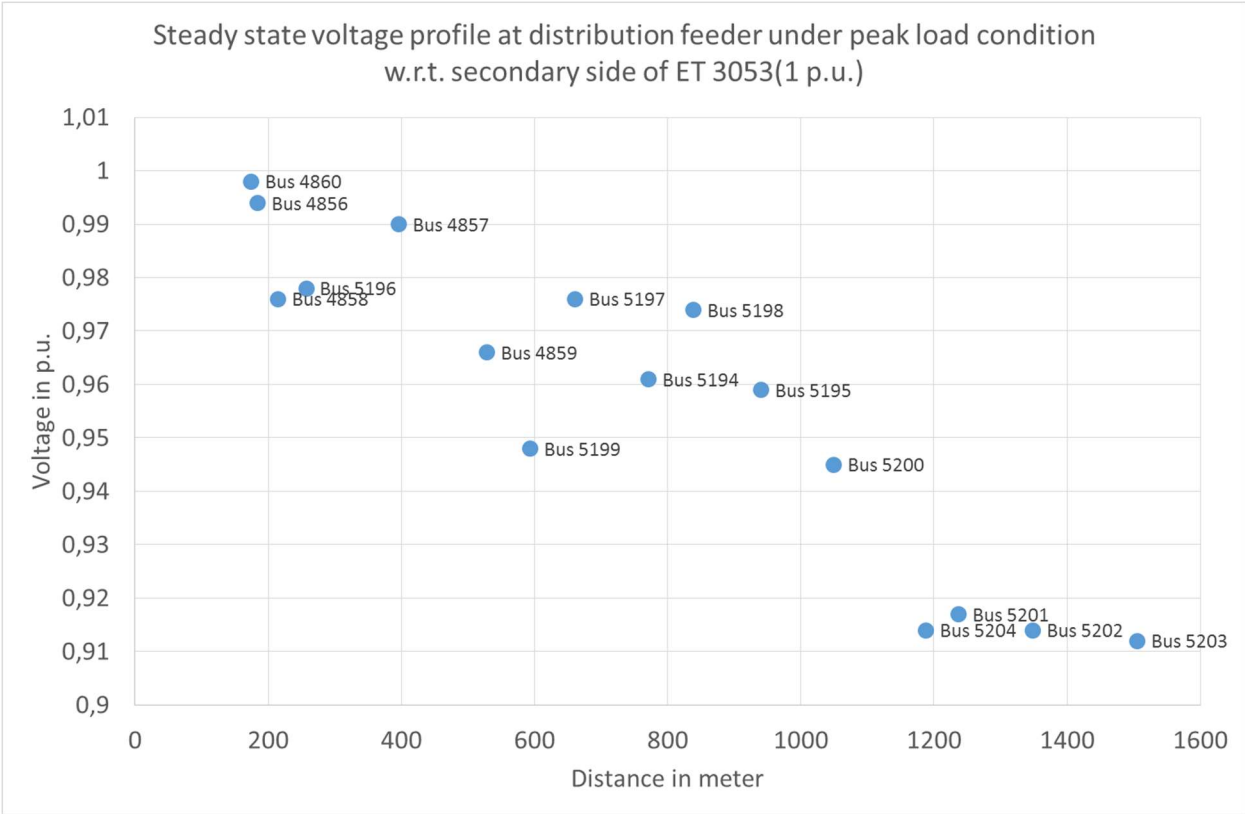


Figure 31: Voltage profile for load buses for peak load condition

The second simulation is aimed to evaluate the steady state parameters along the LV distribution line, with low load condition. The parameters of the simulation are:

- voltage value supplied from the MV/LV substation of 412V;
- minimum condition of load

The results from the simulation study is presented in Figure 32. The voltage profile at the distribution feeder shows a good performance of the network.

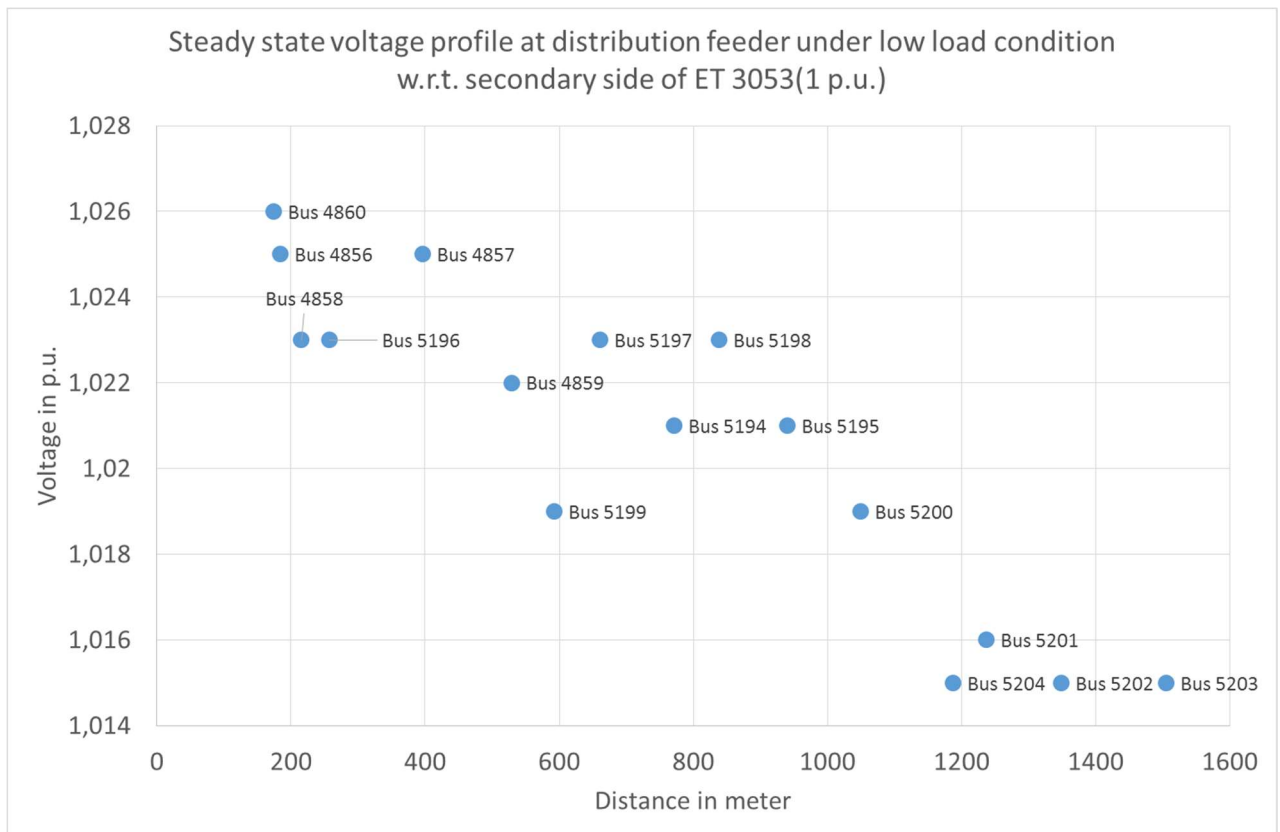


Figure 32: Voltage profile for the load buses for low load condition

5 RESULT

This chapter presents the simulation results for the distribution grids from Mälarenergi Elnät. The results as obtained from the simulation softwares are presented comparing for the base cases (maximum load and minimum load condition) without PV integration and with integration of PV generation. These results are for voltage level, system losses, voltage unbalancing and harmonics.

5.1 Overvoltage impact

Output from a PV system is not a constant for all around but varies depending on the time of the day and the climatic conditions prevailing at that time. Additionally, the consumption of active and reactive power for residential loads equally varies with time. Hence, the power flow simulation must be done in the most critical case of loads (i.e. minimum load and maximum load) under period of high and low solar irradiance respectively in order to get the reference steady state parameters under both extreme cases.

The first simulation is aimed to visualize the improvement in voltage and losses of the system and the second case of simulation for evaluating the over-voltages along the LV distribution line. Scenarios of simulation would be as per following conditions:

- Case I: Minimum generation from the PV system at peak load condition
- Case II: Maximum generation from the PV system at low load condition

The base cases of the grids were simulated in Simscape Power system tool of MATLAB using load flow analysis function without the PV integration. The distribution grid area served from distribution transformer ET 3053 has a maximum and minimum power consumption of 464.21 kW and 224.83 kVAR, 65.2 kW and 31.57 kVAR respectively. The minimum load value is approximately 23% of the maximum load value. For analysis of the impact of PV system integration on the LV network, PV system which has been modelled in the previous section with a capacity of 15 kW has been integrated into the distribution network model at each load bus point. There would be 16 numbers of such PV system integration, one for each distribution feeder node represented as load bus in the simulation. Since there are 16 such load buses, the level of penetration is approximately 50%. The above mentioned PV groups are connected at load buses which is assumed to be the distribution feeder section for the group of houses. In the real case each house is supplied by a line that starts from one node. However, in this work the minimum aggregation of loads is intended as a bulk loading for definite number of houses from a distribution feeder, and the PV system will be installed where the distribution feeder were emerged to supply the houses. Therefore, the connection of the PV system with the grid was done in the node of the distribution line, i.e. in parallel with the houses.

As per daily solar irradiance level during summer days, the maximum solar irradiance level is considered around 960 W/m² at peak sun shine hours and 300 W/m² for low irradiance condition and the ambient temperature of 25 °C. The PV system is modelled with a constant power generator working with unitary power factor for running the load flow simulation. The power output from the PV system under high and low irradiance condition for the above given operating condition is found to be 12.60 kW and 3.7 kW respectively. Simulations have been carried out in different conditions of the systems and the voltage level on the distribution feeders has been shown Figure 33 and Figure 34 for both the cases.

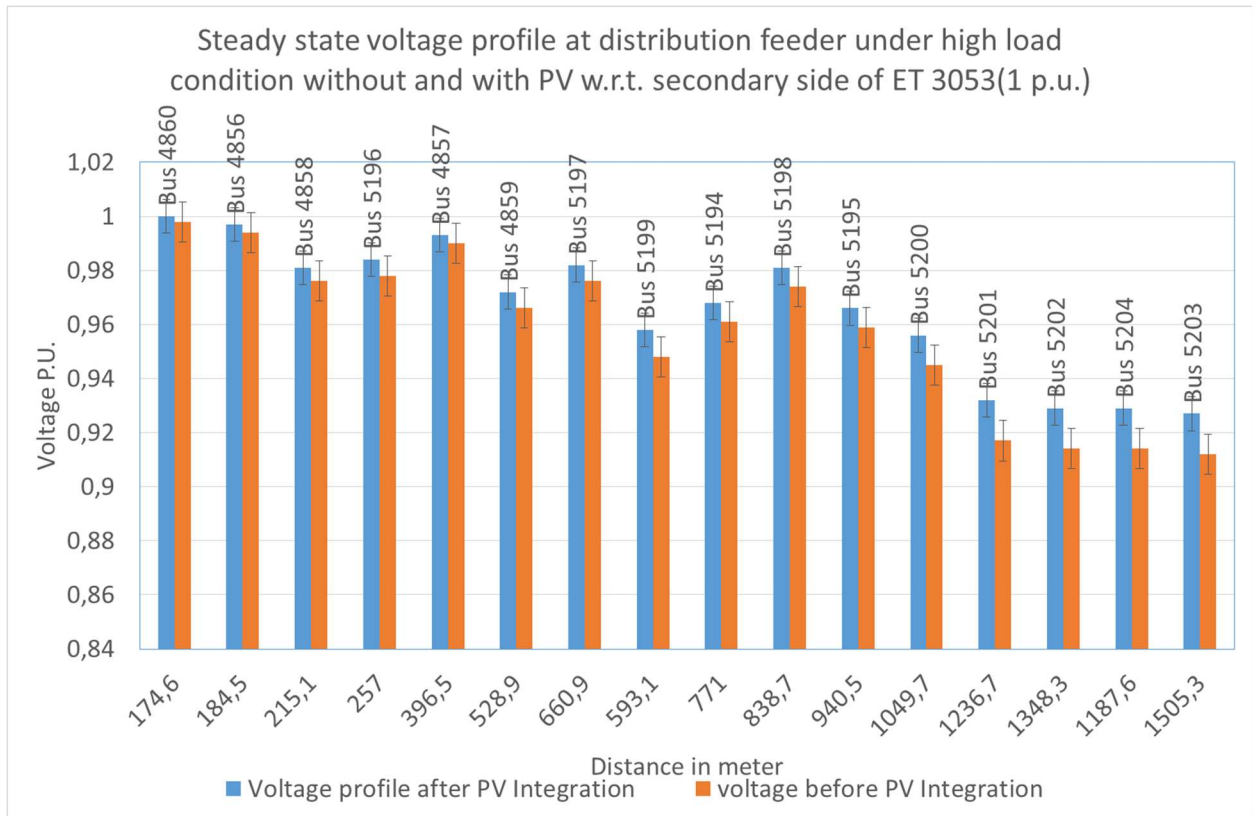


Figure 33: Voltage Profile at distribution feeder for Case I

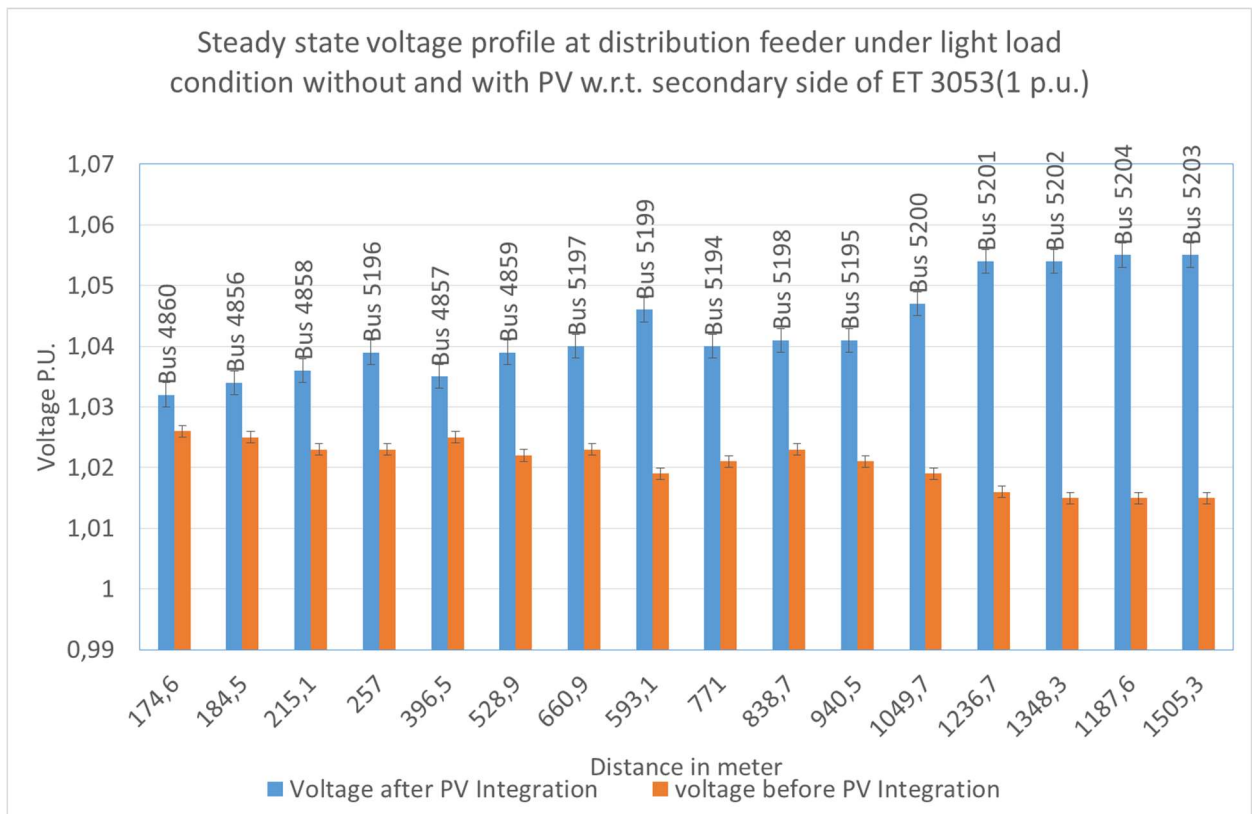


Figure 34: Voltage profile at distribution feeder for case-II

The voltage profile for the minimum load condition before and after PV generation integration was checked for the 103% criteria. It can be seen from Figure 35, that except for few load buses which are situated at distance of 1200 meter and farther away from the DT, the voltage profile for other nodes are within the prescribed limit of 103%.

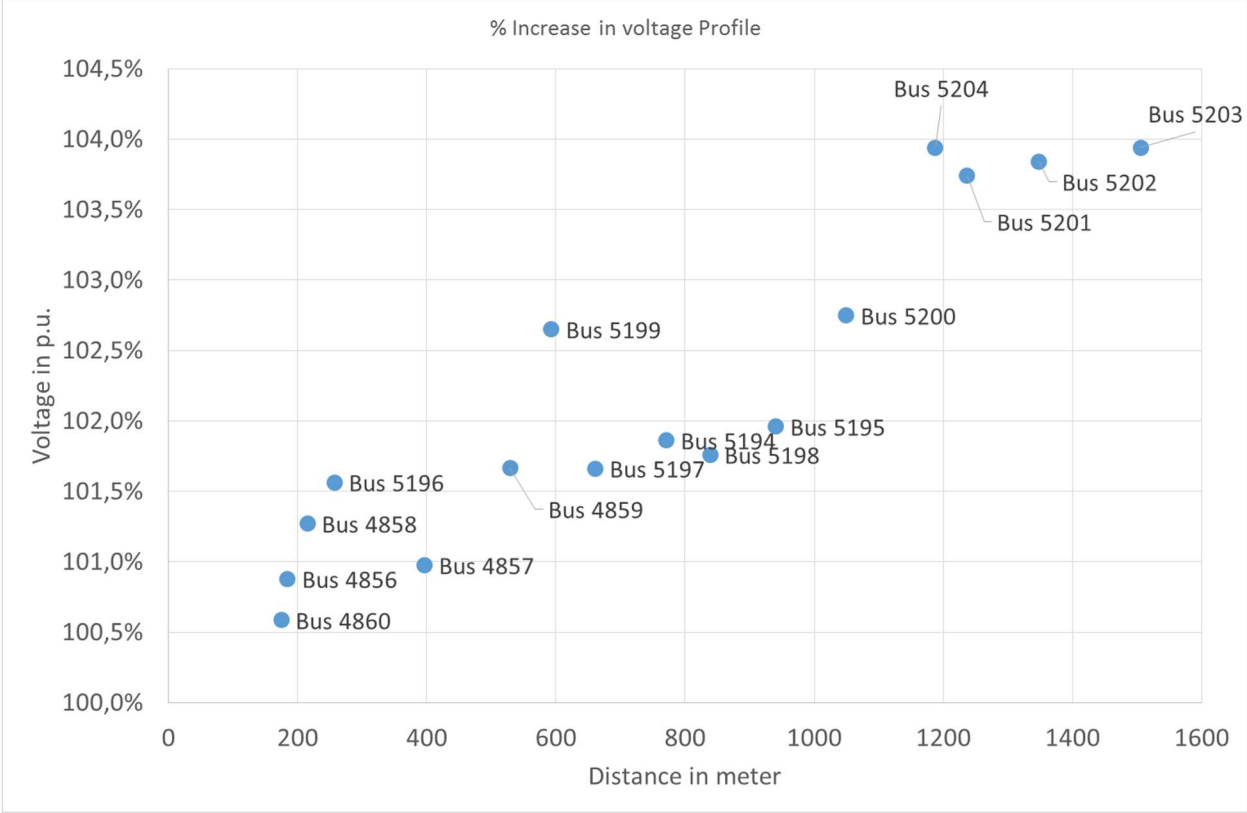


Figure 35: Overvoltage at minimum load condition with PV Integration

5.2 Voltage unbalancing impact

For studying the voltage unbalancing in the grid due to integration of PV system, the modelled 15 kW dynamic PV model is connected to each of the distribution feeder load tapping point. The three phase voltage sequences and magnitudes were logged at a node 5196 located near to the substation and at node 5200 which is located far from the substation, before and after the integration to see the difference in impact at different points of the grid. Figure 36 and Figure 37 represents the voltage sequences at node which is closed to substation DT. Figure 38 and Figure 39 represents the voltage sequences at a node farther to DT. It can be seen that voltage unbalancing is prominent for the node which is located at a distant point from the DT.

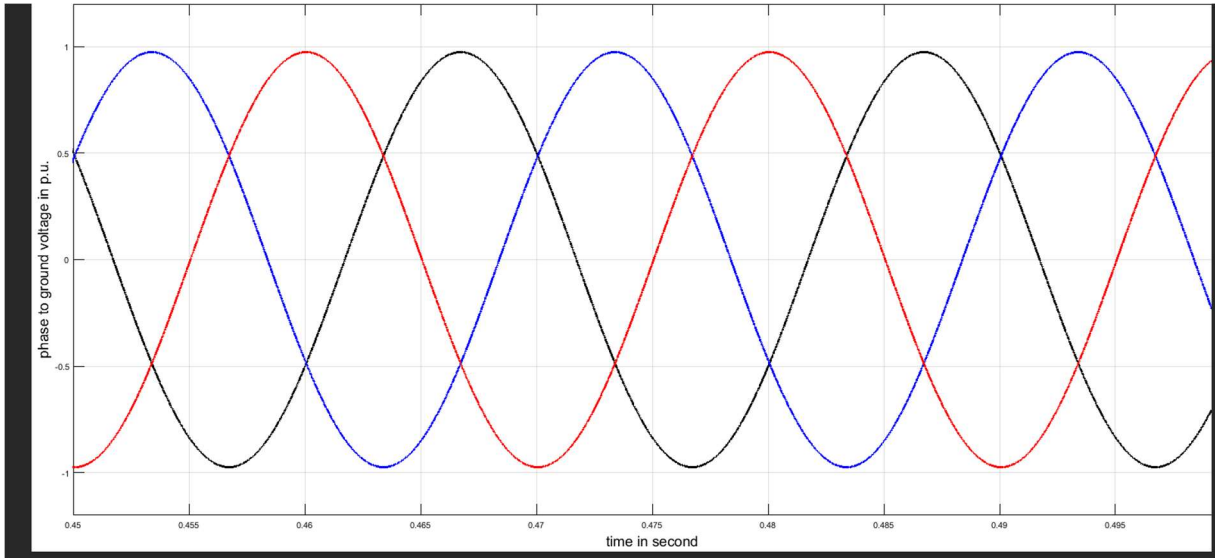


Figure 36: Voltage sequence at node 5196 before PV integration

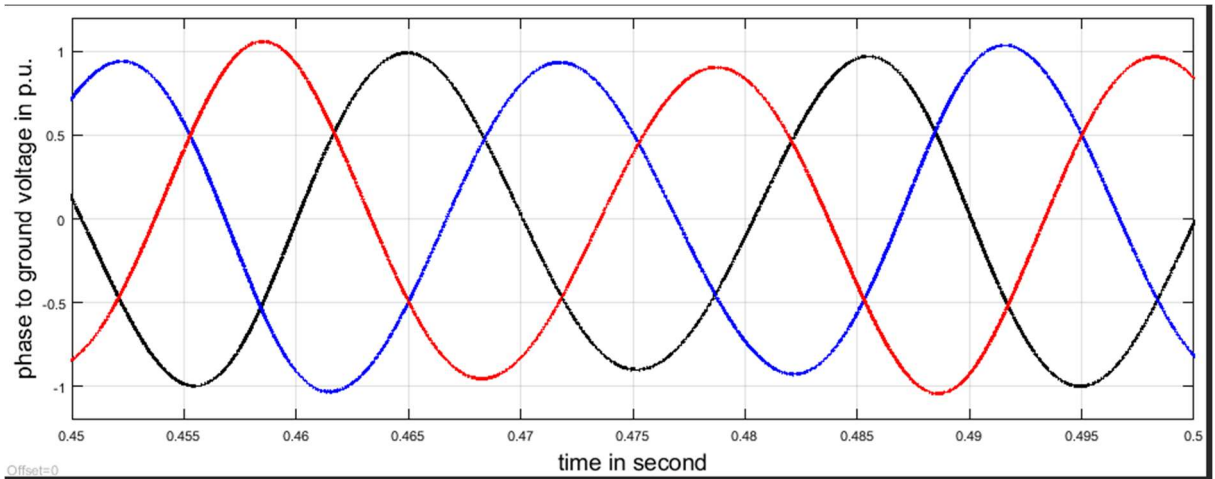


Figure 37: Voltage sequence at node 5196 after PV Integration

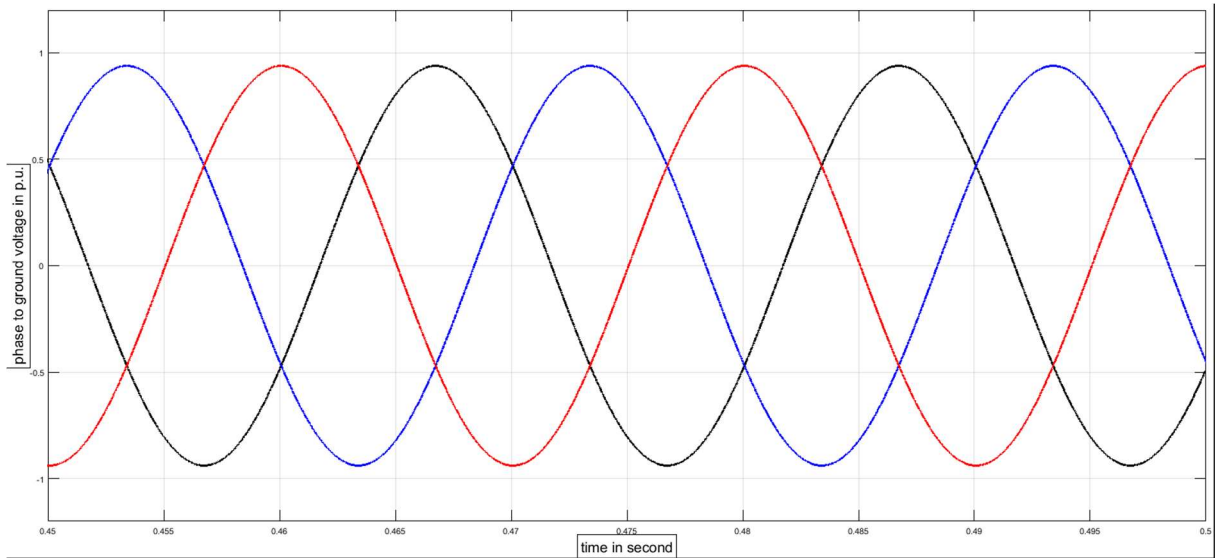


Figure 38: Voltage sequence at node 5200 before PV Integration

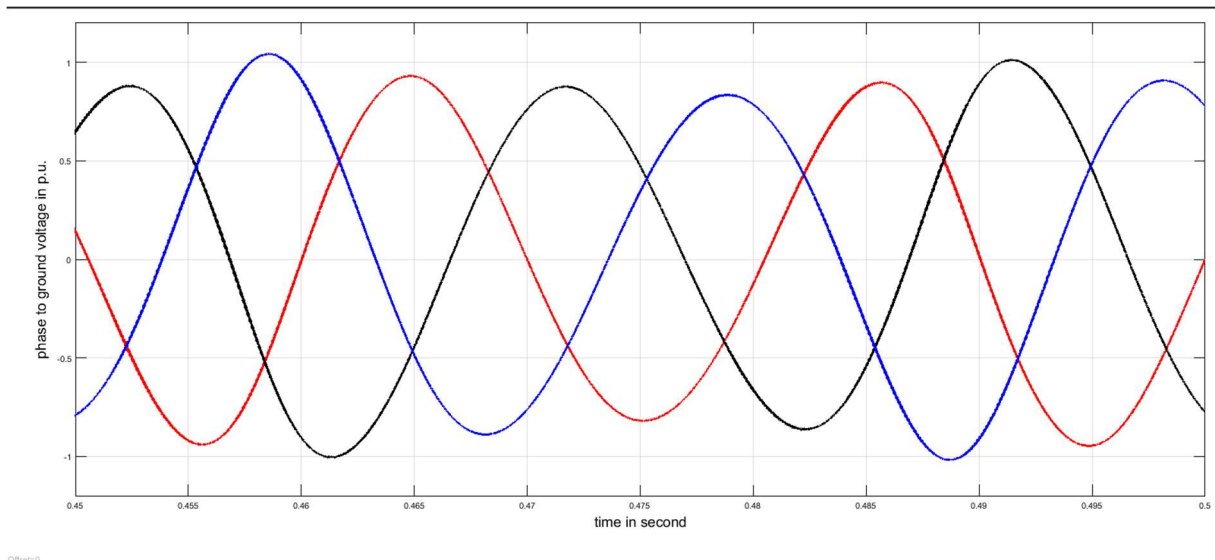


Figure 39: Voltage sequence at node 5200 after PV Integration

5.3 Harmonic distortion impact

In order to show the harmonic content due to integration of PV system, the built in PV dynamic models has been integrated in to each of the load bus of the grid. The impacts on grid under two different operating condition were analyzed. The two scenarios are: the first one is for peak load condition and other is for low load condition. The % THD for both cases were shown at 400V on the secondary side of the DT and 11 kV side of the DT as presented in Figure 40, Figure 41, Figure 42 and Figure 43.

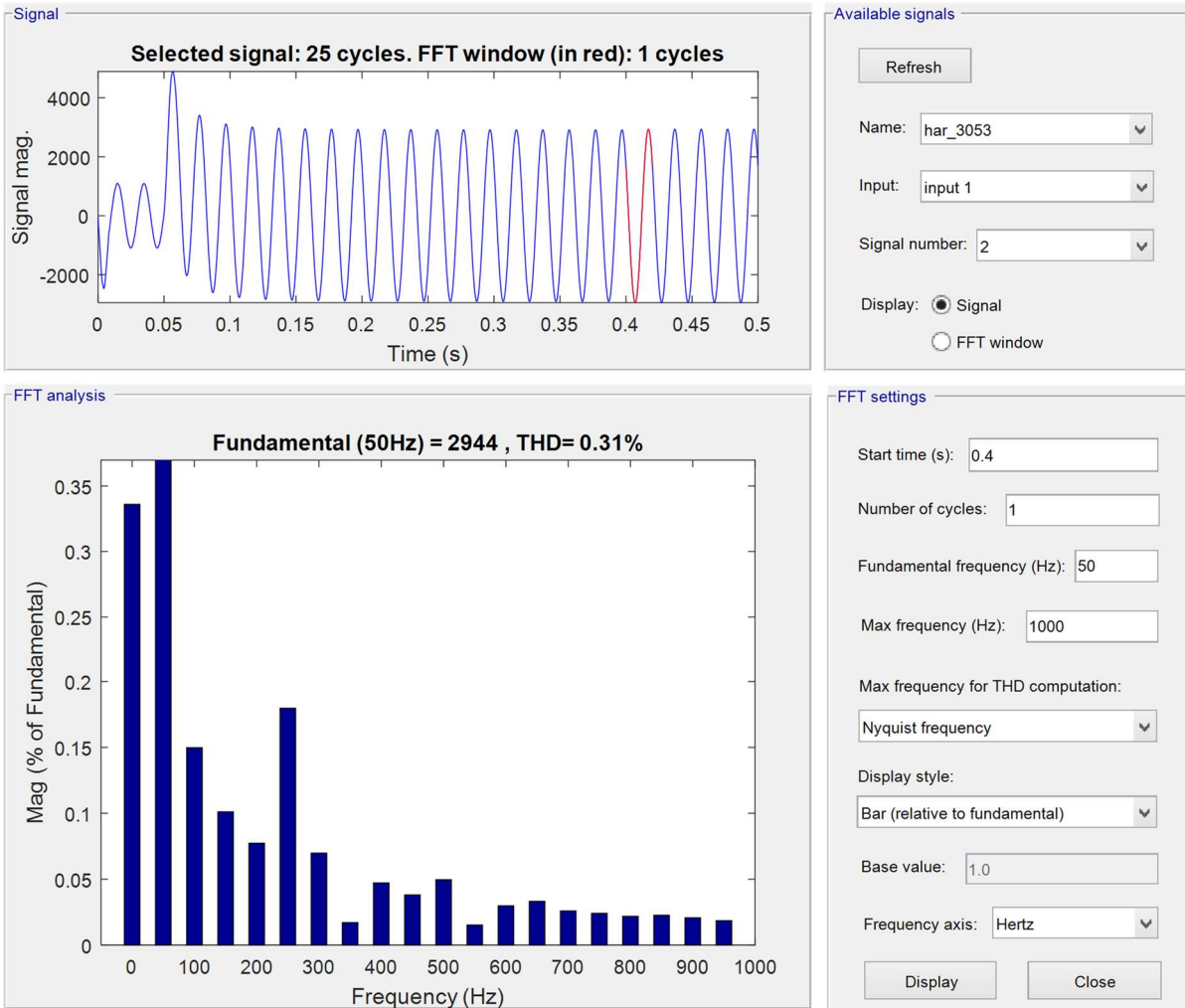


Figure 40: THD at maximum load condition at 400 V side

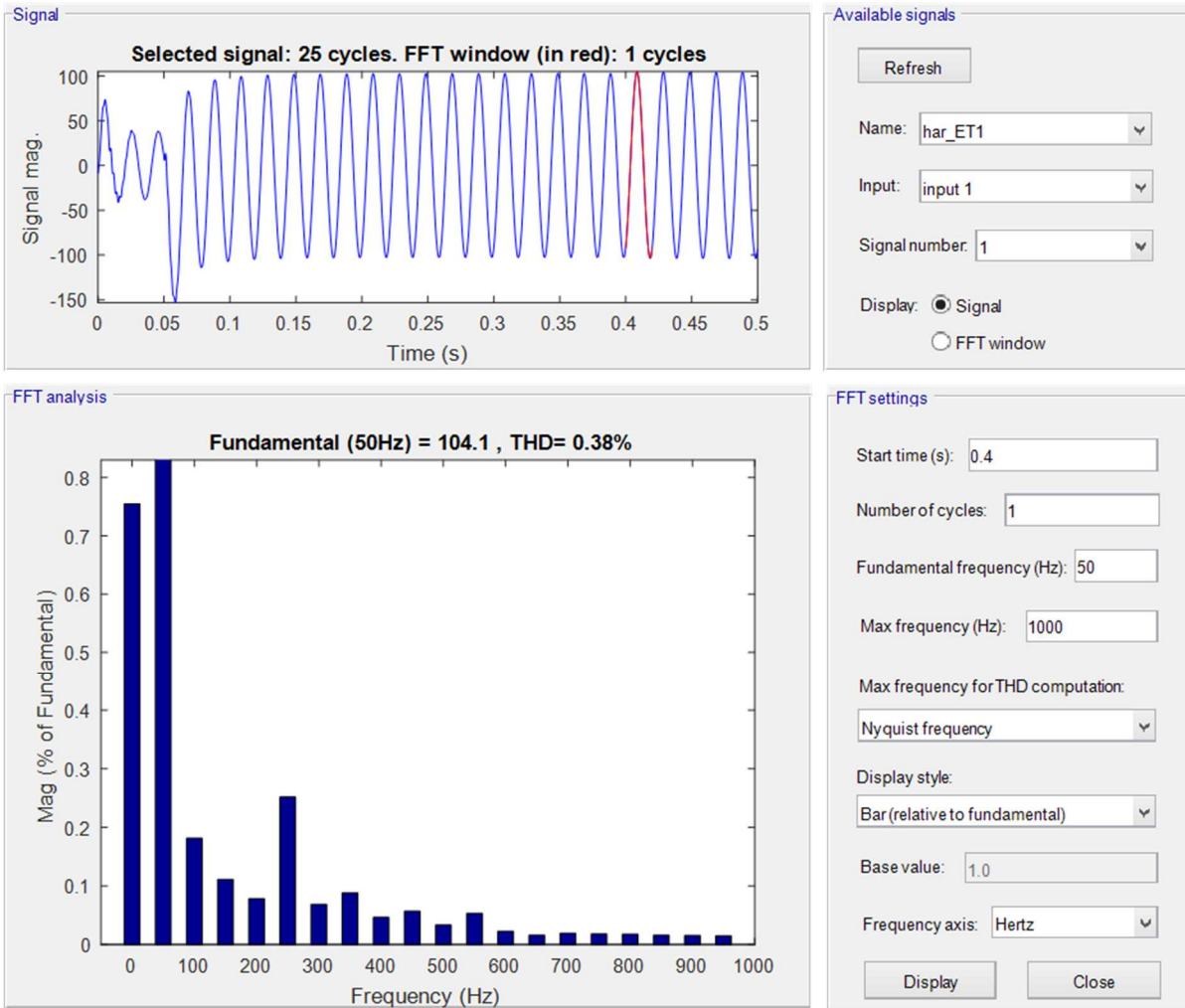


Figure 41: THD at maximum load condition at 11kV side

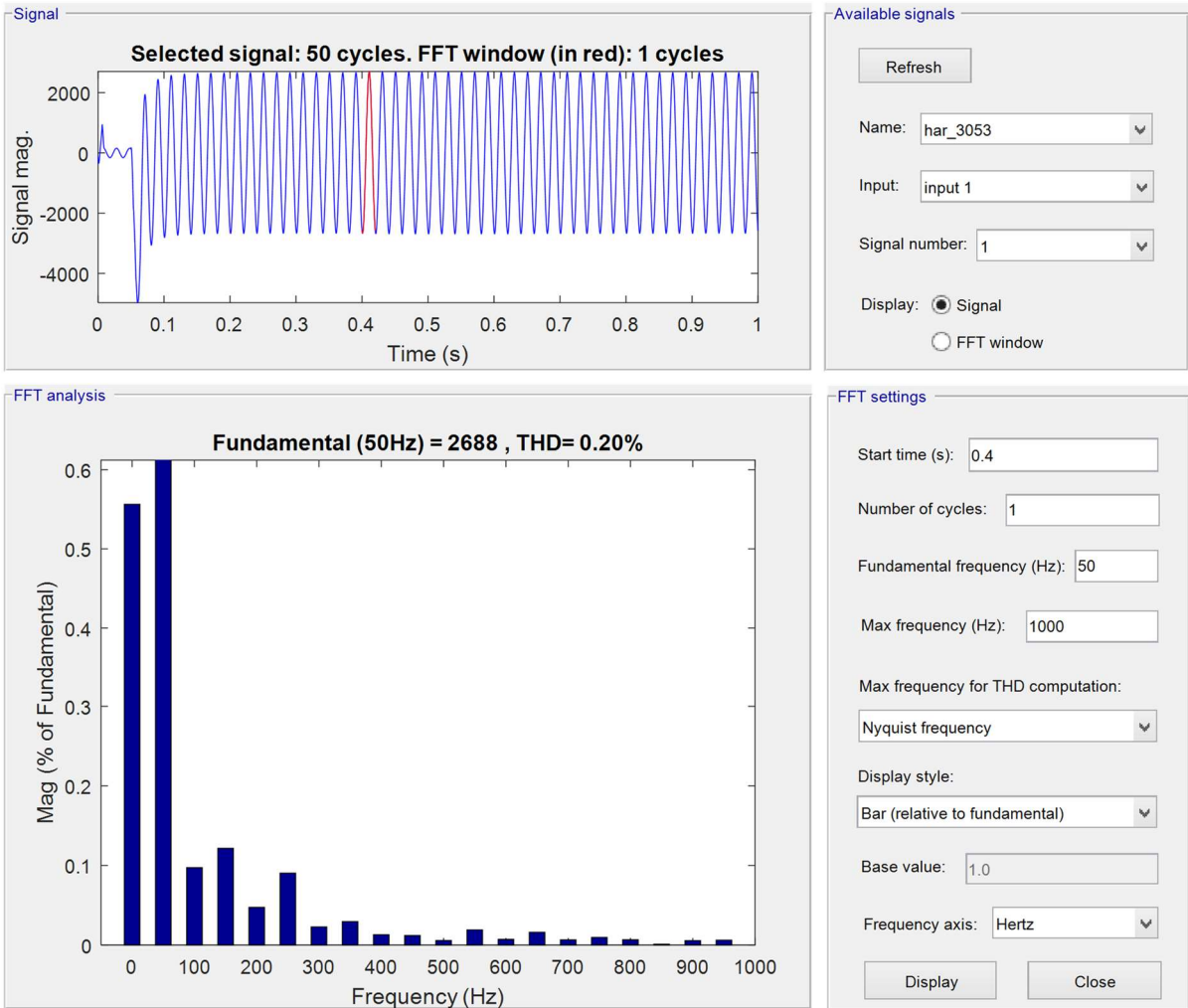


Figure 42: THD for minimum load condition at 400V

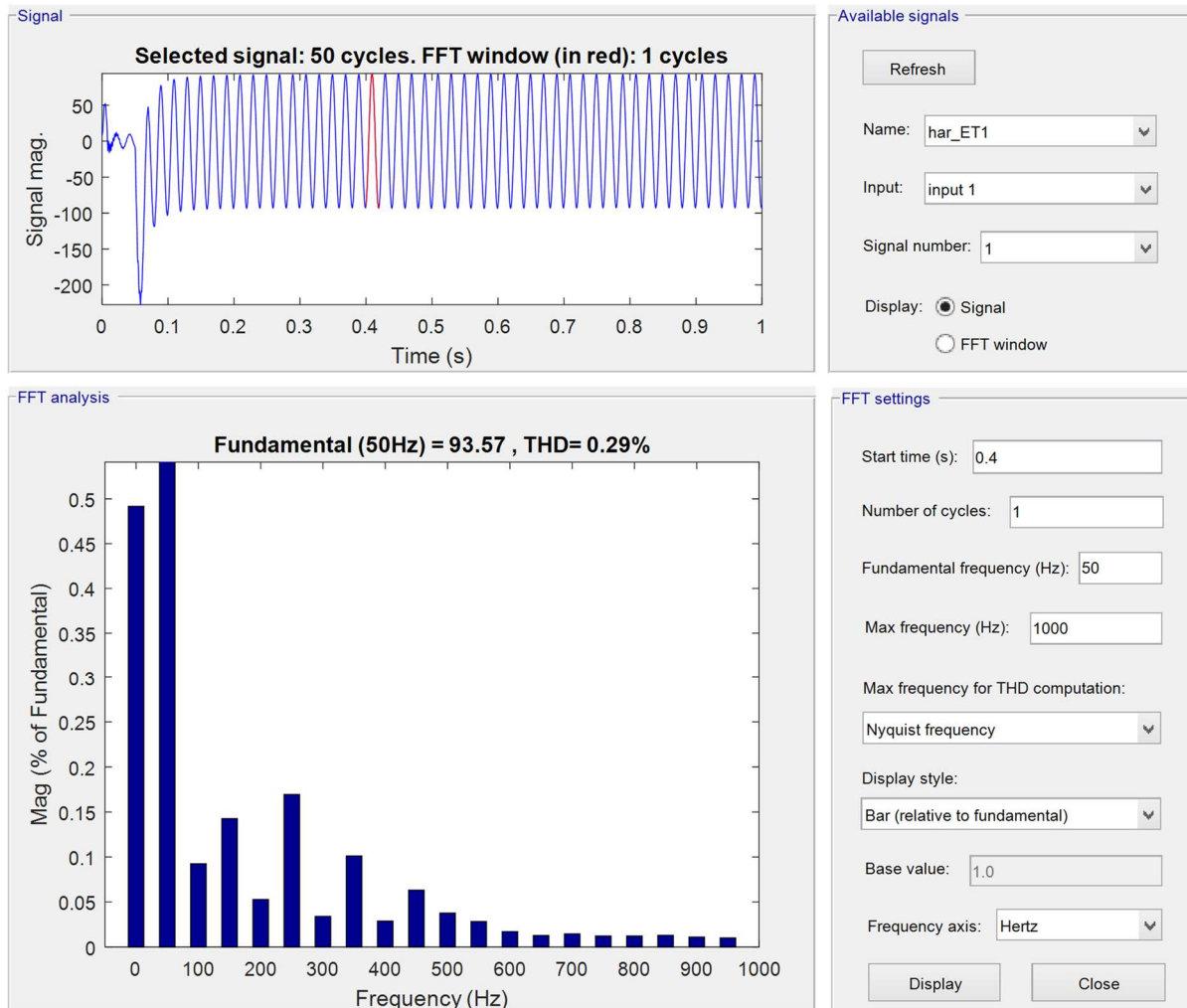


Figure 43: THD at minimum load condition at 11 kV

6 DISCUSSION

Discussions of the results obtained by comparison of base cases and with PV generation are presented.

The integration of PV system to the distribution grid can have significant effects on the grid power quality and those are dependent upon various factors such as characteristics of load, the location for placement of PV system (lumped or distributed, near to substation or far away from substation), network parameters, loading condition of network etc. Thus, it makes various scenarios while conducting the impact study. In this thesis work, the studies were conducted based on certain assumptions and for few scenarios such as: balanced load condition, uniform distribution of PV installation across the feeder etc. Also, the impact study was only limited to PV penetration level of 50%. Under such limitation, the impact study was carried. The impacts were mainly focused for peak load and low load condition in high and low

level of sun irradiance. In the above backdrop, the conclusions drawn from the study are on comparative basis between various scenarios.

Referring to the literature study presented in section 2.5 of the report, where it has been discussed that the high penetration of PV systems can increase in harmonic content at the connection point of the grid, which multiplies with number of PV system integration. The inverter is not the only source of harmonics for the network, other factors which can cause harmonics in the grid are non-linear loads, saturation of transformers etc. In the study, the only source of harmonics considered was from inverters i.e. because the switching frequency involved in the solid state electronic devices. Hence, more the number of PV systems more harmonic content will be introduced to the grid. Further, it is explained that both the switching frequency and filter circuit is responsible for getting good quality power output from the PV inverter. Also current controlled VSI DC-AC inverters are relatively free from the harmonics compared to voltage controlled inverters. Higher the switching frequency, lower the size required for the filter circuit. If both of these chosen for optimum performance, the harmonic content could be less in the power output, in other way, it injects pure sinusoidal wave current in to the grid. The chosen switching frequency for the switches is at 1.65 kHz and the size of inductance (L) in filter circuit is for 5 mH. Besides, the detailed PV model uses a current control strategy to set the switching signals for the PWM inverter to transform DC power to AC power. Hence, the performance of the grid connected inverter is almost harmonic free. In addition, the PV system injects current to the network through a series impedance which acts as a low pass filter to improve power quality.

7 CONCLUSION

The electrical characteristics of a grid connected photovoltaic system, with a three phase voltage source inverter with functionality of MPPT algorithm has been simulated using MATLAB/Simulink platform. Also, the integration of such built in models were done at various distribution feeder nodes of the modelled representative distribution grid of Mälarenergi Elnät. The impacts of such integration on the grid was analyzed for overvoltage issues, loss reduction, and voltage unbalancing and introduction of harmonics. Following conclusions were made based on the results in found from the simulation study.

- The integration of PV system at the load point of the distribution grids caused an increase in voltage level for the network.
- The voltage improvement under high load condition was found to be significant for the nodes located at the farther end of the network (from level of 0.917 p.u. to 0.932 p.u.) compared to a node nearer to the substation feeder.
- With 50% PV penetration level under minimum load condition and with maximum solar irradiance, the voltage profile for the load buses located at farther end of the

network was found marginally higher with respect to the prescribed regulatory benchmark of 103%.

- There is a significant reduction in losses in the network from 27 kW (without PV integration) to 17 kW (with PV Integration) for the scenario under maximum load condition.
- With selection of higher switching frequency, better control technique and filter circuit, the harmonic content in the power output from PV system can be reduced to a satisfactory level as per the regulator prescribed limit.
- The introduction of harmonics to the grid multiplies with each addition of PV system to the network. However, overall the THD content of the grid with multiple number of PV integration was found very minimal and within the regulatory requirement. Further, the THD differs with loading condition of the grid and was found to be more when the grid operates at maximum load condition with low PV generation compared to minimum load condition with high PV generation.
- Voltage unbalancing do occur due to integration of PV system in an unbalanced grid. The unbalancing impact is dependent upon the type of load in the grid and location of the PV system.

Hence, in the above backdrop it can be concluded that, even noticeable values of the current THD at rated power of the PV system have a low impact on the harmonic distortion of the grid voltage and current. Rather, with the foreseeable increase in the large scale integration of PV system, the main problem could be the voltage rise. Regarding the voltage unbalancing phenomenon, three phase grid connected PV system doesn't create voltage unbalancing in the grid as such, if the output from the PV system is pure sinewave with no variation among phases, but is mostly affected from the unbalancing in the grid. The severity of unbalancing is more when the PV integration is at a point located far away from the substation for an unbalanced grid.

8 FUTURE WORK

The work attempted to study both steady state and dynamic state impacts of integrating PV power to the LV distribution grid. The study was carried with many assumptions related to the load profile. The representative grid network, which was modelled to showcase the PV integration impact was assumed to be operated under balanced condition of load. However, in reality most distribution network has a degree of imbalance. Hence, there could be improvement in the study with the help of dynamic load modelling. Dynamic load models are true representative of the characteristics of load with the dynamics involved in real scenario. In the study, the grid-connected PV systems are designed to inject all of the real power produced by PV modules. The power is injected regardless of the voltage level. With injection

or absorption of the reactive power, the PV power can mitigate the overvoltage and under voltage issues of the network, which could also be a complementary work for this kind of study.

The study of voltage stability issues which depends on the variability of PV power production under varying climatic conditions (dynamics), can be extension of this work.

REFERENCES

- Ahmed S. Khalifa, E. F.-S. (Sept. 2010). Control of Three Phase Grid Connected Photovoltaic Power Systems. *Proceedings of 14th International Conference on Harmonics and Quality of Power - ICHQP 2010* (ss. 1 - 7). Bergamo: IEEE.
- Aldo Canova, L. G. (2009). Electrical Impact Of Photovoltaic Plant In Distributed Network. *Industry Applications, IEEE Transactions Volume:45 , Issue: 1*.
- Amakye Dickson, N. M. (May 2014.). Grid Connected Inverter with Unity Power Factor for Renewable Energy (PV) Applications. *International Journal of Innovative Science, Engineering & Technology, Vol. 1 Issue 3*.
- E. Liu, J. B. (February 2008). *Distribution System Voltage Performance Analysis for High-Penetration Photovoltaics*. Natiolal Renewable Energy Lab.
- EN50160. (2004). *Voltage Characteristics in Public Distribution Systems*.
- Erhan Demirok, D. S. (2009). Clustered PV Inverters in LV Networks: An Overview of Impacts and Comparison of works: An Overview of Impacts and Comparison of. *Proceedings of the Electrical Power and Energy Conference, EPEC 2009*, (ss. 1-6).
- Evju, S. E. (June 2007). *Fundamentals of Grid Connected Photo-Voltaic Power Electronic Converter Design* . Norwegian University of Science and Technology.
- Farhad Shahnia, A. G. (2011). Voltage Correction in Low Voltage Distribution Networks with Rooftop PVs using Custom Power Devices. *IECON 2011 - 37th Annual Conference on IEEE Industrial Electronics Society*, (ss. 991 - 996). Melbourne, VIC.
- Farhad Shahnia, R. M. (2010). Sensitivity Analysis of Voltage Imbalance in distribution networks with rooftop PVs. *Power and Energy Society General Meeting, 2010 IEEE* (ss. 1-8). Minneapolis, MN: IEEE.
- Farhan Mahmood, L. V. (May , 2014). Modeling of a Detailed Photovoltaic Generation System for EMT-Type Simulation. *Energy Conference (ENERGYCON), 2014 IEEE International* (ss. 916 - 921). Dubrovnik, Croatia: IEEE.
- Florentin Batrinu, G. C. (May 2006). Impacts of grid-connected photovoltaic plant operation on the harmonic distortion. *Electrotechnical Conference, 2006. MELECON 2006. IEEE Mediterranean*, (ss. 861 - 864). Malaga, Spain.
- Hirofumi Akagi, E. H. (2007). *INSTANTANEOUS POWER THEORY AND APPLICATIONS TO POWER CONDITIONING*. IEEE PRESS.
- Huang Yalin, A. K. (June 2013). Short-term network planning of distribution system with photovoltaic. *22nd International Conference and Exhibition on Electricity Distribution, CIRED 2013*, (ss. 0989- p). Stockholm.
- IEA-PVPS. (2014). *Trends 2014-In Photovoltaic Applications: Survey Report of Selected IEA Countries between 1992 and 2003*.

- Jaan Niitsoo, M. J. (2015). Power Quality Issues Concerning Photovoltaic Generation in Distribution Grids. *Smart Grid and Renewable Energy*, 2015, 6, 148-163. Hämtat från Power Quality Issues Concerning Photovoltaic Generation in Distribution Grids: <http://www.scirp.org/journal/sgre>
- June Seok Lee, K. B. (January 2013). Variable DC-Link Voltage Algorithm with a Wide Range of Maximum Power Point Tracking for a Two-String PV System. *Energies* 2013, vol. 6, 58-78.
- Kashif Ishaque, Z. S. (September 2011). A comprehensive MATLAB Simulink PV system simulator with partial shading capability based on two-diode model. *Solar Energy*, Volume 8, Issues 9, 2217–2227.
- Kun Ding, X. B. (December 2012). A MATLAB-Simulink-Based PV Module Model and Its Application Under Conditions of Nonuniform Irradiance. *IEEE TRANSACTIONS ON ENERGY CONVERSION*, VOL. 27, NO. 4.
- Lindhahl, J. (2014). *National Survey Report of PV Power Applications in Sweden 2014*. Uppsala University : Swdsh Energy Agency .
- M. Chidi, O. I. (July 2012). Investigation of impact of integrating on-grid home based solar power systems on voltage rise in the utility network. *Power and Energy Society General Meeting, 2012 IEEE* (ss. 1 - 7). San Diego, CA: IEEE.
- M. Karimi, H. ., (2016). Photovoltaic penetration issues and impacts in distribution network- A review . *Renewable and Sustainable Energy Reviews* (53), 594-605.
- M.D Singh, K. B. (2011). *Power Electronics*. Tata Mcgraw Hill publishers, Second edition, pp. 135-670.
- Man, E. A. (2011). *Control of Grid Connected PV Systems with Grid Support Functions*. Denmark : Aalborg University .
- Marcelo Gradella Villalva, J. R. (May 2009). Comprehensive Approach to Modeling and and Simulation of Photovoltaic Arrays. *IEEE TRANSACTIONS ON POWER ELECTRONICS*, VOL. 24, NO. 5, 1198 - 1208.
- Massawe, H. B. (June 2013). *Grid Connected Photovoltaic Systems with SmartGrid functionality*. Norwegian University of Science and Technology.
- Minas Patsalides, V. E. (2016). A generic transient PV system model for power quality studies. *Renewable Energy* (89), 526-542.
- Mohamed A. Eltawil, Z. Z. (2010). Grid-connected photovoltaic power systems: Technical and potential problems—A review. *Renewable and Sustainable Energy Reviews*, 112–129.
- Mohammad T. Arif, A. M. (October 2014). Impacts of Distributed Generators on Utility Grid – an Experimental and Simulation Analysis. *Australasian Universities Power*

- Engineering Conference, AUPEC 2014, Curtin University, Perth, Australia, (ss. 1 - 7). Perth, WA: IEEE.*
- Mulenga, E. (2015). *Impacts of integrating solar PV power to an existing grid: Case Studies of Mölndal and Orust energy distribution (10/0.4 kV and 130/10 kV) grids.* y, Gothenburg, Sweden: Chalmers University of Technology.
- Nadeeshani Jayasekara, P. W. (2010). Analysis of power quality impact of high penetration PV in residential feeders. *Universities Power Engineering Conference (AUPEC), 2010 20th Australasian (ss. 1-8).* Christchurch: IEEE.
- Neimane, V. (2001). *On Development Planning of Electricity Distribution Networks .* Stockholm: Royal Institute of Technology .
- NREL. (August 2003). *DG Power Quality, Protection and Reliability Case Studies.* Niskayuna, New York: GE Corporate Research and Development.
- NREL. (February 2008). *Distribution System Voltage Performance Analysis for High-Penetration Photovoltaics.* NREL.
- P. Trichakis, P. T. (2006). An Investigation of Voltage Unbalance In Low Voltage Distribution Networks With High Levels of SSEG. *Universities Power Engineering Conference, 2006. UPEC '06. Proceedings of the 41st International (ss. 182 - 186).* Newcastle upon Tyne: IEEE.
- Patil, K. (November 2013). Harmonic Analysis of Sine PWM and hysteresis current controller. *International Journal of Advanced Research in Electrical, Electronics and Instrumentation Engineering, Vol. 2, Issue 11.*
- Pedro A. B. Block, H. L. (March 2014). Power quality analyses of a large scale photovoltaic system. *Renewable Energy Congress (IREC), 2014 5th International (ss. 1 - 6).* Hammamet: IEEE.
- Povslen, A. F. (February 2002). *Impacts of power penetration from photovoltaic power systems in distribution networks.* IEA PVPS .
- Rangy Sunny, R. A. (December, 2013). Harmonics Control and Performance Analysis of a Grid Connected Photovoltaic System. *International Conference on Advanced Computing and Communication Systems (ICACCS -2013).* Coimbatore, INDIA.
- Ravi Bhatt, B. C. (August 2011). Grid frequency and voltage support using PV systems with energy storage. *North American Power Symposium (NAPS), 2011 (ss. 1 - 6).* Boston, MA: IEEE.
- REN21. (2015). *Renewables 2015: Global Status Report : Key findings 2015.* Hämtat från REN21: http://www.ren21.net/wp-content/uploads/2015/07/GSR2015_KeyFindings_lowres.pdf
- S.M.A.Faisal. (2011). Model of Grid Connected Photovoltaic System Using MATLAB/SIMULINK. *Journal of Electrical Engineering.*

- S.V. Swarna Kumary, V. A. (2014). Modelling and Power quality analysis of a Grid-connected Solar PV System. *Australasian Universities Power Engineering Conference, AUPEC 2014*. Australia.
- Sam KoohiKamali, S. Y. (2010). Impacts of Grid-Connected PV System on the Steady-State Operation of a Malaysian Grid. *Power and Energy (PECon), 2010 IEEE International Conference on Year: 2010* (ss. 858 - 863). Kuala Lumpur: IEEE.
- SANDIA Report. (February 2008). *Renewable Systems Interconnection Study:Advanced Grid Planning and Operations*. California: Sandia National Laboratories.
- Sanjuan, S. L. (2010). *Voltage Oriented Control of Three-Phase Boost PWM Converters:Design, simulation and implementation of a 3-phase boost battery*. Göteborg,Sweden: CHALMERS UNIVERSITY OF TECHNOLOGY.
- Skalík, L., Lulkoviová, O., Furbo, S., Perers, B., Dragsted, J., & Nielsen, K. P. (February 2016). *Evaluation of long-term global radiation measurements in Denmark and Sweden*. Technical University of Denmark .
- Stefania Conti, S. R. (2005). Simulink Modelling of LV Photovoltaic Grid-connected Distributed Generation. *18th International Conference on Electricity Distribution,CIRED*. Turin,Italy.
- Tan, Y. T. (February 2004). *Impact on the power system with a large penetration of photovoltaic generation*. Department of Electrical Engineering and Electronics ,UMIST.
- Tao Ma, H. Y. (2014). Solar photovoltaic system modeling and performance prediction . *Renewable and Sustainable Energy Reviews* 36, 304–315.
- Vattenfall. (2007). *Europe's energy markets:Major Challenges for the Energy Sector*. Hämtat från http://www.vattenfall.com/en/file/3-Europes-energy-marketsElect_8460610.pdf
- VDE. (2011). *VDE-AR-N 4105 : Generators connected to the low-voltage distribution network* . VDE.
- Víctor H., M. Q. (May 2006). Assessment of energy distribution losses for increasing penetration of distributed generation. *Power Systems, IEEE Transactions on (Volume:21 , Issue: 2)*, 533 - 540.
- Williams K. Francis, P. S. (December 2014). MATLAB/Simulink PV Module Modelof P&O And DC Link CDC MPPT Algorithmswith Labview Real Time Monitoring And Control Over P&O Technique. *International Journal of Advanced Research in Electrical,Electronics and Instrumentation Engineering*.
- Xu Xiaoyan, H. Y. (April 2009). Modeling of large grid-integrated PV station and analysis its impact on grid voltage. *Sustainable Power Generation and Supply, 2009. SUPERGEN '09. International Conference on*. Nanjing: IEEE.

Yalin Huang, E. H. (2013). Short-term Network Planning of Distribution System with Photovoltaic. *22nd International Conference on Electricity Distribution* . Stockholm: CIRED.

Yun Tiam Tan, D. S. (June 2007). Impact on the Power System of a Large Penetration of Photovoltaic Generation. *Power Engineering Society General Meeting, 2007. IEEE* (ss. 1 - 8). Tampa, FL: IEEE.

APPENDIX A: MATLAB SCRIPT FOR PV MODULE MODELLING

```
function Iout = fcn(S1,T,V)
%#codegen
% clc; clear; close all;
% S1, T inputs, log is natural logarithm
Isc_r=3;
Voc_r=22;
Impp_r=2.77;
Vmpp_r=17.98;
a=0.0004;
b=-0.0033;
c=0.066;
% Rs=0.085;
% Tref=25;
% Sref=1000;
% DT=T-Tref;
% Isc=Isc_r*(S1/Sref)*(1+a*DT);
% Voc=Voc_r*(1+b*DT+c*log(S1/Sref));
% k=(1-Impp_r/Isc_r)^(Voc_r/(Vmpp_r-Voc_r+Rs*Impp_r));
up1= Vmpp_r+(Impp_r*(Voc_r-Vmpp_r)/((Isc_r-Impp_r)*log(1-(Impp_r/Isc_r)));
lo1= Impp_r+Impp_r^2/((Isc_r-Impp_r)*log(1-(Impp_r/Isc_r)));
Rs=up1/lo1;
Sr=1000;
Tr=25;
DT= T-Tr;
Isc= Isc_r*(S1/Sr)*(1+a*DT);
Voc=Voc_r*(1+b*DT+c*log(S1/Sr));
k = (1-(Impp_r/Isc_r)^(Voc_r/(Vmpp_r+Rs*Impp_r-Voc_r)));
Iref=1.5;
DIref=1.5;
V1=Voc-(Rs*Iref*Isc/Isc_r)+Voc_r*(log(1-Iref/Isc_r))/log(k);
%%

for i=1:50
    DIref=DIref/2;
    if (V1-V < 0.01)
        Iref=Iref-DIref;
    elseif (V1-V > 0.01)
        Iref=Iref+DIref;
    %     else
    %         i=1000;
    end
    V1=Voc-(Rs*Iref*Isc/Isc_r)+Voc_r*(log(1-Iref/Isc_r))/log(k);
end
Iout=Iref*Isc/Isc_r;
% display Iref;
```

APPENDIX B: MATLAB SCRIPT FOR P&O ALGORITHM

```
function D = PandO( Vpv, Ipv, T )

persistent Pn Po dP d dd n;

if isempty(Vpv)
    Vpv=55;
end
if isempty(Ipv)
    Ipv=0;
end
if isempty(Po)
    Po=0;
end
if isempty(Pn)
    Pn=0;
end
if isempty(dP)
    dP=0;
end
if isempty(d)
    d=1;
end
if isempty(dd)
    dd=0;
end
if isempty(n)
    n=1;
end

if (T>n*0.02)
    n=n+1;
    Po=Pn;
    Pn=Vpv*Ipv;
    dP=Pn-Po;

    if (dd==0) % to avoid dP/dd=inf
        if dP>1
            dd=0.01;
            d=d+dd;
        else
            if (dP<-1)
                dd=-0.01;
                d=d+dd;
            else
                dd=0;
            end
        end
    end
else
    if ((dP<1)&&(dP>-1)) % leave little margin
        dd=0;
        d=d+dd;
    else
        if ((dP/dd)>0) % positive slop
            dd=0.01;
            d=d+dd;
        end
    end
end
```

```

        else % negative and zero slop
            dd=-0.01;
            d=d+dd;
        end
    end
end
end

D=d/(d+1); % calculate duty

% code to avoid duty less than 0.1 and more than 0.9
if (D<0.1)
    D=0.1;
    d=D/(1-D);
else
    if (D>0.9)
        D=0.9;
        d=D/(1-D);
    else
        end
end
end
end

```



**MÄLARDALEN UNIVERSITY
SWEDEN**